EUROPEAN UNION
European Structural and Investment Funds
Operational Programme Research,
Development and Education

Optical Waves in Planar Systems

Jaroslav Vlček

April 2020

This work has been supported by the Ministry
of Education, Youth and Sport of the Czech Republic
by the project

"Technology for the Future 2.0"

No. CZ.02.2.69/0.0/0.0/18_058/0010212

Contents

Preface 5
List of Notation 5

1 Field Mathematics for Photonics **8**
1.1 Tensor calculus 8
1.1.1 Introducing notions 8
1.1.2 Orthogonal transformation 11
1.1.3 Cartesian tensors 15
1.1.4 Symmetric second rank tensors 21
1.1.5 Levi-Civita tensor 24
1.1.6 Selected tensor applications 26

2 Electromagnetic Field Equations **28**
2.1 Maxwell's Equations in Anisotropic Medium 28
2.1.1 Optical waves in material media 28
2.1.2 Maxwell's equations 29
2.1.3 The wave vector 30
2.1.4 Solution of wave equation 32
2.2 Polarization states 33
2.2.1 Optical waves in an isotropic medium 33
2.2.2 Electrically anisotropic medium 36
2.2.3 Polarization states in magnetooptics 38
2.2.4 Representation of polarization states 42
2.2.5 Medium with both electric and magnetic anisotropy . . 43
2.2.6 Excersise 46

3 Optical Waves in Multilayers **47**
3.1 Waves at single planar interface 47
3.1.1 Boundary conditions 47
3.1.2 Wave coupling principle 49
3.1.3 Interface between isotropic media 52

3.1.4 Interface between isotropic media and anisotropic substrate . . . 58
3.2 Optical multilayers . . . 62
3.2.1 Multilayer matrix construction . . . 62
3.2.2 Reflection and transmission . . . 64
3.2.3 Implementation remarks . . . 66
3.2.4 A single layer structure . . . 67
3.3 Selected applications . . . 69
3.3.1 An interface with metallic film . . . 69
3.3.2 Prism coupling . . . 70
3.3.3 Magnetooptics . . . 71
3.3.4 Spectral ellipsometry . . . 72
3.3.5 Inverse problems . . . 73
3.3.6 Excersise . . . 75

4 Planar Optical Waveguides **77**
4.1 Introduction . . . 77
4.2 Dispersion relations . . . 79
4.2.1 Transverse resonance . . . 79
4.2.2 Dispersion relations . . . 79
4.2.3 Equivalence of resonance relations . . . 81
4.2.4 Electromagnetic field model . . . 82
4.3 Waveguide modes . . . 83
4.3.1 Classification . . . 83
4.3.2 Symmetric waveguide . . . 85
4.3.3 Weakly guided modes . . . 87
4.3.4 Waveguiding structures with coupling prism . . . 89
4.3.5 Excersise . . . 90

5 Plasmon Waves **92**
5.1 Plasmon polaritons in planar structures . . . 92
5.1.1 Plasmon wave generation . . . 92
5.1.2 Surface plasmon dispersion relations . . . 93
5.1.3 Examples . . . 95
5.2 Surface pasmon polariton applications . . . 96
5.2.1 Plasmonic sensing principle . . . 96
5.2.2 MIM and IMI plasmonic structures . . . 98
5.2.3 Excersise . . . 101
Excersises in Chapter 2-5: Answers and Solutions . . . 102
References . . . 104

Preface

Present technologies of planar optical nanostructures enable an implementation of new devices for photonics, sensing or electronics. Optical methods used to characterize such devices offer spatial resolution on the nanometer scale. This text is intent on analytical investigation of the properties of free, guided and evanescent electromagnetic waves with given polarization in nanostructures being generally anisotropic and absorbing. Among other, this work is addressed to Ph.D. students and postdocs who deal with wave optics, nanotechnologies or applied physics. The objective is to summarize an overview of theoretical background for study of properties important for characterization, design or application of optical nanostructures.

Presented matter is divided into two parts. The first (and the most extensive) chapter is devoted to the vector and tensor calculus with selected applications. There the mathematical themes known from the graduate courses are upgraded to make easy the orientation in following text. Since there are current written or web-site sources at disposal, we only point out three titles [1], [2] and [3] in the list of references. The Chapter 2 covers basic physical relations describing propagation of electromagnetic waves in (homogeneous) anisotropic media. The third chapter aims to show principles in mathematical modeling of nanostructured optical multilayers, especially the rigorous coupled waves method and its algorithmization. The two subsequent parts contains several meaningful applications realized with the use of formerly introduced theoretical background. Planar waveguides as well as plasmonic structures are discussed in the coupling gap setup.

Note, that all presented numerical outputs were realized using own procedures implemented as Matlab codes.

Overall, there is no attempt in this text-book to provide a comprehensive list of references. Rather, the intention is to give representative examples that lead to fundamental physical understanding, and, that can serve as starting points for more in-depth investigations.

List of Notation

The following overview brings notation of the most used quantities in the chapters 2 - 5. The other symbols are either well-known or these are explained “ad hoc”. Notation in the first “mathematical” chapter is a bit different. We give up the exact distinguishing of the row and column vectors typing – the particular form is allways perceptible by a context.

Latin symbols

$\boldsymbol{B}$	magnetic flux density vector
c	free space light velocity
d	layer thickness
$\mathbf{D}$	dynamical matrix
$\boldsymbol{D}$	electric flux density vector
$\boldsymbol{e}$	polarization vector of electric intensity
$\boldsymbol{E}$	electric field vector
$\boldsymbol{h}$	polarization vector of magnetic intensity
$\boldsymbol{H}$	magnetic field vector
$\mathbf{I}$	unit matrix
k	wave number
$\boldsymbol{k}$	wave vector
k_0	free space wave number
$\mathbf{K}$	matrix of the operation $\boldsymbol{k}\times$
$\mathbf{M}$	matrix of multilayer
n	refractive index
N	effective refractive index
$\boldsymbol{o}$	null vector
$\mathbf{O}$	null matrix
$\mathbf{P}$	propagation matrix
$\mathbf{R}$	rotation matrix
Q	Voigt parameter
r	reflection coefficient
$\boldsymbol{r}$	position vector
S	sensitivity
$\mathbf{S}$	characteristic matrix
t	transmission coefficient
u	amplitude coefficient
$\boldsymbol{u}$	vector of amplitude coefficients

Greek symbols

α	wave vector component
β	longitudinal propagation constant
γ	transversal propagation constant
δ_{ij}	Kronecker tensor
ε	relative permittivity
$\boldsymbol{\varepsilon}$	relative permittivity tensor
ϵ	ellipticity

$\boldsymbol{\epsilon}$	Levi-Civita tensor
Θ	rotation
φ	incidence angle
λ	wavelength
μ	relative permeability
$\boldsymbol{\mu}$	relative permeability tensor
$\boldsymbol{\nu}$	normal vector
ω	frequency
Δ	ellipsometrical angle
ψ	ellipsometrical angle
τ	exponent, equal to $k_0 n \gamma d$

Indices

p, s	polarization states
(κ)	layer index

Other symbols

∇	Hamilton operator
$\times$	vector product
$\otimes$	tensor product
$\cdot$	scalar product
$*$	complex conjugation

Chapter 1

Field Mathematics for Photonics

1.1 Tensor calculus

1.1.1 Introducing notions

1.1.1.1 Euclidean space

Consider a space containing points $X = [x_1, x_2, \ldots, x_n]$, $Y = [y_1, y_2, \ldots, y_n]$ etc. and vectors $\boldsymbol{u} = (u_1, u_2, \ldots, u_n)$, $\boldsymbol{v} = (v_1, v_2, \ldots, v_n)$. If needed, we write $\boldsymbol{u}^\top$ for column (i.e. transposed) vector. The coordinates of points as well as vector components are real ($\mathbb{R}$) or complex ($\mathbb{C}$) numbers. Therefore, we denote these spaces of n-tuples simply as $\mathbb{R}^n$, $\mathbb{C}^n$, respectively; in this text, the space dimension n is generally $n = 2$ or $n = 3$. If the vector location is of importance, we assign the vector $\boldsymbol{u} = \overline{XY} = (y_1 - x_1, y_2 - x_2, \ldots, y_n - x_n)$ to the pair of the points X, Y.

Vector operations in $\mathbb{R}^n$

1. summation: $(\boldsymbol{u} + \boldsymbol{v})_i = u_i + v_i, \quad i = 1, \ldots, n,$
2. multiplication by a number: $(k.\boldsymbol{u})_i = k.u_i, \quad k \in \mathbb{R}.$

Linearity of $\mathbb{R}^n$

$$\forall\, \boldsymbol{u},\, \boldsymbol{v} \in \mathbb{R}^n \quad \forall\, a_1,\, a_2 \in \mathbb{R} \quad a_1\boldsymbol{u} + a_2\boldsymbol{v} \in \mathbb{R}^n\,.$$

Scalar product

$$\boldsymbol{u} \cdot \boldsymbol{v} = u_1v_1 + u_2v_2 + \cdots + u_nv_n = \sum_{i=1}^{n} u_iv_i\,. \tag{1.1}$$

Metric characteristics

In what follows, we consider the Cartesian coordinate system with the axes x_i, $i = 1, \ldots, n$.

(Euclidean) norm of the vector $\boldsymbol{u}$:

$$\|\boldsymbol{u}\| = \sqrt{\boldsymbol{u} \cdot \boldsymbol{u}} = \left(\sum_{i=1}^{n} u_i^2 \right)^{\frac{1}{2}} . \tag{1.2}$$

The vector $\tilde{\boldsymbol{u}} = \boldsymbol{u}/\|\boldsymbol{u}\|$ is called as normed, because of $\|\tilde{\boldsymbol{u}}\| = 1$. The ratio

$$\frac{u_i}{\|\boldsymbol{u}\|} = \cos \alpha_i \tag{1.3}$$

gives the cosine of direction angle α_i, i.e. the angle between the vector $\boldsymbol{u}$ and the x_i axis. Geometrical interpretation of scalar product (φ is the vector deviation):

$$\boldsymbol{u} \cdot \boldsymbol{v} = \|\boldsymbol{u}\| . \|\boldsymbol{v}\| . \cos \varphi \, . \tag{1.4}$$

Orthogonality: $\boldsymbol{u} \cdot \boldsymbol{v} = 0 \Longleftrightarrow \boldsymbol{u} \perp \boldsymbol{v} \quad (\boldsymbol{u}, \boldsymbol{v} \neq \boldsymbol{o})$.

Resume: the **Euclidean space $\mathbb{R}^n$ is the metric linear space with scalar product**.

1.1.1.2 Vector as linear combination of basis vectors

Let $\{\boldsymbol{u}_1, \boldsymbol{u}_2, \ldots, \boldsymbol{u}_m\}$ is a set of vectors in $\mathbb{R}^n$. **Linear combination** of these vectors is the sum

$$k_1 \boldsymbol{u}_1 + k_2 \boldsymbol{u}_2 + \ \ldots \ + k_m \boldsymbol{u}_m = \sum_{i=1}^{m} k_i \boldsymbol{u}_i \, , \tag{1.5}$$

where the numbers $k_1, k_2, \ldots, k_m \in \mathbb{R}$ are the coefficients.

The vectors $\boldsymbol{u}_1, \boldsymbol{u}_2, \ldots, \boldsymbol{u}_m$ are said to be **linearly dependent**, if there exist scalars $k_1, k_2, \ldots, k_m$, not all zero, such that

$$k_1 \boldsymbol{u}_1 + k_2 \boldsymbol{u}_2 + \ \ldots \ + k_m \boldsymbol{u}_m = \boldsymbol{o} \, , \tag{1.6}$$

where $\boldsymbol{o}$ denotes the null vector. This implies that arbitrary vector from the set can be represented as a linear combination of the remaining vectors in the set. On the other hand, a set of vectors is **linearly independent** if the only representations of $\boldsymbol{o}$ as a linear combination of its vectors is the trivial representation in which all the scalars k_i are zero.

In a vector space of dimension n at most n vectors are linearly independent. It means that another vectors can be expressed as linear combination of them.

Any n-tuple of linearly independent vectors forms a **basis of the vector space**. Considering the basis $\{\boldsymbol{h}_1, \boldsymbol{h}_2, \ldots, \boldsymbol{h}_n\}$, for instance, it holds for a vector $\boldsymbol{u}$,

$$\boldsymbol{u} = u_1\boldsymbol{h}_1 + u_2\boldsymbol{h}_2 + \ldots + u_n\boldsymbol{h}_n = \sum_{i=1}^{n} u_i\boldsymbol{h}_i = (u_1, u_2, \ldots, u_n)\,. \tag{1.7}$$

Therefore, the vector coordinates $u_1, u_2, \ldots, u_n$ are the coefficients of linear combination through which is this vector represented with respect to given basis.

Let $\{\boldsymbol{h}'_1, \boldsymbol{h}'_2, \ldots, \boldsymbol{h}'_n\}$ is another basis. We express each vector of it as linear combination of primal basis:

$$\begin{aligned} \boldsymbol{h}'_1 &= a_{11}\boldsymbol{h}_1 + a_{12}\boldsymbol{h}_2 + \cdots + a_{1n}\boldsymbol{h}_n\,, \\ \boldsymbol{h}'_2 &= a_{21}\boldsymbol{h}_1 + a_{22}\boldsymbol{h}_2 + \cdots + a_{2n}\boldsymbol{h}_n\,, \\ &\cdots \\ \boldsymbol{h}'_n &= a_{n1}\boldsymbol{h}_1 + a_{n2}\boldsymbol{h}_2 + \cdots + a_{nn}\boldsymbol{h}_n\,. \end{aligned} \tag{1.8}$$

The coefficients a_{ij} forms the transition matrix $\mathbf{A}$ from the original basis to the new one:

$$\mathbf{A} = \begin{bmatrix} a_{11} & a_{12} & \cdots & a_{1n} \\ a_{21} & a_{22} & \cdots & a_{2n} \\ \vdots & \vdots & & \vdots \\ a_{n1} & a_{n2} & \cdots & a_{nn} \end{bmatrix}\,. \tag{1.9}$$

Coordinates of the vector

$$\boldsymbol{u} = (u_1, u_2, \ldots, u_n) = u_1\boldsymbol{h}_1 + u_2\boldsymbol{h}_2 + \cdots + u_n\boldsymbol{h}_n, \tag{1.10}$$

regarding the new basis can be written by (1.8) as

$$\boldsymbol{u} = (u'_1, u'_2, \ldots, u'_n) = u'_1\boldsymbol{h}'_1 + u'_2\boldsymbol{h}'_1 + \cdots + u'_n\boldsymbol{h}'_n =$$

$$= u'_1(a_{11}\boldsymbol{h}_1 + a_{12}\boldsymbol{h}_2 + \cdots + a_{1n}\boldsymbol{h}_n) + \cdots + u'_n(a_{n1}\boldsymbol{h}_1 + a_{n2}\boldsymbol{h}_2 + \cdots + a_{nn}\boldsymbol{h}_n)\,. \tag{1.11}$$

Comparing (1.10) to (1.11) we obtain the system of algebraic equations

$$\begin{aligned} u_1 &= a_{11}u'_1 + a_{21}u'_2 + \cdots + a_{n1}u'_n\,, \\ u_2 &= a_{12}u'_1 + a_{22}u'_2 + \cdots + a_{n2}u'_n\,, \\ &\cdots \\ u_n &= a_{1n}u'_1 + a_{2n}u'_2 + \cdots + a_{nn}u'_n \end{aligned} \qquad \text{or in matrix form} \qquad \boldsymbol{u}^\top = \mathbf{A}^\top\boldsymbol{u}'^\top\,.$$

Thus, the new vector coordinates we find as the solution of algebraic problem

$$\boldsymbol{u}'^{\top} = \left(\mathbf{A}^{\top}\right)^{-1} \boldsymbol{u}^{\top} \ , \tag{1.12}$$

where the **transition matrix** $\mathbf{A}$ is of key importance. Regularity of this one follows from the linear independence of basis vectors.

1.1.1.3 Linear mapping in $\mathbb{R}^n$

Any square matrix $\mathbf{T}$ of the dimension n defines a linear mapping in the space $\mathbb{R}^n$, thereby it maps vector $\boldsymbol{u}$ on the vector $\boldsymbol{v}$ by the relation

$$\boldsymbol{v}^{\top} = \mathbf{T}\boldsymbol{u}^{\top} \ . \tag{1.13}$$

The linearity follows from the fact, that $\mathbf{T}$ maps linear combination of vectors again on linear combination of them with the same coefficients, because of

$$\mathbf{T}(k_1\boldsymbol{u}_1 + k_2\boldsymbol{u}_2 + \cdots + k_m\boldsymbol{u}_m) = k_1\mathbf{T}\boldsymbol{u}_1 + k_2\mathbf{T}\boldsymbol{u}_2 + \cdots + k_m\mathbf{T}\boldsymbol{u}_m =$$

$$k_1\boldsymbol{v}_1 + k_2\boldsymbol{v}_2 + \cdots + k_m\boldsymbol{v}_m.$$

Moreover, if matrix $\mathbf{T}$ is regular, i.e. $\det(\mathbf{T}) \neq 0$, there exists the inverse matrix $\mathbf{T}^{-1}$, which realizes inverese mapping

$$\boldsymbol{u}^{\top} = \mathbf{T}^{-1}\boldsymbol{v}^{\top} \ .$$

This relation is changed under the trasformation of basis with given matrix $\mathbf{A}$. Inserting $\boldsymbol{u}'$, $\boldsymbol{v}'$ instead $\boldsymbol{u}$, $\boldsymbol{v}$ in (1.12) leads to the new matrix $\mathbf{T}'$ of linear mapping:

$$\boldsymbol{v}'^{\top} = \mathbf{T}'\boldsymbol{u}'^{\top} \quad \rightarrow \quad (\mathbf{A}^{\top})^{-1}\boldsymbol{v}^{\top} = \mathbf{T}'(\mathbf{A}^{\top})^{-1}\boldsymbol{u}^{\top} \ ,$$

therefore,

$$(\mathbf{A}^{\top})^{-1}\mathbf{T}\boldsymbol{u}^{\top} = \mathbf{T}'(\mathbf{A}^{\top})^{-1}\boldsymbol{u}^{\top} \ .$$

Comparison of the both sides yields

$$\mathbf{T}' = (\mathbf{A}^{\top})^{-1}\mathbf{T}\mathbf{A}^{\top} \ . \tag{1.14}$$

1.1.2 Orthogonal transformation

1.1.2.1 Orthonormal basis

Any basis $\{\mathbf{e}_1, \mathbf{e}_2, \ldots \mathbf{e}_n\}$ v $\mathbb{R}^n$ containing mutually orthogonal unit vectors is called orthonormal. It means, that

$$|\mathbf{e}_i\| = 1, \quad \mathbf{e}_i \cdot \mathbf{e}_j = \delta_{ij} = \begin{cases} 1\,, \, i = j\,, \\ 0\,, \, i \neq j\,. \end{cases} \ , \tag{1.15}$$

where δ_{ij} stands for the Kronecker symbol. In the case of principal orthonormal basis one holds $(\mathbf{e}_i)_j = \delta_{ij}$, i.e. the components of the i-th vector are zero excluding the j-th being equal to one. In geometrical sense, these basis vectors are the direction vectors of axes in Cartesian coordinate system in $\mathbb{R}^n$.

Let derive the transition matrix from a basis (1.15) to the other orthonormal basis $\{\mathbf{e}'_1, \mathbf{e}'_2, \dots \mathbf{e}'_n\}$. At first, we express the i-th vector of new basis under the original one:

$$\mathbf{e}'_i = a_{i1}\mathbf{e}_1 + a_{i2}\mathbf{e}_2 + \cdots + a_{in}\mathbf{e}_n = \sum_{j=1}^{n} a_{ij}\mathbf{e}_j = a_{ij}\mathbf{e}_j \,. \tag{1.16}$$

The last term represents **summation convention**, in which the summation runs over the index obeying two-fold in the expression without the "sum" writting. An use of this convention is obvious from following examples:

$$u_i v_i = \sum_{i=1}^{n} u_i v_i = \boldsymbol{u}\cdot\boldsymbol{v} \,, \quad a_{ij}u_j = a_{i1}u_1 + a_{i2}u_2 + \cdots + a_{in}u_n \,,$$

$$\tau_{ii} = \tau_{11} + \tau_{22} + \tau_{33} = \sum_{i=1}^{3} \tau_{ii} \ (\text{in}\,\mathbb{R}^3) \,.$$

Scalar product (1.16) of a vector $\mathbf{e}'_i$ belonging to new basis and vector $\mathbf{e}_j$ of original basis reads

$$\mathbf{e}'_i \cdot \mathbf{e}_j = a_{ij} \Rightarrow a_{ij} = \|\mathbf{e}'_i\|.\|\mathbf{e}_j\|.\cos(\widehat{x'_i x_j}) = \cos(\widehat{x'_i x_j}). \tag{1.17}$$

In the geometric meaning, the coefficient a_{ij} of the transition matrix $\mathbf{A}$ is cosine of the angle between the new i-th axis and j-th original axis. Similar form as (1.16) has the reversal transformation (1.16),

$$\mathbf{e}_j = \sum_{i=1}^{3} b_{ji}\mathbf{e}'_i = b_{ji}\mathbf{e}'_i, \tag{1.18}$$

where $b_{ji} = \mathbf{e}_j \cdot \mathbf{e}'_i = \cos(\widehat{x_j x'_i})$ are elements of a matrix $\mathbf{B}$. Since $\cos(\widehat{x_j x'_i}) = \cos(\widehat{x'_i x_j})$, we have $a_{ij} = b_{ji}$, i.e. $\mathbf{B} = \mathbf{A}^\top$. The composed transformation must give the original basis, therefore, $\mathbf{AB} = \mathbf{I}$ is true, thus

$$\mathbf{A}\mathbf{A}^\top = \mathbf{I} \qquad \Rightarrow \qquad \mathbf{A}^\top = \mathbf{A}^{-1} \,, \tag{1.19}$$

where $\mathbf{I}$ denotes the unit matrix. Matrices exhibiting the property (1.19) are called as othonormal or (simply and more frequently) **orthogonal matrices**.

1.1.2.2 Properties of orthogonal matrices

If the matrix $\mathbf{A}$ is orthogonal, then

(1) $\det(\mathbf{A}) = \pm 1$.
As $\det(\mathbf{A}.\mathbf{B}) = \det(\mathbf{A}).\det(\mathbf{B})$ together with $\det(\mathbf{A}) = \det(\mathbf{A}^\top)$, in the case of orthogonal matrix must be $\det(\mathbf{A}).\det(\mathbf{A}^\top) = \det^2(\mathbf{A}) = 1$.

(2) $a_{ik}a_{jk} = \sum_k a_{ik}a_{jk} = \delta_{ij}, \quad a_{ij}.a_{ik} = \delta_{jk}$.
Scalar product of two different rows (columns) of orthogonal matrix is zero; the rows (columns) are normed.

(3) Product of two othogonal matrices is orthogonal matrix.
If $\mathbf{C} = \mathbf{AB}$, then $\mathbf{C}^{-1} = (\mathbf{AB})^{-1} = \mathbf{B}^{-1}.\mathbf{A}^{-1} = \mathbf{B}^\top\mathbf{A}^\top = (\mathbf{AB})^\top = \mathbf{C}^\top$.

Consider an orthogonal matrix in its geometric sense (1.17). Thus, the multiplication by this matrix can be viewed as rotation of Cartesian coordinate system about its center – for a situation in $\mathbb{R}^3$ see Figure 1.1.

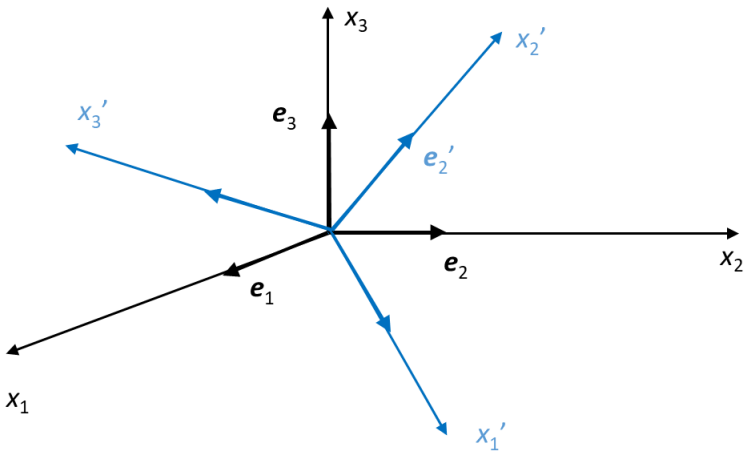

Fig. 1.1 Original Cartesian coordinate system (black) and rotated one (blue).

Examples

(a) It can be easy shown that the matrix

$$\mathbf{A} = \begin{bmatrix} \cos\phi & -\sin\phi \\ \sin\phi & \cos\phi \end{bmatrix}.$$

is orthogonal. It represents counterclockwise rotation about the point $[0,0]$ in $\mathbb{R}^2$ by an angle ϕ.

(b) Rotation in $\mathbb{R}^3$ about the x_3 axis by the angle ϑ is described by the matrix

$$\mathbf{R}_\vartheta = \begin{bmatrix} \cos\vartheta & -\sin\vartheta & 0 \\ \sin\vartheta & \cos\vartheta & 0 \\ 0 & 0 & 1 \end{bmatrix};$$

similarly, the matrix

$$\mathbf{R}_\varphi = \begin{bmatrix} 1 & 0 & 0 \\ 0 & \cos\varphi & -\sin\gamma \\ 0 & \sin\varphi & \cos\varphi \end{bmatrix}$$

represents rotation about the x_1 axis by the angle φ. The composition of the both rotations (in presented order) leads again to the rotation with the transformation matrix $\mathbf{R} = \mathbf{R}_\vartheta.\mathbf{R}_\varphi$.

(c) The matrix $\mathbf{A}$ is orthogonal, because of $\mathbf{A}\mathbf{A}^\top = \mathbf{I}$:

$$\mathbf{A} = \begin{bmatrix} \frac{1}{\sqrt{2}} & \frac{1}{2} & \frac{1}{2} \\ -\frac{1}{\sqrt{2}} & \frac{1}{2} & \frac{1}{2} \\ 0 & -\frac{1}{\sqrt{2}} & \frac{1}{\sqrt{2}} \end{bmatrix}.$$

1.1.2.3 Orthogonal transformation of linear mapping

Orthogonal transformation of vector

In (1.12) we showed that it holds by a change of basis $\boldsymbol{u}'^\top = \left(\mathbf{A}^\top\right)^{-1}\boldsymbol{u}^\top$. If $\mathbf{A}$ is orthogonal, then $\left(\mathbf{A}^\top\right)^{-1} = \left(\mathbf{A}^\top\right)^\top = \mathbf{A}$. It means, that the vector $\boldsymbol{u}$ is transformed by transition between two orthogonal bases (e.g. by a coordinate system rotation) on the vector

$$\boldsymbol{u}'^\top = \mathbf{A}\boldsymbol{u}^\top\ , \qquad \text{i.e.} \qquad u'_i = a_{ij}u_j\ . \tag{1.20}$$

It follows important statement: scalar product of vectors in space of arbitrary dimension n is invariant by orthogonal transformation. Really, we have

$$\boldsymbol{u}' \cdot \boldsymbol{v}' = u'_i v'_i = a_{ij}u_j\, a_{ik}v_k = a_{ij}a_{ik}u_j v_k = \delta_{jk}u_j v_k = u_j v_j = \boldsymbol{u}\cdot\boldsymbol{v}\ . \tag{1.21}$$

Orthogonal transformation of matrix

Consider a linear mapping with the matrix $\mathbf{T}$. We obtain its transformed feature with orthogonal matrix $\mathbf{A}$ using the relation (1.14) :

$$\mathbf{T}' = (\mathbf{A}^\top)^{-1}\mathbf{T}\mathbf{A}^\top = \mathbf{A}\mathbf{T}\mathbf{A}^\top \,. \tag{1.22}$$

Indexed form of this result yields

$$T'_{ij} = a_{ik}T_{kl}a_{lj}\,, \qquad \text{i.e.} \qquad T'_{ij} = a_{ik}a_{jl}T_{kl}\,. \tag{1.23}$$

1.1.2.4 Excersise

(1) Find transformed vector $\boldsymbol{u} = (2, \sqrt{3})$ by the rotation in the Example **(a)** on the page 13. Solve generally at first, then for the angle $\phi = \frac{\pi}{3}$.

(2) Calculate matrix $\mathbf{R}$ in the Example **(b)** inserting the angles $\alpha = \gamma = \pi/2$. Then rotate the vector $\boldsymbol{b} = (2, 1, 0)$.

(3) Verify that $\mathbf{R}_\alpha.\mathbf{R}_\gamma \neq \mathbf{R}_\gamma.\mathbf{R}_\alpha$.

(4) Given linear mapping with the matrix

$$\mathbf{T} = \begin{bmatrix} 2 & 0 & 1 \\ -1 & 3 & 0 \\ 0 & 1 & 1 \end{bmatrix} .$$

Derive its transform $\mathbf{T}'$ due the coordinate system rotation about x_2 axis by the angle $\beta = \pi/2$.

1.1.3 Cartesian tensors

The laws of physics do not depend on the choice of coordinate system. However, a symbolic (mathematical) representation of them can be changed, when another coordinate system is chosen. Here, we are concerned with linear transformations of the especial type, where the new coordinates are linked with original ones by rotation of Cartesian coordinate system. Therefore, our transformation method of non-invariant quantities is based on orthogonal matrices.

1.1.3.1 Introduction

At first we remind two important relations (1.20), (1.23) in previous part that serve to orthogonal transformation of a vector and matrix. We write those in the indexed form with the use of summation convention:

$$u'_i = a_{ij}u_j \ , \qquad T'_{ij} = a_{ik}a_{jl}T_{kl} \ .$$

Consider a mapping $\mathbf{W}$ of the vector $\boldsymbol{u}$ on the matrix $\mathbf{T}$ that we write in the both forms:

$$\mathbf{T} = \mathbf{W}\boldsymbol{u}^\top \ , \qquad T_{lm} = W_{lmn}u_n \ .$$

Now, we apply orthogonal transformation with matrix $\mathbf{A}$ and write the result $\mathbf{T}' = \mathbf{W}'\boldsymbol{u}'^\top$ in the indexed form being advantageous. Successive arrangement using particular transformations reads:

$$T'_{ij} = W'_{ijk}u'_k \quad \rightarrow \quad a_{il}a_{jm}T_{lm} = W'_{ijk}a_{kn}u_n \quad \rightarrow \quad a_{il}a_{jm}W_{lmn}u_n = W'_{ijk}a_{kn}u_n \ .$$

Final transformation rule for the mapping $\mathbf{W}$ follows from the last relation as

$$W'_{ijk} = a_{il}a_{jm}a_{kn}W_{lmn} \ . \tag{1.24}$$

In this sense, quantities with arbitrary number M of indices are transformed by the application of corresponding number of rotation matrices $\mathbf{A}$ to each one of the indices. This consideration leads to the notion **tensor** that we define as follows.
The n-tuple $\boldsymbol{u} = (u_1, u_2, \ldots, u_n)$ that fulfils by orthogonal transformation the relation

$$u'_i = a_{ij}u_j \tag{1.25}$$

is called **the first rank tensor** or the vector. The matrix $\mathbf{T} = (T_{ij})$, $i, j = 1, \ldots, n$ is called as **second rank tensor**, when its elements are transformed by the relation

$$T'_{ij} = a_{ik}a_{jl}T_{kl}. \tag{1.26}$$

The quantity with M indices that fulfils transformation relation

$$T'_{i_1 i_2 \cdots i_M} = a_{i_1 j_1}a_{i_2 j_2} \ldots a_{i_M j_M}T_{j_1 j_2 \cdots j_M}. \tag{1.27}$$

is called **Cartesian tensor of the rank** M.

Remarks

- the form of transformation relations does not depend on the dimension of space, where the tensor lives,

- scalars are tensors of the rank $M = 0$,
- number of rank M tensor components in $\mathbb{R}^n$ equals n^M,
- any second rank tensor can be written as a square matrix, the elements of which are numbers or functions:

$$\mathbf{T} = \begin{bmatrix} T_{11} & T_{12} & T_{13} \\ T_{21} & T_{22} & T_{23} \\ T_{31} & T_{32} & T_{33} \end{bmatrix} .$$

  However, it is distinguished from an arbitrary square matrix by the transformation properties of its components.

Example
We verify tensor properties of dyadic product of two vectors $\mathbf{W} = \boldsymbol{u} \otimes \boldsymbol{v}$ in $\mathbb{R}^n$ with the elements $W_{kl} = u_k v_l$. Transformation by (1.26) gives

$$W'_{ij} = u'_i v'_j = a_{ik} u_k a_{jl} v_l = a_{ik} a_{jl} u_k v_l = a_{ik} a_{jl} W_{kl}.$$

1.1.3.2 Tensor operations

(A) Addition of tensors
The corresponding components are added; it makes the sense when both have the same rank. When a tensor $\mathbf{R}$ is said to be the sum of the tensors $\mathbf{P}$ and $\mathbf{Q}$, this means (e.g. for the tensors of the rank 3):

$$\mathbf{P} + \mathbf{Q} = \mathbf{R} \quad \Leftrightarrow \quad P_{ijk} + Q_{ijk} = R_{ijk}.$$

(B) Multiplication of tensor by a scalar
means multiplication of all its elements by this scalar:

$$\mathbf{P} = k\mathbf{Q} \quad \Leftrightarrow \quad P_{ijk} = kQ_{ijk} \ .$$

(C) Contraction of tensor
When there exist two identic tensor indices, the summation over this common index results in the tensor having its rank by two less than original tensor. In other words, the summation convention is the direct consequence of this operation. We can demonstrate this principle by a four rank tensor $\mathbf{B}$ in $\mathbf{R}^3$:

$$B_{ijkj} = B_{i1k1} + B_{i2k2} + B_{i3k3} = B_{ik} \ .$$

Contraction of a second rank tensor gives the scalar

$$T_{ii} = T_{11} + T_{22} + T_{33} = \mathrm{Tr}(\mathbf{T}) \ .$$

Here, we denoted as Tr the trace of 3×3 matrix.

(D) Multiplication of tensors

(D1) ***Outer product of tensors*** means the multiplication of each component of the first tensor by each component of the second tensor. Thus, the rank of resulting tensor is the sum of the both factors ranks – see following example.

$$\mathbf{P} \otimes \mathbf{Q} = \mathbf{R} \quad \Leftrightarrow \quad P_{ijk}.Q_{lm} = R_{ijklm} \quad \text{and the like.}$$

Note, that the outer product is not commutative. Dyadic product of two vectors in $\mathbb{R}^3$ is a simple case of this operation.

$$\mathbf{W} = \boldsymbol{u} \otimes \boldsymbol{v} = \begin{pmatrix} u_1v_1 & u_1v_2 & u_1v_3 \\ u_2v_1 & u_2v_2 & u_2v_3 \\ u_3v_1 & u_3v_2 & u_3v_3 \end{pmatrix} \quad , \text{ e.g.} \quad W_{ij} = u_iv_j \neq W_{ji} \, .$$

(D2) ***Inner product of tensors*** arises when an outer product is contracted. As an example we take outer product of a matrix and vector that leads to the third rank tensor $T_{ij}u_k = W_{ijk}$. Algebraic product of matrix with vector (i.e. the vector $\mathbf{T}\boldsymbol{u}^\top = \boldsymbol{v}^\top$) we obtain as the inner product of those, i.e. by contraction of the third rank tensor over the index $j = k$:

$$T_{ij}u_j = W_{ijj} = v_i \, .$$

Examples

(a) Contraction of dyadic product $\boldsymbol{u} \otimes \boldsymbol{v}$ of two vectors gives the scalar product of vectors, because of

$$u_iv_i = \boldsymbol{u} \cdot \boldsymbol{v} = \mathrm{Tr}\,(\boldsymbol{u} \otimes \boldsymbol{v}) \, .$$

(b) Kronecker tensor δ_{ij} is the second rank tensor representing the unit matrix $\mathbf{I}$. Therefore it holds in $\mathbf{R}^3$

$$\delta_{ij}\delta_{ik} = \delta_{jk} \, , \quad \delta_{ii} = 3 \, .$$

1.1.3.3 Especial properties of tensors

(a) Isotropic tensors

These tensors are invariant by orthogonal transformation. The Kronecker tensor is typical example because of

$$\delta'_{ij} = a_{ik}a_{jl}\delta_{kl} = a_{ik}a_{jk} = \delta_{ij}.$$

Example
We prove that the tensor

$$\eta_{ijkl} = A.\delta_{ij}\delta_{kl} + B.\delta_{ik}\delta_{jl} + C.\delta_{il}\delta_{jk} \tag{1.28}$$

is isotropic tensor of the rank 4 by arbitrary constants A, B, C. With regard to tensor definition we have

$$\eta'_{ijkl} = a_{ir}a_{js}a_{kt}a_{lu}\eta_{rstu} = a_{ir}a_{js}a_{kt}a_{lu}.(A.\delta_{rs}\delta_{tu} + B.\delta_{rt}\delta_{su} + C.\delta_{ru}\delta_{ts}) =$$

$$= A\underbrace{a_{ir}\delta_{rs}}_{a_{is}}a_{js}a_{kt}\underbrace{a_{lu}\delta_{tu}}_{a_{lt}} + B\underbrace{a_{ir}\delta_{rt}}_{a_{it}}\underbrace{a_{js}\delta_{su}}_{a_{ju}}a_{kt}a_{lu} + C\underbrace{a_{ir}\delta_{ru}}_{a_{ir}}\underbrace{a_{js}\delta_{ts}}_{a_{jt}}a_{kt}a_{lu} =$$

$$= A.\underbrace{a_{is}a_{js}}_{\delta_{ij}}\underbrace{a_{kt}a_{tl}}_{\delta_{kl}} + B.\underbrace{a_{it}a_{kt}}_{\delta_{ik}}\underbrace{a_{ju}a_{lu}}_{\delta_{jl}} + C.\underbrace{a_{iu}a_{lu}}_{\delta_{il}}\underbrace{a_{kt}a_{jt}}_{\delta_{jk}} = \eta_{ijkl}\ .$$

(b) Symmetric and antisymmetric tensors

- Symmetric second rank tensor: $T_{ij} = T_{ji}$.
- Antisymmetric second rank tensor: $T_{ij} = -T_{ji}$.
- Higher rank tensors: symmetry or antisymmetry is related to particular couple of indices. For example, the third rank tensor $\mathbf{W}$ is antisymmetric in the indices j, k, when $W_{ijk} = -W_{ikj}$.

There exists direct analogy to (anti)symmetric matrices for second rank tensors. Among other it holds that arbitrary second rank tensor can be decomposed into symmetric and antisymmetric part as follows:

$$T_{ij} = \frac{1}{2}(T_{ij} + T_{ji}) + \frac{1}{2}(T_{ij} - T_{ji}) = S_{ij} + A_{ij}\ . \tag{1.29}$$

Evidently, the symmetric tensor S_{ij} is given by six elements, and the antisymmetric tensor A_{ij} by three elements. In the other frequently used decomposition isotropic term containing the trace T_{kk} is detached:

$$T_{ij} = \frac{1}{3}T_{kk}\delta_{ij} + A_{ij} + P_{ij}\ , \qquad \text{where} \qquad P_{ij} = S_{ij} - \frac{1}{3}T_{kk}\delta_{ij}\ . \tag{1.30}$$

The symmetrical "traceless" tensor $\mathbf{P}$ is denoted as deviatoric part, when the original tensor $\mathbf{T}$ itself is symmetric (asymmetric term $\mathbf{A}$ vanishes).

(c) Parity of tensors

Consider physical quantity $f(\boldsymbol{r})$ as a function of position vector $\boldsymbol{r}$ =

(x_1, x_2, x_3). The parity $\mathcal{P}(f)$ is either equal to 1 or -1 by the change of signum quantity f, when the position vector $\boldsymbol{r}$ is replaced by $-\boldsymbol{r}$:

$$\mathcal{P}(f)f(\boldsymbol{r}) = f(-\boldsymbol{r}) \qquad \rightarrow \qquad \mathcal{P}(f) = \pm 1 \ . \tag{1.31}$$

In parrticular, one holds for the velocity $\boldsymbol{v}(\boldsymbol{r})$ and force $\boldsymbol{F}(\boldsymbol{r})$:

$$\boldsymbol{v} = \frac{d\boldsymbol{r}}{dt} \, , \qquad \boldsymbol{F} = m\frac{d\boldsymbol{v}}{dt} = m\frac{d^2\boldsymbol{r}}{dt^2} \, .$$

Since $\boldsymbol{v}(-\boldsymbol{r}) = -\boldsymbol{v}(\boldsymbol{r})$, $\boldsymbol{F}(-\boldsymbol{r}) = -\boldsymbol{F}(\boldsymbol{r})$ the both vectors have negative parity.

Generally, we distinguish two kinds of tensors of any rank M by their parity $\mathcal{P}$:

- **eigen tensors**, if $\mathcal{P} = (-1)^M$,
- **pseudotensors**, if $\mathcal{P} = -(-1)^M = (-1)^{M+1}$.

Usual multiplication rule is true:

$$\mathbf{P} \otimes \mathbf{Q} = \mathbf{R} \quad \rightarrow \quad \mathcal{P}(\mathbf{P})\mathcal{P}(\mathbf{Q}) = \mathcal{P}(\mathbf{R}) \ .$$

In the case of vectors ($M = 1$) the notation 'polar vector' , 'axial vector' is used instead 'eigenvector' and 'pseudovector'.
It is unavoidable for tensor equations describing real physical processes to keep their parity.

Example

Lorentz force $\boldsymbol{F}$ acting on a particle moving in magnetic field with the velocity $\boldsymbol{v}$ is the function of particle charge q and magnetic induction $\boldsymbol{B}$:

$$\boldsymbol{F} = q\boldsymbol{v} \times \boldsymbol{B} \ .$$

Since $\boldsymbol{F}$ and $\boldsymbol{v}$ are polar vectors with negative parity, then the induction $\boldsymbol{B}$ is axial vector as its parity must be $+1$.

(d) Cross product of vectors

In the space $\mathbb{R}^3$ we consider the fundamental orhonormal basis

$$\boldsymbol{e}_1 = (1,\, 0,\, 0) \, , \quad \boldsymbol{e}_2 = (0,\, 1,\, 0) \, , \quad \boldsymbol{e}_3 = (0,\, 0,\, 1) \ .$$

Besides scalar or dyadic product we introduce cross product of two vectors:

$$\boldsymbol{u} \times \boldsymbol{v} = (u_2v_3 - u_3v_2,\, u_3v_1 - u_1v_3,\, u_1v_2 - u_2v_1) = \begin{vmatrix} \boldsymbol{e}_1 & \boldsymbol{e}_2 & \boldsymbol{e}_3 \\ u_1 & u_2 & u_3 \\ v_1 & v_2 & v_3 \end{vmatrix} \ .$$

Geometric properties

- norm: $\|\boldsymbol{u} \times \boldsymbol{v}\| = \|\boldsymbol{u}\|.\|\boldsymbol{v}\|.\sin\alpha$, where α is the angle between vectors,
- direction: resulting vector is pependicular to the both factors: $\boldsymbol{u} \perp \boldsymbol{u} \times \boldsymbol{v}$, $\boldsymbol{v} \perp \boldsymbol{u} \times \boldsymbol{v}$,
- orientation: the vectors $\boldsymbol{u}$, $\boldsymbol{v}$, $\boldsymbol{u} \times \boldsymbol{v}$ forms counter-clockwise system.

The last one means that cross product is axial vector because of

$$\mathcal{P}(\boldsymbol{u} \times \boldsymbol{v}) = \mathcal{P}(\boldsymbol{u})\mathcal{P}(\boldsymbol{v}) = 1 \text{ by } \mathcal{P}(\boldsymbol{u}) = \mathcal{P}(\boldsymbol{v}) = -1.$$

Decomposition of dyadic product $T_{ij} = u_i v_j$ of two vectors by (1.29) enables to write its antisymmetric part as

$$A_{ij} = (\boldsymbol{u} \times \boldsymbol{v})_{6-i-j} \ , \tag{1.32}$$

where the order of indices i, j correspond to even permutation on the index triple 123.

The cross product is defined only in the space of the dimension 3. The reason is as follows: antisymmetric second rank tensor in $\mathbb{R}^n$ is defined by $(n^2 - n)/2$ elements; this value should be equal to the number n of vector components in such space; however, the relation $(n^2 - n)/2 = n$ is true only if $n = 3$.

1.1.4 Symmetric second rank tensors

1.1.4.1 Associate quadric and invariants

The symmetric second rank tensors, for which $S_{ij} = S_{ji}$, represent important group because of widely used applications. Moreover, the most of their properties can be illustrated with the help of symmetric matrices. Any tensor

$$\mathbf{S} = \begin{bmatrix} S_{11} & S_{12} & S_{13} \\ S_{12} & S_{22} & S_{23} \\ S_{13} & S_{23} & S_{33} \end{bmatrix} \tag{1.33}$$

can be viewed as a matrix of quadratic form in the variables x_1, x_2, x_3 that form the vector $\underline{\mathrm{x}}$.s The algebraic notation

$$S_{11}x_1^2 + S_{22}x_2^2 + S_{33}x_3^2 + 2S_{12}x_1x_2 + 2S_{13}x_1x_3 + 2S_{23}x_2x_3$$

is equivalent to tensor expression $S_{ij}x_ix_j$ (using summation rule). Contraction of this four rank tensor in the both indices results in (positive or negative) scalar value:

$$S_{ij}x_ix_j = \pm K^2 \ . \tag{1.34}$$

Obtained relation represents a quadratic surface in $\mathbb{R}^3$ that is called **associated quadric to the tensor** S_{ij}. The quadric type is given by eigenvalues of the matrix $\mathbf{S}$; corresponding eigenvectors agree with the principal axes of quadric. The eigenvectors $\boldsymbol{u}$ can be found as a solution of the equation

$$\mathbf{S}\boldsymbol{u}^\top = \lambda \boldsymbol{u}^\top, \quad \text{or, by tensor notation,} \quad S_{ij}u_j = \lambda u_i\,, \tag{1.35}$$

where an eigenvalue λ must be real because of tensor symmetry. In order to find non-trivial solution $\boldsymbol{u} \neq \boldsymbol{o}$ of the algebraic problem

$$(\mathbf{S} - \lambda\mathbf{I})\boldsymbol{u}^\top = \boldsymbol{o}^\top, \qquad (S_{ij} - \lambda\delta_{ij})u_j = 0\,, \tag{1.36}$$

the determinant must be equal to zero,

$$|\, S_{ij} - \lambda\delta_{ij} \,| = 0\,, \tag{1.37}$$

i.e.

$$\begin{vmatrix} S_{11}-\lambda & S_{12} & S_{13} \\ S_{12} & S_{22}-\lambda & S_{23} \\ S_{13} & S_{23} & S_{33}-\lambda \end{vmatrix} = 0\,. \tag{1.38}$$

Resolving this relation we obtain third degree algebraic equation

$$\lambda^3 - I_1\lambda^2 + I_2\lambda - I_3 = 0\,, \tag{1.39}$$

the roots of which are the **eigenvalues** λ_1, λ_2, λ_3. The associate quadric classification (for non-zero eigenvalues) is demonstrated by several typical examples:

- mutualy different λ_1, λ_2, $\lambda_3 > 0$ correspond to non-rotational elliptic surface,
- $\lambda_1 = \lambda_2 = \lambda_3 \neq 0$ means a sphere,
- $\lambda_1 = \lambda_2 > 0$, $\lambda_3 < 0$ estimate an uniaxial hyperbolic surface with the symmetry axis x_3.

Obviously, a multiplicity of eigenvalues means certain symmetry of quadric. The coefficients I_1, I_2, I_3 in the equation (1.39) do not depend on the choose of coordinate system. In other words, the values

$$I_1 = S_{11} + S_{22} + S_{33} = S_{ii}, \quad I_2 = \begin{vmatrix} S_{11} & S_{12} \\ S_{12} & S_{22} \end{vmatrix} + \begin{vmatrix} S_{11} & S_{13} \\ S_{13} & S_{33} \end{vmatrix} + \begin{vmatrix} S_{22} & S_{23} \\ S_{23} & S_{33} \end{vmatrix},$$

$$I_3 = |\mathbf{S}| \quad \text{(the determinant of } \mathbf{S}\text{)}$$

are invariant with regard to orthogonal transformation.

1.1.4.2 Principal axes

In following example the method of eigenvectors estimate is demonstrated.

Example
Determine principal axes and associated quadric type of the tensor

$$\mathbf{S} = \begin{bmatrix} 6 & -2 & 2 \\ -2 & 5 & 0 \\ 2 & 0 & 7 \end{bmatrix} .$$

(1) Eigenvalues:
The equation

$$|\mathbf{S} - \lambda\mathbf{I}| = \begin{vmatrix} 6-\lambda & -2 & 2 \\ -2 & 5-\lambda & 0 \\ 2 & 0 & 7-\lambda \end{vmatrix} = \cdots = -\lambda^3 + 18\lambda^2 - 99\lambda + 162 = 0$$

has the roots $\lambda_1 = 3,\ \lambda_2 = 6,$ a $\lambda_3 = 9$. It means, that the associated quadric

$$6x_1^2 + 5x_2^2 + 7x_3^2 - 4x_1x_2 + 4x_1x_3 = K^2$$

represents a general (non-rotational) elliptic surface.

(2) **Eigenvectors** (principal axes of associate quadric):
Putting eigenvalue λ_i into the equation (1.36) we obtain homogeneous algebraic system for the components of corresponding eigenvector $\boldsymbol{u}_i$:

$$\lambda_1 = 3\ \ldots \begin{bmatrix} 3 & -2 & 2 \\ -2 & 2 & 0 \\ 2 & 0 & 4 \end{bmatrix} \cdot \begin{bmatrix} u_{11} \\ u_{12} \\ u_{13} \end{bmatrix} = \begin{bmatrix} 0 \\ 0 \\ 0 \end{bmatrix} .$$

Arbitrary multiple of the eigenvector $\boldsymbol{u}_1 = (2,\, 2,\, -1)$ represents one from principal axes of the quadric associated with given tensor. The other two eigenvectors

$$\lambda_2 = 6\ \ldots\ \boldsymbol{u}_2 = (-1,\, 2,\, 2)\ , \qquad \lambda_3 = 9\ \ldots\ \boldsymbol{u}_3 = (2,\, -1,\, 2)$$

can be found by similar way.

1.1.5 Levi-Civita tensor

1.1.5.1 Levi-Civita tensor

The third rank tensor ϵ defined as

$$\epsilon_{ijk} = \begin{cases} 1 & \text{by even permutation of indices,} \\ -1 & \text{by odd permutation of indices,} \\ 0 & \text{for } i = j \text{ or } j = k \text{ or } k = i \end{cases} \tag{1.40}$$

is called Levi-Civita tensor. In the three-dimensional space it haves $3^3 = 27$ components, however, only 6 ones are non-zero – see Figure 1.2.

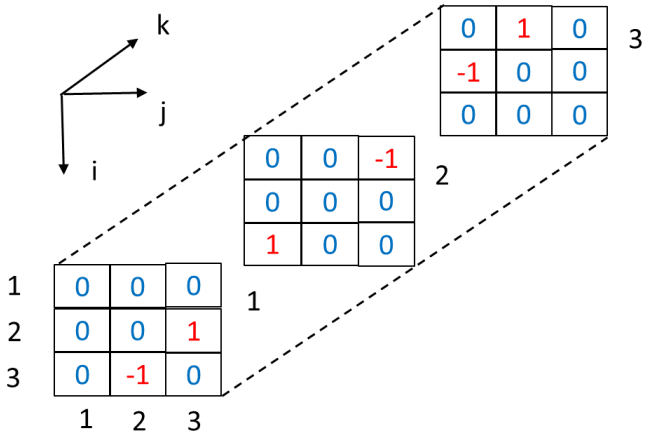

Fig. 1.2 The Levi-Civita tensor scheme.

Let we show its properties by orthogonal transformation:

$$\epsilon'_{ijk} = a_{il}a_{jm}a_{kn}\epsilon_{lmn} = a_{i1}.(a_{j2}a_{k3} - a_{j3}a_{k2}) +$$

$$+a_{i2}.(a_{j3}a_{k1} - a_{j1}a_{k3}) + a_{i3}.(a_{j1}a_{k2} - a_{j2}a_{k1}) =$$

$$= \begin{vmatrix} a_{i1} & a_{i2} & a_{i3} \\ a_{j1} & a_{j2} & a_{j3} \\ a_{k1} & a_{k2} & a_{k3} \end{vmatrix} = \left\{ \begin{array}{ll} 1, & ijk = 123,\ 231,\ 312, \\ -1, & ijk = 321,\ 213,\ 132, \\ 0, & \text{otherwiles} \end{array} \right\} = \epsilon_{ijk}.$$

When all three indices are different, the resulting determinant of orthogonal matrix **A** equals ± 1 depending on the order of its rows. If some two indicices

are equal one to the other, then two of rows become identical, therefore, the determinant equals 0.

Since $\epsilon'_{ijk} = \epsilon_{ijk}$, the Levi-Civita tensor is invariant regarding orthogonal transformation, therefore it is isotropic tensor of rank 3. Moreover, this one is antisymmetric with respect to any couple of indices, e.g. $\epsilon_{ijk} = -\epsilon_{jik}$ etc.

Example

We prove that it holds for the cross product of two vectors

$$\boldsymbol{u} \times \boldsymbol{v} = \epsilon_{ijk} \mathbf{e}_i u_j v_k \ . \tag{1.41}$$

By the Levi-Civita tensor definition:

$$\epsilon_{ijk} \mathbf{e}_i u_j v_k = \mathbf{e}_1(u_2 v_3 - u_3 v_2) + \mathbf{e}_2(-u_1 v_3 + u_3 v_1) + \mathbf{e}_3(u_1 v_2 - u_2 v_1) =$$

$$= \begin{vmatrix} \mathbf{e}_1 & \mathbf{e}_2 & \mathbf{e}_3 \\ u_1 & u_2 & u_3 \\ v_1 & v_2 & v_3 \end{vmatrix} = \boldsymbol{u} \times \boldsymbol{v} \ .$$

1.1.5.2 Excersise

(1) Find the associate quadric and its principal axes of the tensor

$$\mathbf{T} = \begin{bmatrix} 4 & 0 & 1 \\ 0 & 4 & 2 \\ 1 & 2 & 0 \end{bmatrix} .$$

(2) Prove the identity $\epsilon_{ijk}\epsilon_{klm} = \delta_{jm}\delta_{il} - \delta_{jl}\delta_{im}$.

(3) Use the result of Excersise **(2)** to verify the double cross product rule

$$\boldsymbol{u} \times (\boldsymbol{v} \times \boldsymbol{w}) = (\boldsymbol{u} \cdot \boldsymbol{w})\boldsymbol{v} - (\boldsymbol{u} \cdot \boldsymbol{v})\boldsymbol{w} \ . \tag{1.42}$$

(4) Levi-Civita tensor maps a vector on antisymmetric second rank tensor as

$$\epsilon_{ijk} u_k = U_{ij} \ , \quad U_{ij} = -U_{ji} \ . \tag{1.43}$$

Prove this property. Use this relation to write matrix representation of cross product.

1.1.6 Selected tensor applications

The most tensor applications in optics or more generally in theory of electromagnetic field bear relation to material anisotropy. Conventionaly, we distinguish between natural anisotropy having persistent character (crystals, composite materials) and artificial anisotropy raised by external factor that goes off together with this one (e.g. Kerr effect – see the Chapter 2). Note that only homogeneous materials are supposed in what follows.

1.1.6.1 General form of Hooke's law

We cannot omit this well-known application field because of its intuitive use of tensor apparatus. We start with the effect of external force $\boldsymbol{T}$ acting on unit surface area characterized by the normal $\boldsymbol{\nu}$. The caused stress is generally described by nine components of the symmetric **stress tensor** $\boldsymbol{\tau}$ by the relation

$$T_i = \tau_{ij}\nu_j \ . \tag{1.44}$$

Resulting **displacement** $\boldsymbol{u}$ of an element is connected to the **strain tensor** $\boldsymbol{e}$:

$$e_{kl} = \frac{1}{2}\left(\frac{\partial u_k}{\partial x_l} + \frac{\partial u_l}{\partial x_k}\right) \ . \tag{1.45}$$

The **generalized Hooke's law** for a material is given as

$$\tau_{ij} = C_{ijkl}e_{kl} \ , \quad i,j,k,l = 1,2,3 \ , \tag{1.46}$$

where C_{ijkl} is a fourth order stiffness tensor. In the case of isotropic material, the stiffness tensor becomes also isotropic. Therefore, it can be written in the form (1.28) that yields well-known feature of **Hooke's law** that we write with Lamé coefficients λ and μ:

$$\tau_{ij} = \lambda\delta_{ij}e_{kk} + 2\mu e_{ij} \ . \tag{1.47}$$

1.1.6.2 Ohm's law in an anisotropic medium

The vector form of Ohm's Law says that an applied electric field $\boldsymbol{E}$ produces a current density $\boldsymbol{J}$ (current per unit area) in the same direction: $\boldsymbol{J} = \sigma\boldsymbol{E}$, where σ is the conductivity. This only holds for conducting media that are isotropic, i.e. the same in all directions. This is certainly not the case in crystalline media, where the regular lattice will favour conduction in some directions more than in others. The most general relation between $\boldsymbol{J}$ and $\boldsymbol{E}$ is of the form

$$J_i = G_{ij}E_j \ , \tag{1.48}$$

where G_{ij} are the components of the **conductivity tensor** in the chosen basis.

1.1.6.3 Piezoelectric effect

An ability of given material to exhibit an electrical response to external mechanical loading is characterized by **piezoelectric modulus** $\mathbf{D}$, what is the tensor of rank 3. Knowing the stress tensor τ the piezoelectric effect is expressed by dipole moment $\boldsymbol{P}$ as

$$P_i = D_{ijk}\tau_{jk} \ . \tag{1.49}$$

Especially, in the case of three-axis crystal the tensor $\mathbf{D}$ has only 18 mutually different components as a consequence of the stress tensor symmetry. Increasing level of crystal symmetry leads to further simplification of piezoelectric modulus.

1.1.6.4 Permittivity and permeability

In linear optics (and electromagnetics), the constitutive relation describing the electric flux $\boldsymbol{D}$ in terms of the applied electric field intensity $\boldsymbol{E}$ is given by the relation

$$\boldsymbol{D} = \varepsilon_0 \boldsymbol{\varepsilon} \boldsymbol{E} \ , \qquad \text{i.e.} \qquad D_i = \varepsilon_0 \varepsilon_{ij} E_j \ , \tag{1.50}$$

where ε_0 is the free space permittivity and ε_{ij} are the components of medium **relative permittivity**. The symmetric traceless part $\hat{\boldsymbol{\varepsilon}}$ of the symmetric permittivity tensor $\boldsymbol{\varepsilon}$ characterizes the optical anisotropy of medium in the decomposition by (1.30) :

$$\varepsilon_{ij} = \varepsilon_{kk}\delta_{ij}/3 + \hat{\varepsilon}_{ij} \ . \tag{1.51}$$

Thus the **birefringence** of light occurs only when $\hat{\boldsymbol{\varepsilon}}$ is not zero for optical frequencies.

In contrast, the term nonlinear is used, for instance, when the field $\boldsymbol{E}$ changes several components of $\boldsymbol{\varepsilon}$. Thus, the higher order tensors come into constitutive relation that can be written as

$$D_i = \varepsilon_0 \left(\varepsilon^{(1)}_{ij} E_j + \varepsilon^{(2)}_{ijk} E_j E_k + \varepsilon^{(3)}_{ijkl} E_j E_k E_l + \cdots \right) \ . \tag{1.52}$$

The magnetic permeability acts as material characteristic in the constitutive relation between magnetic flux $\boldsymbol{B}$ and magnetic field intensity $\boldsymbol{H}$,

$$B_i = \mu_0 \mu_{ij} H_j \ , \tag{1.53}$$

where again μ_0, $\boldsymbol{\mu}$ are the free space permeability and **relative permeability** of optical medium, respectively.

Chapter 2

Electromagnetic Field Equations

2.1 Maxwell's Equations in Anisotropic Medium

In order to need not use the transposition we suppose column vectors in the Chapter 2.

2.1.1 Optical waves in material media

A classical description of an interaction between light and material medium starts with solution of Maxwell's equations. We consider monochromatic light wave of the wavelength λ, the angular frequence ω of which is

$$\omega = \frac{2\pi}{\lambda} c\,, \qquad c = \frac{1}{\sqrt{\varepsilon_0 \mu_0}}\,, \tag{2.1}$$

where c is the light velocity in vacuum; and, ε_0, μ_0 are the free space permittivity and permeability, respectively:

$$\varepsilon_0 \approx 8.85 \times 10^{-12}\ \mathrm{F/m}, \qquad \mu_0 = 4\pi \times 10^{-7}\ \mathrm{H/m}\,.$$

In the most cases the components of planar optical system (layers etc.) are very thin, therefore, we can suppose the homogeneity of them. An anisotropic optical medium is characterized by complex second rank tensors of relative permittivity and permeability

$$\boldsymbol{\varepsilon} = \begin{bmatrix} \varepsilon_{11} & \varepsilon_{12} & \varepsilon_{13} \\ \varepsilon_{21} & \varepsilon_{22} & \varepsilon_{23} \\ \varepsilon_{31} & \varepsilon_{32} & \varepsilon_{33} \end{bmatrix}, \qquad \boldsymbol{\mu} = \begin{bmatrix} \mu_{11} & \mu_{12} & \mu_{13} \\ \mu_{21} & \mu_{22} & \mu_{23} \\ \mu_{31} & \mu_{32} & \mu_{33} \end{bmatrix}. \tag{2.2}$$

In this general case the materials are called bi-gyrotropic. If only the anisotropy of permittivity takes place, then the specification gyrotropic is used.

At optical frequencies the field vectors are harmonic functions of the time t, for which we use the convention with time factor $\exp\{\mathrm{i}\omega t\}$. Thus, the corresponding notation reads as

$$\boldsymbol{\mathcal{E}} = \boldsymbol{E}\,\mathrm{e}^{\mathrm{i}\omega t}\,, \qquad \boldsymbol{\mathcal{H}} = \boldsymbol{H}\,\mathrm{e}^{\mathrm{i}\omega t}\,, \qquad \boldsymbol{\mathcal{D}} = \boldsymbol{D}\,\mathrm{e}^{\mathrm{i}\omega t}\,, \qquad \boldsymbol{\mathcal{E}} = \boldsymbol{B}\,\mathrm{e}^{\mathrm{i}\omega t}\,. \tag{2.3}$$

The electric and magnetic intensities are combined with with flux densities and with free current density $\boldsymbol{J}$ by constitutive relations

$$\boldsymbol{J} = \gamma\boldsymbol{E}\,, \quad \boldsymbol{D} = \varepsilon_0\boldsymbol{\varepsilon}\boldsymbol{E}\,, \quad \boldsymbol{B} = \mu_0\boldsymbol{\mu}\boldsymbol{H}\,. \tag{2.4}$$

An influence of the conductivity γ is incorporated into complex permittivity in what follows. Further, we will suppose media free of charges, i.e. we set the charge density $q = 0$.

2.1.2 Maxwell's equations

Rewrite differential forms (**??**), (**??**) and (**??**) of Maxwell's equations derived in previous chapter:

$$\begin{aligned} \nabla\times\boldsymbol{\mathcal{E}} &= -\frac{\partial\boldsymbol{\mathcal{B}}}{\partial t} & \qquad \nabla\times\boldsymbol{\mathcal{H}} &= \boldsymbol{J} + \frac{\partial\boldsymbol{\mathcal{D}}}{\partial t}\,, \\ \nabla\cdot\boldsymbol{\mathcal{D}} &= \rho\,, & \qquad \nabla\cdot\boldsymbol{\mathcal{E}} &= 0\,. \end{aligned} \tag{2.5}$$

The derivatives of exponential time factor including above assumptions lead to typical arrangement of Maxwell's equations in wave optics:

$$\begin{aligned} \nabla\times\boldsymbol{E} &= -\mathrm{i}\omega\mu_0\boldsymbol{\mu}\boldsymbol{H}\,, & \qquad \nabla\times\boldsymbol{H} &= \mathrm{i}\omega\varepsilon_0\boldsymbol{\varepsilon}\boldsymbol{E}\,, \\ \nabla\cdot(\boldsymbol{\varepsilon}\boldsymbol{E}) &= 0\,, & \qquad \nabla\cdot(\boldsymbol{\mu}\boldsymbol{H}) &= 0\,. \end{aligned} \tag{2.6}$$

In the following text we work only with time independent factors of field vectors, but the nomenclature remains unchanged for more clarity.

In order to introduce the wavelength λ in the governing set of equations instead the angular frequence ω, we apply the relations (2.1). Denoting $k_0 = 2\pi/\lambda$ the wavenumber, the first two equations are of the form

$$\nabla\times\boldsymbol{E} = -\mathrm{i}k_0\sqrt{\mu_0/\varepsilon_0}\,\boldsymbol{\mu}\boldsymbol{H}\,, \tag{2.7}$$

$$\nabla\times\boldsymbol{H} = \mathrm{i}k_0\sqrt{\varepsilon_0/\mu_0}\,\boldsymbol{\varepsilon}\boldsymbol{E}\,. \tag{2.8}$$

If we put the intensity $\boldsymbol{H}$ expressed from the first equation into the second one, then we obtain **bi-gyrotropic form of wave equation** for the intensity $\boldsymbol{E}$:

$$\nabla \times \boldsymbol{\mu}^{-1}(\nabla \times \boldsymbol{E}) = k_0^2 \boldsymbol{\varepsilon} \boldsymbol{E} \ . \tag{2.9}$$

It is obvious that this step can be "mirrored" with the similar result for the field $\boldsymbol{H}$.

Consider the **isotropic variant** of this equation with the scalar material characteristics that reads as

$$\nabla \times \nabla \times \boldsymbol{E} = k_0^2 \varepsilon \mu \boldsymbol{E} \ . \tag{2.10}$$

The double cross product on the left-hand side can be written as (see the Subsection 1.2.2.3)

$$\operatorname{rot} \operatorname{rot} \boldsymbol{E} = \operatorname{grad} \operatorname{div} \boldsymbol{E} - \Delta \boldsymbol{E} \ , \qquad \Delta \boldsymbol{E} = (\Delta E_1, \, \Delta E_2, \, \Delta E_3) \, .$$

Since $\operatorname{div} \boldsymbol{E} = 0$ due the divergence theorem, the Eq. (2.10) takes the well-known form

$$\Delta \boldsymbol{E} + k_0^2 \varepsilon \mu \boldsymbol{E} = \boldsymbol{o} \ , \tag{2.11}$$

i.e. three **scalar Helmholtz's equations**

$$\Delta E_i + k_0^2 \varepsilon \mu E_i = 0 \ , \qquad i = 1, 2, 3 \tag{2.12}$$

for the field $\boldsymbol{E}$ components.

2.1.3 The wave vector

The space dependent part of any component E_i is of the form

$$\mathrm{e}^{-\mathrm{i}\boldsymbol{k}\cdot\boldsymbol{x}} \ , \qquad \boldsymbol{x} = (x_1, \, x_2, \, x_3)^\top \, , \tag{2.13}$$

where

$$\boldsymbol{k} = (k_1, \, k_2, \, k_3)^\top = k_0(\alpha, \, \beta, \, \gamma)^\top \ , \qquad \|\boldsymbol{k}\| = k_0^2 \varepsilon \mu \tag{2.14}$$

is the wave vector of the field $\boldsymbol{E}$. Thus, if the scalar field (2.13) fulfills Helmholtz's equation, then it must hold

$$\Delta \left(\mathrm{e}^{-\mathrm{i}\boldsymbol{k}\cdot\boldsymbol{x}} \right) = -k^2 \mathrm{e}^{-\mathrm{i}\boldsymbol{k}\cdot\boldsymbol{x}} \ .$$

Really, rewritting the Laplace operator we have

$$\Delta \left(\mathrm{e}^{-\mathrm{i}\boldsymbol{k}\cdot\boldsymbol{x}} \right) = \nabla \cdot \left[\nabla \left(\mathrm{e}^{-\mathrm{i}\boldsymbol{k}\cdot\boldsymbol{x}} \right) \right] = \nabla \cdot \left[-\mathrm{i}\boldsymbol{k} \ \mathrm{e}^{-\mathrm{i}\boldsymbol{k}\cdot\boldsymbol{x}} \right] = -\mathrm{i}\mathrm{e}^{-\mathrm{i}\boldsymbol{k}\cdot\boldsymbol{x}} \, \nabla \cdot \boldsymbol{k} - \mathrm{i}\boldsymbol{k} \cdot \nabla \left(\mathrm{e}^{-\mathrm{i}\boldsymbol{k}\cdot\boldsymbol{x}} \right) \ .$$

Since $\nabla \cdot \boldsymbol{k} = 0$ the remaining term gives

$$-\mathrm{i}\boldsymbol{k} \cdot \left(-\mathrm{i}\boldsymbol{k}\ \mathrm{e}^{-\mathrm{i}\boldsymbol{k}\cdot\boldsymbol{x}}\right) = -k^2 \mathrm{e}^{-\mathrm{i}\boldsymbol{k}\cdot\boldsymbol{x}}\ .$$

As we know (see Example **(3)** in the Subsection 1.2.1.1) the function (2.13) represents the wavefront of planar optical wave with the normal vector $\boldsymbol{k}$. In an isotropic medium with the refractive index

$$n = \sqrt{\varepsilon\mu} \tag{2.15}$$

we introduce the coordinate system as in the Figure 2.1, where the wave vector $\boldsymbol{k}$ lies in the incidence plane given by this vector and the x_3 axis. Thus, its components are generally functions of the incidence angle φ and the angle ϑ of the incidence plane turning:

$$\boldsymbol{k} = k_0 n(\sin\vartheta \sin\varphi,\ \cos\vartheta \sin\varphi,\ \cos\varphi)^\top\ . \tag{2.16}$$

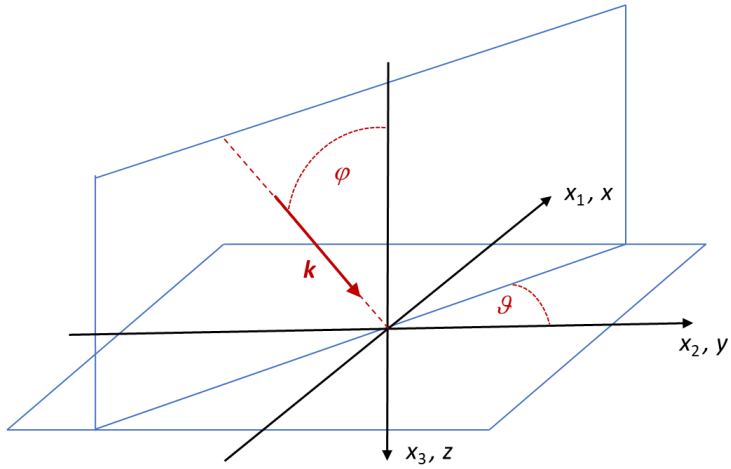

Fig. 2.1 A wave vector in the coordinate system.

This form can be obtained e.g. by successive applying of two rotations $\mathbf{R}_\varphi$, $\mathbf{R}_\vartheta$ (see Example **(b)** in 1.1.2.2) on the basis vector $\mathbf{e}_3$:

$$\boldsymbol{k} = k_0 n\ \mathbf{R}_\vartheta^\top \mathbf{R}_\varphi^\top (0,\ 0,\ 1)^\top\ .$$

As long as optical wave propagates in a lossy medium, where the refractive index becomes complex, its amplitude exponentially decrases that is way we expect a damping in propagation direction. By this reason the imaginary part of refractive index must be negative,

$$n = \nu - \mathrm{i}\kappa\,, \quad \kappa > 0\,. \tag{2.17}$$

If we rewrite corresponding part of exponential factor assuming wave propagation in the increasing x_3 coordinate as

$$\exp\{-\mathrm{i}k_0(\nu-\mathrm{i}\kappa)x_3\cos\varphi\} = \exp\{-k_0\kappa x_3\cos\varphi\}\,\exp\{-\mathrm{i}k_0\nu x_3\cos\varphi\}\ ,$$

then the first right-hand term manifests itself as the amplitude attenuation.

2.1.4 Solution of wave equation

We express the field vector $\boldsymbol{E}$ of planar wave arbitrary medium as

$$\boldsymbol{E} = u\boldsymbol{e}\,\mathrm{e}^{-\mathrm{i}\boldsymbol{k}\cdot\boldsymbol{x}}\ , \tag{2.18}$$

where $\boldsymbol{k} = k_0(\alpha,\,\beta,\,\gamma)$. Further, the vector $\boldsymbol{e}$ represents polarization state of the wave; and, u is the wave amplitude. Seeing that is easy to show that

$$\nabla\times\boldsymbol{e}\mathrm{e}^{-\mathrm{i}\boldsymbol{k}\cdot\boldsymbol{x}} = -\mathrm{i}\,\boldsymbol{k}\times\boldsymbol{e}\mathrm{e}^{-\mathrm{i}\boldsymbol{k}\cdot\boldsymbol{x}}\ ,$$

the wave equation (2.9) takes the simplified form

$$\boldsymbol{k}\times\left[\boldsymbol{\mu}^{-1}(\boldsymbol{k}\times\boldsymbol{e})\right] + k_0^2\boldsymbol{\varepsilon}\,\boldsymbol{e} = \boldsymbol{o}\ . \tag{2.19}$$

The result of Excersise 1.1.5.2 **(4)** enables to write cross product $\boldsymbol{k}\times\bullet$ as multiplication by antisymmetric tensor (matrix)

$$k_0\mathbf{K} = k_0\begin{bmatrix} 0 & -\gamma & \beta \\ \gamma & 0 & -\alpha \\ -\beta & \alpha & 0 \end{bmatrix}\ . \tag{2.20}$$

As the consequence we obtain from (2.19) homogeneous algebraic system for polarization vectors,

$$\left(\mathbf{K}\boldsymbol{\mu}^{-1}\mathbf{K} + \boldsymbol{\varepsilon}\right)\boldsymbol{e} = \boldsymbol{o} \tag{2.21}$$

where the **propagation constants** α, β, γ are the other unknowns. To have non-trivial solutions, the determinant must be equal to zero that leads to the fourth degree algebraic equation for the longitudinal propagation constant γ. The roots γ_q, $q = 1,\ldots,4$ correspond to four **polarization states** represented by their **polarization vectors** $\boldsymbol{e}_q$. The two couples of polarizations differ mutually by the propagation direction that allows distinguish the forward and backward waves. Resulting field of electric intensity is then superposition of the four partial waves

$$\boldsymbol{E} = \sum_{q=1}^{4} u_q\boldsymbol{e}_q\mathrm{e}^{-\mathrm{i}\boldsymbol{k}_q\cdot\boldsymbol{x}} = \sum_{q=1}^{4} u_q\boldsymbol{e}_q\mathrm{e}^{-\mathrm{i}k_0(\alpha x_1+\beta x_2+\gamma_q x_3)}\ . \tag{2.22}$$

The relation between polarization vectors $\boldsymbol{e}$, $\boldsymbol{h}$ follows immediatelly from the first two Maxwell's equations (2.7, 2.8):

$$\boldsymbol{k} \times \boldsymbol{e} = k_0 \sqrt{\mu_0/\varepsilon_0}\ \boldsymbol{\mu}\, \boldsymbol{h}\ , \qquad \boldsymbol{k} \times \boldsymbol{h} = -k_0 \sqrt{\varepsilon_0/\mu_0}\ \boldsymbol{\varepsilon}\, \boldsymbol{e}\,. \tag{2.23}$$

As a consequence we get the structured formula for the magnetic intensity $\boldsymbol{H}$:

$$k_0 \sqrt{\frac{\mu_0}{\varepsilon_0}} \mu \boldsymbol{H} = \boldsymbol{k} \times \boldsymbol{E} = k_0 \sum_{q=1}^{4} u_q \mathbf{K}_q \boldsymbol{e}_q \mathrm{e}^{-\mathrm{i}\boldsymbol{k}_q \cdot \boldsymbol{x}} \tag{2.24}$$

with the matrices $\mathbf{K}_q$ defined by (2.20) with particular propagation constants γ_q.

In the next section we will discuss wave equation solution with regard to the material properties of the media, in which the optical wave propagates.

2.2 Polarization states

2.2.1 Optical waves in an isotropic medium

The described approach does not depend on the orientation of incidence plane, therefore, we can choose this one advantageously at most as possible. In particular, if we take the angle $\vartheta = 0$ in the Figure 2.1, the incidence plane is coincident with the coordinate plane $x_1 = 0$. This implies that

$$\boldsymbol{k} = k_0 (0,\, \beta,\, \gamma)^{\top}\ , \qquad \mathbf{K} = \begin{bmatrix} 0 & -\gamma & \beta \\ \gamma & 0 & 0 \\ -\beta & 0 & 0 \end{bmatrix}\ . \tag{2.25}$$

Since the material characteristics of isotropic media are of the form $\boldsymbol{\varepsilon} = \varepsilon \mathbf{I}$, $\boldsymbol{\mu} = \mu \mathbf{I}$, where $\mathbf{I}$ is the identity matrix, the Eq. (2.21) takes the form

$$\left(\mathbf{K}^2 + \varepsilon\mu \mathbf{I}\right) \boldsymbol{e} = \boldsymbol{o}\ . \tag{2.26}$$

This system has non-trivial solution, only if

$$\det\left(\mathbf{K}^2 + \varepsilon\mu \mathbf{I}\right) = \begin{vmatrix} \varepsilon\mu - \beta^2 - \gamma^2 & 0 & 0 \\ 0 & \varepsilon\mu - \gamma^2 & \beta\gamma \\ 0 & \beta\gamma & \varepsilon\mu - \beta^2 \end{vmatrix} = 0\ , \tag{2.27}$$

i.e., when

$$(\varepsilon\mu - \beta^2 - \gamma^2)^2 = 0\,. \tag{2.28}$$

In lossless media the analysis of two-fold roots couple brings following results, where we set $\varepsilon\mu = n^2$:

- $n^2 - \beta^2 > 0$ gives two real propagation constants

$$\gamma^{(+)} = \sqrt{n^2 - \beta^2}\,, \qquad \gamma^{(-)} = -\sqrt{n^2 - \beta^2}\,, \tag{2.29}$$

- $n^2 - \beta^2 < 0$ leads to imaginary propagation constants that can be written as

$$\gamma^{(+)} = -\mathrm{i}\sqrt{|n^2 - \beta^2|}\,, \qquad \gamma^{(-)} = \mathrm{i}\sqrt{|n^2 - \beta^2|}\,. \tag{2.30}$$

In a lossy medium with non-zero imaginary part of refractive index $n = \sqrt{\varepsilon\mu}$ there the forward wave must have the propagation constant with negative imaginary part – see Subsection 2.1.3. Note, that the upper symbols + and – denote forward and backward wave (it is not the sign of the propagation constant!).

The singular case $\varepsilon\mu - \beta^2 = 0$ means an existence of resonance state that is not discussed.

As the next step we derive polarization vectors related to propagation constants. Putting γ into the matrix of algebraic system (2.26) we get

$$\mathbf{K}^2 + \varepsilon\mu\mathbf{I} \sim \begin{bmatrix} 0 & 0 & 0 \\ 0 & \beta & \gamma \\ 0 & \beta & \gamma \end{bmatrix}. \tag{2.31}$$

Thus, the polarization vectors $\boldsymbol{e} = (e_1,\, e_2,\, e_3)^\top$ appear in the two forms. The choose $e_1 \neq 0$ implies the same solution for the both propagation directions,

$$\boldsymbol{e}_s^{(+)} = \boldsymbol{e}_s^{(-)} = \begin{bmatrix} 1 \\ 0 \\ 0 \end{bmatrix}, \tag{2.32}$$

where the subscript s denotes the ***s*-polarized wave**. In this case the vector $\boldsymbol{E}$ is perpendicular to the incidence plane $x = 0$; we call this wave as **transversal electric** (TE). The second variant $e_1 = 0$ leads to two normed ***p*-polarization states**[1] (**transversal magnetic** T(M) **wave**)

$$\boldsymbol{e}_p^{(+)} = \frac{1}{\sqrt{\varepsilon\mu}} \begin{bmatrix} 0 \\ \gamma^{(+)} \\ -\beta \end{bmatrix}, \qquad \boldsymbol{e}_p^{(-)} = \frac{1}{\sqrt{\varepsilon\mu}} \begin{bmatrix} 0 \\ \gamma^{(-)} \\ -\beta \end{bmatrix}, \tag{2.33}$$

[1] the s, p notation stems from german words *senkrecht* (perpendicular) and *paralel*

for which the intensity $\boldsymbol{E}$ is linearly polarized in the plane $x = 0$. Taking into account that

$$\mathbf{K}\boldsymbol{e} = \sqrt{\mu_0/\varepsilon_0}\ \mu\,\boldsymbol{h}\ , \tag{2.34}$$

the resulting field is transversal magnetic (TM) with the magnetic intensity $\boldsymbol{H}$ perpendicular to the incidence plane. The eigen polarizations of the field $\boldsymbol{H}$ follow from above relations as

$$\frac{1}{\mu}\sqrt{\frac{\varepsilon_0}{\mu_0}}\mathbf{K}_s^{(\pm)}\boldsymbol{e}_s^{(\pm)} = \frac{1}{\mu}\sqrt{\frac{\varepsilon_0}{\mu_0}}\begin{bmatrix} 0 \\ \gamma^{(\pm)} \\ -\beta \end{bmatrix} = \boldsymbol{h}_s^{(\pm)}\ , \tag{2.35}$$

$$\frac{1}{\mu}\sqrt{\frac{\varepsilon_0}{\mu_0}}\mathbf{K}_p^{(\pm)}\boldsymbol{e}_p^{(\pm)} = \frac{1}{\mu}\sqrt{\frac{\varepsilon_0}{\mu_0}}\begin{bmatrix} -\sqrt{\varepsilon\mu} \\ 0 \\ 0 \end{bmatrix} = \boldsymbol{h}_p^{(\pm)}\ . \tag{2.36}$$

Note, that optical wave in a medium with real refractive index n has the wave vector with the transversal components $\alpha = 0$, $\beta = \sin\varphi$. Hence, the longitudinal components are obtained easy as

$$\gamma_{s,p}^{(\pm)} = \pm\, n\cos\varphi\,, \qquad n = \sqrt{\varepsilon\mu} \tag{2.37}$$

that enables to write the polarization vectors (2.33) of TM wave as

$$\boldsymbol{e}_p^{(\pm)} = \begin{bmatrix} 0 \\ \pm\cos\varphi \\ -\sin\varphi \end{bmatrix}\ . \tag{2.38}$$

We can summarize: field vectors in an isotropic medium are expressed by (2.22) as the superposition of the four linearly polarized waves:

$$\begin{aligned}\boldsymbol{E} = \mathrm{e}^{-\mathrm{i}k_0(\alpha x_1+\beta x_2)}\Big[&\left(u_s^{(+)}\boldsymbol{e}_s^{(+)} + u_p^{(+)}\boldsymbol{e}_p^{(+)}\right)\mathrm{e}^{-\mathrm{i}k_0\gamma^{(+)}x_3} + \\ &+ \left(u_s^{(-)}\boldsymbol{e}_s^{(-)} + u_p^{(-)}\boldsymbol{e}_p^{(-)}\right)\mathrm{e}^{-\mathrm{i}k_0\gamma^{(-)}x_3}\Big]\ ,\end{aligned} \tag{2.39}$$

$$\begin{aligned}\boldsymbol{H} = \mathrm{e}^{-\mathrm{i}k_0(\alpha x_1+\beta x_2)}\Big[&\left(u_s^{(+)}\boldsymbol{h}_s^{(+)} + u_p^{(+)}\boldsymbol{h}_p^{(+)}\right)\mathrm{e}^{-\mathrm{i}k_0\gamma^{(+)}x_3} + \\ &+ \left(u_s^{(-)}\boldsymbol{h}_s^{(-)} + u_p^{(-)}\boldsymbol{h}_p^{(-)}\right)\mathrm{e}^{-\mathrm{i}k_0\gamma^{(-)}x_3}\Big]\ .\end{aligned} \tag{2.40}$$

2.2.2 Electrically anisotropic medium

We will analyse the situation, when relative permittivity exhibits natural or artificial anisotropy characterized by the tensor $\boldsymbol{\varepsilon}$ whereas the magnetic permeability μ remains a scalar quantity. Media of this type are called **gyrotropic**; assuming also their magnetically neutral state, we set $\mu = 1$. Under previous considerations the modified wave equation (2.21)

$$\left(\mathbf{K}^2 + \boldsymbol{\varepsilon}\right) \boldsymbol{e} = \boldsymbol{o} \tag{2.41}$$

has non-trivial solution, if

$$\det \begin{bmatrix} \varepsilon_{11} - \beta^2 - \gamma^2 & \varepsilon_{12} & \varepsilon_{13} \\ \varepsilon_{21} & \varepsilon_{22} - \gamma^2 & \varepsilon_{23} + \beta\gamma \\ \varepsilon_{31} & \varepsilon_{32} + \beta\gamma & \varepsilon_{33} - \beta^2 \end{bmatrix} = 0 \ . \tag{2.42}$$

It results in algebraic equation of 4-th degree with generally complex coefficients for the unknown γ:

$$\varepsilon_{33}\gamma^4 + (\varepsilon_{23} + \varepsilon_{32})\gamma^3 - \left[\varepsilon_{22}(\varepsilon_{33} - \beta^2) + \varepsilon_{33}(\varepsilon_{11} - \beta^2) - \varepsilon_{31}\varepsilon_{13} - \varepsilon_{32}\varepsilon_{23}\right]\gamma^2 -$$

$$\beta\left[(\varepsilon_{11} - \beta^2)(\varepsilon_{23} + \varepsilon_{32}) - \varepsilon_{31}\varepsilon_{12} - \varepsilon_{13}\varepsilon_{21}\right]\gamma +$$

$$\varepsilon_{22}\left[(\varepsilon_{11} - \beta^2)(\varepsilon_{33} - \beta^2) - \varepsilon_{31}\varepsilon_{13}\right] - \varepsilon_{12}\varepsilon_{21}(\varepsilon_{33} - \beta^2) - \varepsilon_{32}\varepsilon_{23}(\varepsilon_{11} - \beta^2) +$$

$$\varepsilon_{23}\varepsilon_{31}\varepsilon_{12} + \varepsilon_{32}\varepsilon_{13}\varepsilon_{21} = 0 \ , \tag{2.43}$$

Again, the roots correspond to longitudinal propagation constants in medium with given material properties.

Usually, we meet the natural anisotropy as a property of crystals, for which the permittivity tensor exhibit certain symmetry that simplifies the computation as in the following example.

Example

We consider uniaxial crystal with principal axes identic with coordinate ones. The optical axis lies in the x_2 axis. Thus, the permittivity tensor is diagonal,

$$\boldsymbol{\varepsilon} = \begin{bmatrix} \varepsilon_1 & 0 & 0 \\ 0 & \varepsilon_2 & 0 \\ 0 & 0 & \varepsilon_1 \end{bmatrix} \ . \tag{2.44}$$

Let turn this crystal around the x_3 axis by the angle ϑ. We get new crystal permittivity tensor using the transformation $\mathbf{R}_\vartheta$ (see Figure 2.1):

$$\mathbf{R}_\vartheta \boldsymbol{\varepsilon} \mathbf{R}_\vartheta^\top = \begin{bmatrix} \varepsilon_1 \cos^2\vartheta + \varepsilon_2 \sin^2\vartheta & (\varepsilon_1 - \varepsilon_2)\cos\vartheta \sin\vartheta & 0 \\ (\varepsilon_1 - \varepsilon_2)\cos\vartheta \sin\vartheta & \varepsilon_2 \cos^2\vartheta + \varepsilon_1 \sin^2\vartheta & 0 \\ 0 & 0 & \varepsilon_1 \end{bmatrix} . \tag{2.45}$$

Arising off-diagonal tensor elements enable among other detailed view on the optical birefringence principle that we will demonstrate for the angle $\vartheta = 45°$. If the wave vector lies in the plane $x = 0$, the matrix in Eq. (2.41) takes the form

$$\mathbf{K}^2 + \mathbf{R}_\vartheta \boldsymbol{\varepsilon} \mathbf{R}_\vartheta^\top = \begin{bmatrix} (\varepsilon_1 + \varepsilon_2)/2 - \beta^2 - \gamma^2 & (\varepsilon_1 - \varepsilon_2)/2 & 0 \\ (\varepsilon_1 - \varepsilon_2)/2 & (\varepsilon_1 + \varepsilon_2)/2 - \gamma^2 & \beta\gamma \\ 0 & \beta\gamma & \varepsilon_1 - \beta^2 \end{bmatrix} . \tag{2.46}$$

The condition $\det(\mathbf{K}^2 + \boldsymbol{\varepsilon}) = 0$ leads to algebraic equation

$$\varepsilon_1\gamma^4 - \left[\varepsilon_1(\varepsilon_1 + \varepsilon_2) - (3\varepsilon_1 + \varepsilon_2)\beta^2/2\right] \gamma^2 + (\varepsilon_1 - \beta^2)\left[\varepsilon_1\varepsilon_2 - (\varepsilon_1 + \varepsilon_2)\beta^2/2\right] = 0 , \tag{2.47}$$

the roots of which give longitudinal propagation constants

$$\gamma_{1,2} = \pm\sqrt{\varepsilon_1 - \beta^2} , \qquad \gamma_{3,4} = \pm\sqrt{\varepsilon_2 - \frac{\varepsilon_1 + \varepsilon_2}{2\varepsilon_1}\beta^2} . \tag{2.48}$$

Polarization vectors of the field $\boldsymbol{E}$ are obtained as the solution of homogeneous system with the matrix (2.46):

$$\boldsymbol{e}_1 = \begin{bmatrix} \gamma_1 \\ \gamma_1 \\ -\beta \end{bmatrix} , \quad \boldsymbol{e}_2 = \begin{bmatrix} -\gamma_1 \\ -\gamma_1 \\ -\beta \end{bmatrix} , \quad \boldsymbol{e}_3 = \begin{bmatrix} \varepsilon_1 \\ -\gamma_1^2 \\ \beta\gamma_3 \end{bmatrix} , \quad \boldsymbol{e}_4 = \begin{bmatrix} \varepsilon_1 \\ -\gamma_1^2 \\ -\beta\gamma_3 \end{bmatrix} . \tag{2.49}$$

Polarization states of the field $\boldsymbol{H}$ follow from the relation $\boldsymbol{h} = \sqrt{\varepsilon_0/\mu_0}\mathbf{K}\boldsymbol{e}$ (the vacuum impedance factor is suppressed):

$$\boldsymbol{h}_1 = \begin{bmatrix} -\varepsilon_1 \\ \gamma_1^2 \\ -\beta\gamma_1 \end{bmatrix} , \quad \boldsymbol{h}_2 = \begin{bmatrix} -\varepsilon_1 \\ \gamma_1^2 \\ \beta\gamma_1 \end{bmatrix} , \quad \boldsymbol{h}_3 = \begin{bmatrix} \varepsilon_1\gamma_3 \\ \varepsilon_1\gamma_3 \\ -\varepsilon_1\beta \end{bmatrix} , \quad \boldsymbol{h}_4 = \begin{bmatrix} -\varepsilon_1\gamma_3 \\ -\varepsilon_1\gamma_3 \\ -\varepsilon_1\beta \end{bmatrix} , \tag{2.50}$$

2.2.3 Polarization states in magnetooptics

In a ferromagnetic materials the anisotropy of permittivity can be induced by external magnetic field that influences polarization states of light beam propagating through the media. This phenomena is said to be **Kerr effect** in the reflected field or **Faraday effect** for the transmitted wave. The permittivity tensor components are represented by the expansion

$$\varepsilon_{ij} = \varepsilon_{ij}^{[0]} + \left[\frac{\partial \varepsilon_{ij}}{\partial M_k}\right]_{\boldsymbol{M}=\boldsymbol{o}} M_k + \frac{1}{2}\left[\frac{\partial^2 \varepsilon_{ij}}{\partial M_k \partial M_l}\right]_{\boldsymbol{M}=\boldsymbol{o}} M_k M_l + \cdots \,, \tag{2.51}$$

where $\boldsymbol{M} = (M_1,\, M_2,\, M_3)$ is the magnetization vector. If we restrict to linear and quadratic effects, then

$$\boldsymbol{\varepsilon} = \boldsymbol{\varepsilon}^{[0]} + \boldsymbol{\varepsilon}^{[1]} + \boldsymbol{\varepsilon}^{[2]} \,, \tag{2.52}$$

where

$$\varepsilon_{ij}^{[0]} = \delta_{ij}\varepsilon \,, \qquad \varepsilon_{ij}^{[1]} = K_{ijk} M_k \,, \qquad \varepsilon_{ij}^{[2]} = G_{ijkl} M_k M_l \,. \tag{2.53}$$

The first term corresponds to non-magnetized (i.e. isotropic) state. The third and four rank tensors $\mathbf{K}$, $\mathbf{G}$, respectively, are introduced for the linear and quadratic MO effects.

In practice, there are magnetooptical characteristics depending on experimental methods used to their derivation. Typically, we meet the **Voigt parameter** Q in linear magnetooptics; and, the **Lissberger parameter** f by quadratic effects. For more detailled discussion see e.g. [3, 5, 6, 7]. Here, we confine ourself to the cubic crystals because of highest symmetry. It can be shown that first order anisotropy is described by antisymmetric second rank tensor

$$\varepsilon_{ij}^{[1]} = \mathrm{i}\, \varepsilon \epsilon_{ijk} Q_k \,, \qquad Q_k = Q \frac{M_k}{M_s} \,, \tag{2.54}$$

where ϵ_{ijk} is the Levi-Civita tensor; and, M_s is saturated magnetization. If the magnetization vector $\boldsymbol{M}$ is oriented in the direction of some coordinate axis, the second order term can be written as

$$\varepsilon_{ij}^{[2]} = f \varepsilon \delta_{ij} (\delta_{kk} - \delta_{ik}) Q_k^2 \,. \tag{2.55}$$

Resulting formula for the tensor (2.52) is obtained in the form

$$\varepsilon_{ij} = \varepsilon \left[\delta_{ij} + \mathrm{i}\epsilon_{ijk} Q_k + f \delta_{ij} (\delta_{kk} - \delta_{ik}) Q_k^2\right] \,. \tag{2.56}$$

The triad "incidence plane – interface – magnetization vector" determines uniquelly a **configuration of magneto-optical effect**. Conventionally,

three basic types are used for experimental procedures called as polar, longitudinal and transversal. Their definition is obvious from the Fig. 2.2, where the incident and reflected beam lie in the plane $x = 0$; and, magnetization vector $\boldsymbol{M} = (M_1, M_2, M_3)$ is parallel to several coordinate axis.

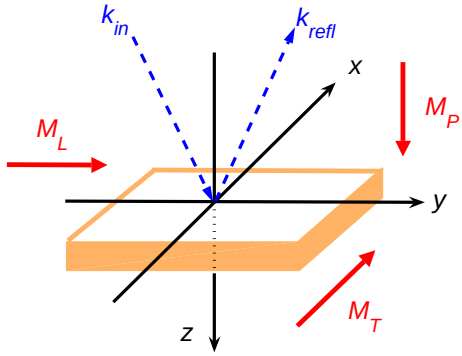

Fig. 2.2 Basic magneto-optical configurations.

The permittivity tensor is of specific form in any case as presented bellow in the linear approximation [8].

(a) Polar configuration: $\boldsymbol{M_P} = (0,\, 0,\, M_3)$:

$$\hat{\boldsymbol{\varepsilon}}_P = \begin{bmatrix} \varepsilon & \mathrm{i}\varepsilon_P & 0 \\ -\mathrm{i}\varepsilon_P & \varepsilon & 0 \\ 0 & 0 & \varepsilon \end{bmatrix} . \tag{2.57}$$

(b) Longitudinal configuration: $\boldsymbol{M_L} = (0,\, M_2,\, 0)$:

$$\hat{\boldsymbol{\varepsilon}}_L = \begin{bmatrix} \varepsilon & 0 & -\mathrm{i}\varepsilon_L \\ 0 & \varepsilon & 0 \\ \mathrm{i}\varepsilon_L & 0 & \varepsilon \end{bmatrix} . \tag{2.58}$$

(c) Transversal configuration: $\boldsymbol{M_T} = (M_1,\, 0,\, 0)$:

$$\hat{\boldsymbol{\varepsilon}}_T = \begin{bmatrix} \varepsilon & 0 & 0 \\ 0 & \varepsilon & \mathrm{i}\varepsilon_T \\ 0 & -\mathrm{i}\varepsilon_T & \varepsilon \end{bmatrix} . \tag{2.59}$$

From the practical point of view, one is suitable to introduce the Voigt magneto-optical parameter as

$$Q_k = \frac{\varepsilon_k}{\varepsilon}\,, \qquad k = T,\, P,\, L \tag{2.60}$$

indexed in agreement with actual MO configuration.

2.2.3.1 Transversal configuration

The bi-quadratic equation (2.43) is reduced to more simple form

$$[\gamma^2 - (\varepsilon - \beta^2)][\varepsilon\gamma^2 - \varepsilon(\varepsilon - \beta^2) + \varepsilon_T^2] = 0\,. \tag{2.61}$$

Resolving this one we obtain four roots

$$\begin{aligned} \gamma_1^{\pm} &= \pm\sqrt{\varepsilon - \beta^2}, \\ \gamma_2^{\pm} &= \pm\sqrt{\varepsilon\,(1 - Q_T^2) - \beta^2}, \end{aligned} \tag{2.62}$$

for which we can briefly write

$$\gamma_1 = \gamma_1^{+} = -\gamma_1^{-}, \quad \gamma_2 = \gamma_2^{+} = -\gamma_2^{-}\,. \tag{2.63}$$

In the case of electric intensity field, the polarization vectors of forward modes result as

$$\boldsymbol{e}_1 = \begin{bmatrix} 1 \\ 0 \\ 0 \end{bmatrix} \quad (s-\text{polarization}), \qquad \boldsymbol{e}_3 = \begin{bmatrix} 0 \\ \varepsilon - \beta^2 \\ \mathrm{i}\varepsilon Q_T - \beta\gamma_2 \end{bmatrix} \quad (p-\text{polarization}). \tag{2.64}$$

2.2.3.2 Polar configuration

We put elements of the tensor $\hat{\boldsymbol{\varepsilon}}_P$ into characteristic equation (2.43).The rearranged form

$$\varepsilon\gamma^4 - 2\varepsilon(\varepsilon - \beta^2)\gamma^2 + (\varepsilon - \beta^2)[\varepsilon(\varepsilon - \beta^2) - \varepsilon_P^2] = 0 \tag{2.65}$$

gives propagation constants

$$\begin{aligned} \gamma_1^{\pm} &= \pm\sqrt{\varepsilon - \beta^2 - Q_P\sqrt{(\varepsilon - \beta^2)\varepsilon}}\,, \\ \gamma_2^{\pm} &= \pm\sqrt{\varepsilon - \beta^2 + Q_P\sqrt{(\varepsilon - \beta^2)\varepsilon}}\,, \end{aligned} \tag{2.66}$$

for which we write similarly as in the previous case

$$\gamma_1 = \gamma_1^+ = -\gamma_1^-, \quad \gamma_2 = \gamma_2^+ = -\gamma_2^- \ . \tag{2.67}$$

Corresponding polarization vectors of forward modes have the components

$$\boldsymbol{e}_1 = \begin{bmatrix} -\mathrm{i}\varepsilon Q_P(\varepsilon - \beta^2) \\ (\varepsilon - \beta^2)(\varepsilon - \beta^2 - \gamma_1^2) \\ -\beta\gamma_1(\varepsilon - \beta^2 - \gamma_1^2) \end{bmatrix}, \qquad \boldsymbol{e}_3 = \begin{bmatrix} -\mathrm{i}\varepsilon Q_P(\varepsilon - \beta^2) \\ (\varepsilon - \beta^2)(\varepsilon - \beta^2 - \gamma_2^2) \\ -\beta\gamma_2(\varepsilon - \beta^2 - \gamma_2^2) \end{bmatrix}. \tag{2.68}$$

2.2.3.3 Longitudinal configuration

Linear magnetization effect in a layer with longitudinal geometry leads to the permittivity tensor (2.58). Putting its components into (2.43) we obtain bi-quadratic equation

$$\varepsilon\gamma^4 - [2\varepsilon(\varepsilon - \beta^2) - \varepsilon_L^2]\,\gamma^2 + \varepsilon((\varepsilon - \beta^2)^2 - \varepsilon_L^2) = 0 \ , \tag{2.69}$$

the roots of which give propagation constants of the form

$$\begin{aligned} \gamma_1^2 &= \varepsilon - \beta^2 - \tfrac{1}{2}Q_L\left(\varepsilon_L + \sqrt{4\beta^2\varepsilon + \varepsilon_L^2}\right) \ , \\ \gamma_2^2 &= \varepsilon - \beta^2 - \tfrac{1}{2}Q_L\left(\varepsilon_L - \sqrt{4\beta^2\varepsilon + \varepsilon_L^2}\right) \ . \end{aligned} \tag{2.70}$$

Supposing $2\varepsilon(\varepsilon - \beta^2) >> \varepsilon_L^2$ these can be approximated as

$$\begin{aligned} \gamma_1^2 &\approx \varepsilon - \beta^2 + \beta\varepsilon_L/\sqrt{\varepsilon}, \\ \gamma_2^2 &\approx \varepsilon - \beta^2 - \beta\varepsilon_L/\sqrt{\varepsilon} \ . \end{aligned} \tag{2.71}$$

Using again the notation (2.67) the forward modes are characterized by polarization vectors

$$\boldsymbol{e}_1 = \begin{bmatrix} \mathrm{i}\varepsilon_L\beta\gamma_1 \\ (\varepsilon - \beta^2)(\varepsilon - \beta^2 - \gamma_1^2) - \varepsilon_L^2 \\ -\beta\gamma_1(\varepsilon - \beta^2 - \gamma_1^2) \end{bmatrix}, \quad \boldsymbol{e}_3 = \begin{bmatrix} \mathrm{i}\varepsilon_L\beta\gamma_2 \\ (\varepsilon - \beta^2)(\varepsilon - \beta^2 - \gamma_2^2) - \varepsilon_L^2 \\ -\beta\gamma_2(\varepsilon - \beta^2 - \gamma_2^2) \end{bmatrix}. \tag{2.72}$$

2.2.4 Representation of polarization states

The end-point of the intensity vector $\boldsymbol{E}$ periodically copies an ellipse (or a circle or a line segment) in the plane perpendicular to the wave vector $\boldsymbol{k}$ with the centre located on a line having the direction of $\boldsymbol{k}$. We introduce the **polarization angles** in the local coordinate system $[\xi, \eta]$ as the **rotation** θ and **ellipticity** ϵ – see Figure 2.3a.

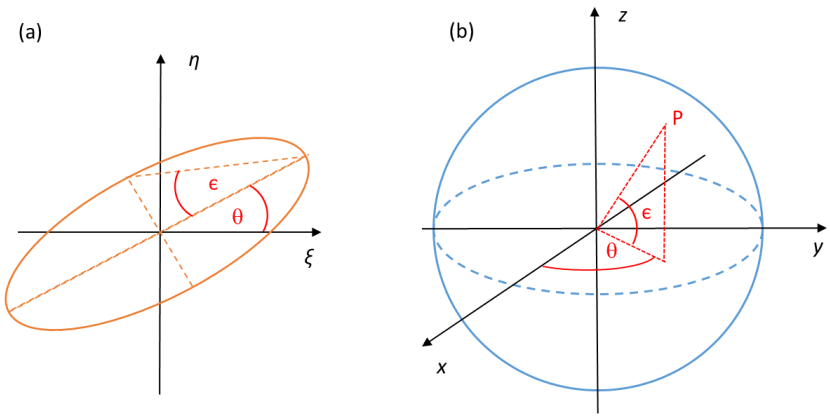

Fig. 2.3 (a) Local coordinate system and ellipsometric angles in a plane perpendicular to wave vector. (b) Coordinates at the Poincaré sphere.

Denote $\chi = e_2/e_1$ for a polarization vector $\boldsymbol{e} = (e_1, e_2, e_3)$. Then the angles θ, ϵ are given as [9]

$$\theta = \frac{1}{2}\text{arctg}\,\frac{2\text{Re}\,(\chi)}{1-|\chi|^2}\,, \qquad \epsilon = \frac{1}{2}\arcsin\frac{2\text{Im}\,(\chi)}{1+|\chi|^2}\,. \tag{2.73}$$

An excellent way to visualize polarized light is representation of polarization state on the **Poincaré sphere** (Fig. 2.3b) [10]. Here P is a point on the surface of the sphere that correspond to the polarization state characterized by the couple (θ, ϵ). For the unit sphere the Cartesian coordinates x, y, z are related to the spherical angles by the equations

$$x = \cos\epsilon\,\cos\theta, \tag{2.74}$$

$$y = \cos\epsilon\,\sin\theta, \tag{2.75}$$

$$z = \sin\epsilon, \tag{2.76}$$

where $-\pi/2 \le \epsilon \le \pi/2$, $0 \le \theta \le 2\pi$. All linear polarization states lie on the equator and right and left circular polarization states are at the north

and south poles, respectively. Elliptically polarized states are represented everywhere else on the surface of the sphere.

We can also realize particular polarization state $\boldsymbol{e}$ as a spatial parametrization of ellipse with the centre at the point [0, 0, 0],

$$\boldsymbol{\psi}(\tau) = \mathrm{Re}\left(\boldsymbol{e}\,\mathrm{e}^{\mathrm{i}\tau}\right) = \begin{bmatrix} x(\tau) \\ y(\tau) \\ z(\tau) \end{bmatrix}, \quad \tau \in \langle 0,\, 2\pi \rangle\ . \tag{2.77}$$

If we use normed vectors, we get an efficient method to comparison of wave eigen polarizations in an anisotropic medium. Let us add that application of the imaginary part of the above relation gives the same ellipse with phase shift $\pi/2$ in variable τ.

Example

As an illustration we discuss polarization states of monochromatic light beam of wavelength $\lambda = 632.8$ nm impinging from the air under the angle φ into amorphous iron, i.e., into lossy medium with refractive index $n = 2.85 - 3.36\mathrm{i}$ and Voigt magneto-optical parameter $Q = 0.054 + 0.004\mathrm{i}$ [6]. To have the full picture, let us note that the values of the Voigt magneto-optical parameter in fact slightly differ for the individual magneto-optical configurations, as the above mentioned formulas among others indicate. This fact is nevertheless not taken into account in the problems presented herein.

We obtain specific results in the case of transversal configuration (Fig. 2.4). One of the waves is linearly polarized in the x axis direction, while the other shows elliptical polarization in the plane perpendicular to it. The next Figure 2.5 demonstrates the output in polar configuration for the angle $\varphi = 60°$; and, longitudinal configuration by the incidence angle $\varphi = 30°$ (Fig. 2.6) is the last variant.

2.2.5 Medium with both electric and magnetic anisotropy

In a bi-anisotropic medium we can observe a common action of electric and magnetic field to magnetic induction. It means that relative permittivity and relative permeability $\boldsymbol{\varepsilon}$, $\boldsymbol{\mu}$ are described by the tensors (2.2). Search for such solution is generally quite complicated especially due to the inverse of permeability matrix. As a demonstration of relatively simple case we present polar configuration in a cubic bi-gyrotropic crystal. The both material tensors are

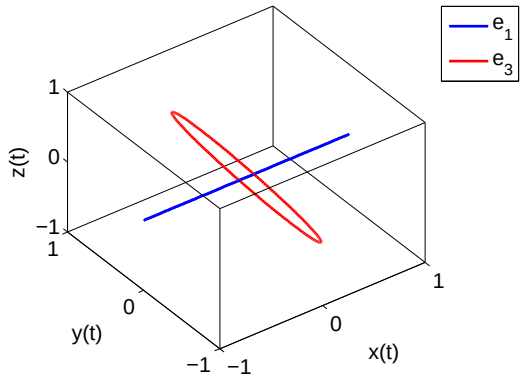

Fig. 2.4 Polarization curves in transversal configuration ($\varphi = 60°$).

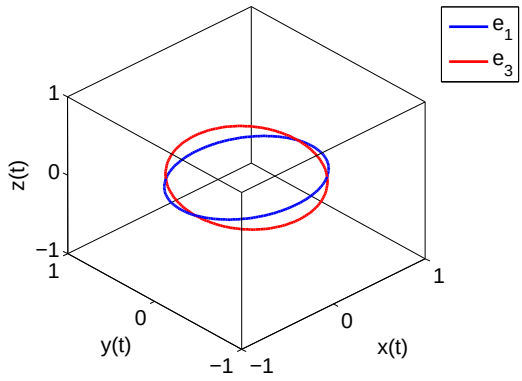

Fig. 2.5 Polarization ellipses in polar configuration ($\varphi = 60°$).

of the similar structure,

$$\boldsymbol{\varepsilon} = \varepsilon \begin{bmatrix} 1 & \mathrm{i}Q_\varepsilon & 0 \\ -\mathrm{i}Q_\varepsilon & 1 & 0 \\ 0 & 0 & 1 \end{bmatrix}, \qquad \boldsymbol{\mu} = \mu \begin{bmatrix} 1 & \mathrm{i}Q_\mu & 0 \\ -\mathrm{i}Q_\mu & 1 & 0 \\ 0 & 0 & 1 \end{bmatrix}. \tag{2.78}$$

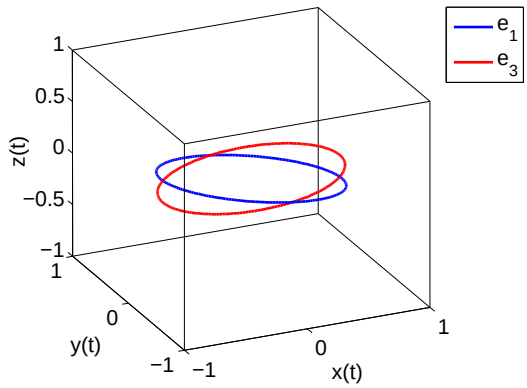

Fig. 2.6 Polarization ellipses in longitudinal configuration ($\varphi = 30°$).

The matrix $\mathbf{K}\boldsymbol{\mu}^{-1}\mathbf{K} + \boldsymbol{\varepsilon}$ is obtained in the form

$$\begin{bmatrix} (\varepsilon\mu^3 - \beta^2)\left(1 - Q_\mu^2\right) - \gamma^2 & \mathrm{i}\left[\varepsilon\mu^3 Q_\varepsilon\left(1 - Q_\mu^2\right) + \gamma^2 Q_\mu\right] & -\mathrm{i}\beta\gamma Q_\mu \\ \mathrm{i}\left[\varepsilon\mu^3 Q_\varepsilon\left(1 - Q_\mu^2\right) + \gamma^2 Q_\mu\right] & \varepsilon\mu^3\left(1 - Q_\mu^2\right)\big) - \gamma^2 & \beta\gamma \\ \mathrm{i}\beta\gamma Q_\mu & \beta\gamma & \varepsilon\mu^3\left(1 - Q_\mu^2\right) - \beta^2 \end{bmatrix}, \tag{2.79}$$

from which we find the longitudinal propagation constants in the compact notation

$$\gamma_q = (-1)^{q-1}\left[\left(\sqrt{\varepsilon\mu - \beta^2} - (-1)^s Q_\varepsilon\sqrt{\varepsilon\mu}\right)\left(\sqrt{\varepsilon\mu - \beta^2} - (-1)^s Q_\mu\sqrt{\varepsilon\mu}\right)\right]^{\frac{1}{2}}, \tag{2.80}$$

where $q = 1, \ldots, 4$, $s = q(q+1)/2$. Putting $\mu = 1$ a $Q_\mu = 0$ these result become the form of (2.66) for gyrotropic medium. Note that the parameter Q_μ is in two or three orders less that Voigt parameter Q_ε.

2.2.6 Excersise

2.2.6.1

Set $\varepsilon_1 = \varepsilon_T = \varepsilon_L$. Find orthogonal matrix (rotation) that transforms permittivity tensor of polar MO configuration in the longitudinal one.

2.2.6.2

Demonstrate graphically the normed polarization states $\boldsymbol{e}_1$ a $\boldsymbol{e}_3$ excited in the rutile crystal (titanium oxide, TiO_2) by monochromatic light beam under following conditions:

- optical configuration as in the Example in the Subsection 2.2.2;
- incidence angle $\varphi = 60°$;
- wavelength $\lambda = 335.14$ nm (3.70 eV);
- ordinary beam refractive index $n_o = 3.65 - 0.81\mathrm{i}$ [11];
- extra-ordinary beam refractive index $n_e = 4.10 - 1.25\mathrm{i}$ [11].

Remark: this is not diffraction problem, that is why $\beta = n \sin \varphi$ changes regarding the refractive index n as $\varepsilon_1 = n_o^2$, $\varepsilon_2 = n_e^2$.

Chapter 3

Optical Waves in Multilayers

3.1 Waves at single planar interface

3.1.1 Boundary conditions

Consider planar interface between two homogeneous regions characterized by relative permittivities $\varepsilon^{(0)}$, $\varepsilon^{(1)}$ and relative permeabilities $\mu^{(0)}$, $\mu^{(1)}$. Monochromatic incident light beam comes from superstrate characterized by the wave vector $\boldsymbol{k}^{(0+)}$ in the incidence plane $x = 0$ under the incidence angle $\varphi^{(0)}$. On the interface, the wave is partially reflected back in superstrate with the wave vector $\boldsymbol{k}^{(0-)}$, and, partially refracted into the substrate with the wave vector $\boldsymbol{k}^{(1+)}$ under the angle $\varphi^{(1)}$ – see Figure 3.1.

In the Subsection 1.2.4.3 we derived general boundary conditions (**??**), (**??**) for the electric and magnetic intensities on a smooth interface with the normal vetor $\boldsymbol{\nu}$ in the form

$$\boldsymbol{\nu} \times (\boldsymbol{E}^{(0)} - \boldsymbol{E}^{(1)}) = \boldsymbol{o}\,, \tag{3.1}$$

$$\boldsymbol{\nu} \times (\boldsymbol{H}^{(0)} - \boldsymbol{H}^{(1)}) = \boldsymbol{o}\,. \tag{3.2}$$

In the situation by the Figure 3.1 the boundary conditions take the simple form

$$E_x^{(0)} = E_x^{(1)}\,, \quad E_y^{(0)} = E_y^{(1)}\,, \tag{3.3}$$

$$H_x^{(0)} = H_x^{(1)}\,, \quad H_y^{(0)} = H_y^{(1)}\,. \tag{3.4}$$

Above conditions must be fullfiled for instantaneous field vectors values with the **time factor** $\mathrm{e}^{\mathrm{i}\omega t}$. It means that the frequency ω is the same for refracted as well as reflected wave. Besides this evident requirement the conditions hold at arbitrary border point characterized by position vector $\boldsymbol{r} = (x, y, z)$ that implies

$$(\boldsymbol{k}^{(0)} - \boldsymbol{k}^{(1)}) \cdot \boldsymbol{r} = 0\,. \tag{3.5}$$

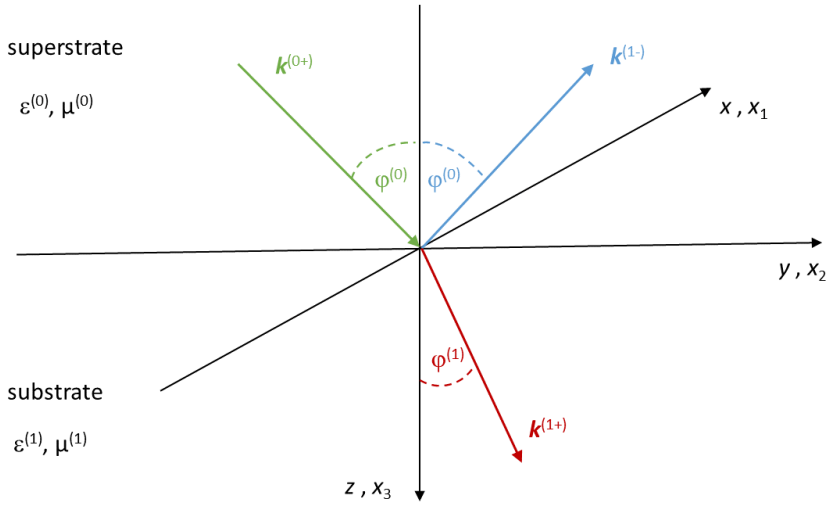

Fig. 3.1 Optical wave diffraction at planar interface.

This relation motivates to several important conclusions. At first, the all three vectors $\boldsymbol{k}^{(0+)}$, $\boldsymbol{k}^{(0-)}$, $\boldsymbol{k}^{(1+)}$ lie in the incidence plane. Further,

(i) the reflection angle equals to the incidence angle because of

$$(\boldsymbol{k}^{(0+)} - \boldsymbol{k}^{(0-)}) \cdot \boldsymbol{r} = 0 \; ;$$

(ii) the variant $(\boldsymbol{k}^{(0+)} - \boldsymbol{k}^{(1+)}) \cdot \boldsymbol{r} = 0$ implies the well-known **Snell law**

$$n^{(0)} \sin \varphi^{(0)} = n^{(1)} \sin \varphi^{(1)} \; . \tag{3.6}$$

In the sense of the last relation the tangential components of wave vector are preserved by the interface throughpass. Since

$$\alpha = \alpha^{(0)} = 0 \, , \quad \beta = \beta^{(0)} = n^{(0)} \sin \varphi^{(0)} \; , \quad n^{(0)} = \sqrt{\varepsilon^{(0)} \mu^{(0)}} \; , \tag{3.7}$$

it suffices to write **wave vectors** in the both media as

$$\boldsymbol{k}^{(\kappa)} = k_0 (0, \, \beta, \, \gamma^{(\kappa)})^\top \; , \quad \kappa = 0, \, 1 \tag{3.8}$$

instead $\boldsymbol{k}^{(\kappa)} = k_0 (\alpha^{(\kappa)}, \, \beta^{(\kappa)}, \, \gamma^{(\kappa)})^\top$.

In order to describe properties of the far field, when $r = \|\boldsymbol{r}\| \to \infty$, the **Sommerfeld radiation conditions** are used in isotropic semi-infinite regions:

$$\lim_{r\to\infty} r^{s/2}\left(\frac{\partial \boldsymbol{E}}{\partial r} - \mathrm{i}k_0\sqrt{\varepsilon\mu}\boldsymbol{E}\right) = \boldsymbol{o}\,, \quad \lim_{r\to\infty} r^{s/2}\left(\frac{\partial \boldsymbol{H}}{\partial r} - \mathrm{i}k_0\sqrt{\varepsilon\mu}\boldsymbol{H}\right) = \boldsymbol{o}\,, \tag{3.9}$$

where $s = 1$ in the two-dimensional case; and, $s = 2$ in the 3D problems.

3.1.2 Wave coupling principle

The intensity fields $\boldsymbol{E}$ and $\boldsymbol{H}$ are composed of the four linearly polarized fields as it has been showed in the Subsection 2.1.4 that are called the optical modes. In agreement with (2.22) we can write

$$\boldsymbol{E}^{(\kappa)} = \mathrm{e}^{-\mathrm{i}k_0\beta y}\sum_{q=1}^{4} u_q^{(\kappa)}\boldsymbol{e}_q^{(\kappa)}\mathrm{e}^{-\mathrm{i}k_0\gamma_q^{(\kappa)}z}\,, \tag{3.10}$$

$$\boldsymbol{H}^{(\kappa)} = \mathrm{e}^{-\mathrm{i}k_0\beta y}\frac{1}{\mu^{(\kappa)}}\sqrt{\frac{\varepsilon_0}{\mu_0}}\sum_{q=1}^{4} u_q^{(\kappa)}\boldsymbol{h}_q^{(\kappa)}\mathrm{e}^{-\mathrm{i}k_0\gamma_q^{(\kappa)}z}\,, \tag{3.11}$$

where we suppose that the polarization vectors are normed in the field $\boldsymbol{E}$ – see (2.32) ,(2.33). Further, we are going to usual assumption of magnetically neutral materials, for which $\mu^{(\kappa)} = 1$.

We organize the modes in (3.10), (3.11) so that the forward modes correspond to the indices $q = 1$, 3, the backward modes are indexed by $q = 2$, 4. To unique specification of fields $\boldsymbol{E}^{(\kappa)}$ and $\boldsymbol{H}^{(\kappa)}$ we must find also amplitude coefficients $u_q^{(\kappa)}$ belonging to the eigen-polarizations $\boldsymbol{e}_q^{(\kappa)}$, $\boldsymbol{h}_q^{(\kappa)}$. To this purpose we apply the boundary conditions (3.3), (3.4) to the tangential components E_j, H_j, $j = 1, 2$. On the boundary $z = 0$ we obtain the four algebraic equation system

$$\sum_{q=1}^{4} u_q^{(0)} e_{jq}^{(0)} = \sum_{q=1}^{4} u_q^{(1)} e_{jq}^{(1)}\,, \tag{3.12}$$

$$\sum_{q=1}^{4} u_q^{(0)} h_{jq}^{(0)} = \sum_{q=1}^{4} u_q^{(1)} h_{jq}^{(1)}\,. \tag{3.13}$$

Remind that $\boldsymbol{E} = (E_1, 0, 0)$, $\boldsymbol{H} = (0, H_2, H_3)$ for the TE field (s-polarization) whereas $\boldsymbol{E} = (0, E_2, E_3)$, $\boldsymbol{H} = (H_1, 0, 0)$ hold for the TM field (p-polarization) by incident wave in the $x = 0$ plane. To differentiate the s- and p-polarized states in above system we write the first two equations for the components e_{1q} a h_{2q} while the equations with the components e_{2q} and h_{1q}

are written as the third and fourth ones. Further, we use the polarization type specification s/p together with sign of propagation direction instead the index q. The structure of rearranged system is obvious from its matrix notation:

$$\mathbf{D}^{(0)}\boldsymbol{u}^{(0)} = \mathbf{D}^{(1)}\boldsymbol{u}^{(1)} \ , \tag{3.14}$$

where

$$\mathbf{D}^{(\kappa)} = \begin{bmatrix} e_{1s}^{(\kappa+)} & e_{1s}^{(\kappa-)} & e_{1p}^{(\kappa+)} & e_{1p}^{(\kappa-)} \\ h_{2s}^{(\kappa+)} & h_{2s}^{(\kappa-)} & h_{2p}^{(\kappa+)} & h_{2p}^{(\kappa-)} \\ e_{2s}^{(\kappa+)} & e_{2s}^{(\kappa-)} & e_{2p}^{(\kappa+)} & e_{2p}^{(\kappa-)} \\ h_{1s}^{(\kappa+)} & h_{1s}^{(\kappa-)} & h_{1p}^{(\kappa+)} & h_{1p}^{(\kappa-)} \end{bmatrix} , \quad \boldsymbol{u}^{(\kappa)} = \begin{bmatrix} u_s^{(\kappa+)} \\ u_s^{(\kappa-)} \\ u_p^{(\kappa+)} \\ u_p^{(\kappa-)} \end{bmatrix} , \quad \kappa = 0, 1 \ . \tag{3.15}$$

In this way we have build **polarization matrices** $\mathbf{D}^{(\kappa)}$ that are frequently refered as **dynamical** ones.

As a rule the amplitude coefficients $u_s^{(0+)}$ or $u_p^{(0+)}$ of incident beam are known, so that this wave has one of the two principal linear polarizations. It means that the vector of amplitude coefficients in the superstrate takes one of the forms

$$\boldsymbol{u}_s^{(0)} = \begin{bmatrix} u_s^{(0+)} \\ u_{ss}^{(0-)} \\ 0 \\ u_{sp}^{(0-)} \end{bmatrix} , \qquad \boldsymbol{u}_p^{(0)} = \begin{bmatrix} 0 \\ u_{ps}^{(0-)} \\ u_p^{(0+)} \\ u_{pp}^{(0-)} \end{bmatrix} . \tag{3.16}$$

In the substrate we suppose only forward modes because no wave enters in the opposite direction to incident wave:

$$\boldsymbol{u}_s^{(1)} = \begin{bmatrix} u_{ss}^{(1+)} \\ 0 \\ u_{sp}^{(1+)} \\ 0 \end{bmatrix} , \qquad \boldsymbol{u}_p^{(1)} = \begin{bmatrix} u_{ps}^{(1+)} \\ 0 \\ u_{pp}^{(1+)} \\ 0 \end{bmatrix} . \tag{3.17}$$

Here, the first lower index denotes the incident wave polarization, whereas the second one relates to coefficients position in the vector $\boldsymbol{u}^{(\kappa)}$ by (3.15). The polarization states with mixed indices sp or ps correspond to the so called **hybrid modes** that take place namely in anisotropic media.

We obtain an efficient algorithm to solve the problem (3.14) when divide the polarization matrices $\mathbf{D}^{(0)}$ and $\mathbf{D}^{(1)}$ into four blocks as

$$\begin{bmatrix} \mathbf{D}_{ss}^{(0)} & \mathbf{D}_{ps}^{(0)} \\ \mathbf{D}_{sp}^{(0)} & \mathbf{D}_{pp}^{(0)} \end{bmatrix} \boldsymbol{u}^{(0)} = \begin{bmatrix} \mathbf{D}_{ss}^{(1)} & \mathbf{D}_{ps}^{(1)} \\ \mathbf{D}_{sp}^{(1)} & \mathbf{D}_{pp}^{(1)} \end{bmatrix} \boldsymbol{u}^{(1)} , \tag{3.18}$$

where the vectors of amplitude coefficients correspond to the incidence wave polarization.

In the both cases we seek for the four unknown with double lower index. Recall relevant optical applications, in which the amplitude coefficients play a key role. At the first place there are **Fresnel reflection and transmission coefficients** that we write here in the general form:

$$r_{ss} = \frac{u_{ss}^{(0-)}}{u_s^{(0+)}} , \quad r_{sp} = \frac{u_{sp}^{(0-)}}{u_s^{(0+)}} \quad \text{by the } s-\text{polarized input} \quad (u_p^{(0+)} = 0) , \tag{3.19}$$

$$r_{ps} = \frac{u_{ps}^{(0-)}}{u_p^{(0+)}} , \quad r_{pp} = \frac{u_{pp}^{(0-)}}{u_p^{(0+)}} \quad \text{by the } p-\text{polarized input} \quad (u_s^{(0+)} = 0) . \tag{3.20}$$

In case of transmission coefficients the notation is analogous:

$$t_{ss} = \frac{u_{ss}^{(1+)}}{u_s^{(0+)}} , \quad t_{sp} = \frac{u_{sp}^{(1+)}}{u_s^{(0+)}} , \quad t_{ps} = \frac{u_{ps}^{(1+)}}{u_p^{(0+)}} , \quad t_{pp} = \frac{u_{pp}^{(1+)}}{u_p^{(0+)}} . \tag{3.21}$$

Reflection coefficients knowledge allows us to estimate another optical characteristics. Among typical experimental techniques based on polarization states the **optical ellipsometry** is of importance. It consist in an analysis of the reflection coefficients quotient

$$\rho = \frac{r_{pp}}{r_{ss}} = \operatorname{tg}\psi \, \mathrm{e}^{\mathrm{i}\Delta} . \tag{3.22}$$

From this formula we obtain definition relations of **ellipsometric angles** ψ and Δ that express relative changes of the optical wave amplitude and phase:

$$\psi = \operatorname{arctg} \left| \frac{r_{pp}}{r_{ss}} \right| , \qquad \Delta = \arg \left(\frac{r_{pp}}{r_{ss}} \right) . \tag{3.23}$$

Ellipsometrical outputs are frequently presented in the form $\tan\psi$ and $\cos\Delta$.

In magnetooptics, the external magnetic field invokes induced anisotropy in ferromagnetic materials that express itself in a change of polarization state of optical beam (see the Section 2.2.3). The geometrical parameters θ and ϵ of polarization ellipse introduced by (2.73) in the previous chapter achieve here

quite poor values that enables to represent these **magnetooptical angles** with the help of reflection coefficients as

$$\begin{aligned} \theta_s &= -\,\mathrm{Re}\left(\frac{r_{sp}}{r_{ss}}\right), & \epsilon_s &= -\,\mathrm{Im}\left(\frac{r_{sp}}{r_{ss}}\right), \\ \theta_p &= \mathrm{Re}\left(\frac{r_{ps}}{r_{pp}}\right), & \epsilon_p &= \mathrm{Im}\left(\frac{r_{ps}}{r_{pp}}\right). \end{aligned} \tag{3.24}$$

These relation have been used in the Section 2.2.4 to compute graphs of polarization states.

3.1.3 Interface between isotropic media

3.1.3.1 Fresnel coefficients

In this case does not happen a generation of hybrid modes, therefore, the matrices $\mathbf{D}^{(\kappa)}$ in (3.18) are blockwise diagonal. Putting components of polarization vectors (2.32), (2.33), (2.35) and (2.36) derived in the Section 2.2.1 we can write

$$\mathbf{D}^{(\kappa)} = \begin{bmatrix} 1 & 1 & 0 & 0 \\ \gamma^{(\kappa+)} & \gamma^{(\kappa-)} & 0 & 0 \\ 0 & 0 & \gamma^{(\kappa+)}/n^{(\kappa)} & \gamma^{(\kappa-)}/n^{(\kappa)} \\ 0 & 0 & -n^{(\kappa)} & -n^{(\kappa)} \end{bmatrix} =$$

$$= \begin{bmatrix} 1 & 1 & 0 & 0 \\ \gamma^{(\kappa)} & -\gamma^{(\kappa)} & 0 & 0 \\ 0 & 0 & \gamma^{(\kappa)}/n^{(\kappa)} & -\gamma^{(\kappa)}/n^{(\kappa)} \\ 0 & 0 & -n^{(\kappa)} & -n^{(\kappa)} \end{bmatrix}. \tag{3.25}$$

Note that unlike the original appearance the vectors of p-polarized states are divided by the refractive index $\sqrt{\varepsilon\mu} = n$ without loss of generality. The second form of polarization matrix corresponds to the assumption of lossless media, where we set $\gamma^{(\kappa)} = \gamma^{(\kappa+)}$.

As a consequence we can split the problem (3.18) into two tasks for the polarizations being of interess:

s-polarization:

$$\begin{bmatrix} 1 & 1 \\ \gamma^{(0)} & -\gamma^{(0)} \end{bmatrix} \begin{bmatrix} u_s^{(0+)} \\ u_s^{(0-)} \end{bmatrix} = \begin{bmatrix} 1 & 1 \\ \gamma^{(1)} & -\gamma^{(1)} \end{bmatrix} \begin{bmatrix} u_s^{(1+)} \\ 0 \end{bmatrix} ; \qquad (3.26)$$

p-polarization:

$$\begin{bmatrix} \gamma^{(0)}/n^{(0)} & -\gamma^{(0)}/n^{(0)} \\ -n^{(0)} & -n^{(0)} \end{bmatrix} \begin{bmatrix} u_p^{(0+)} \\ u_p^{(0-)} \end{bmatrix} = \begin{bmatrix} \gamma^{(1)}/n^{(1)} & -\gamma^{(1)}/n^{(1)} \\ -n^{(1)} & -n^{(1)} \end{bmatrix} \begin{bmatrix} u_p^{(1+)} \\ 0 \end{bmatrix} . \qquad (3.27)$$

The first system leads to the Fresnel coefficients r_s and t_s. Dividing the both equations

$$\begin{aligned} u_s^{(0+)} + u_s^{(0-)} &= u_s^{(1+)} , \\ \gamma^{(0)} u_s^{(0+)} - \gamma^{(0)} u_s^{(0-)} &= \gamma^{(1)} u_s^{(1+)} \end{aligned}$$

by the coefficient $u_s^{(0+)}$ gives

$$\begin{aligned} 1 + r_s &= t_s , \\ \gamma^{(0)}(1 - r_s) &= \gamma^{(1)} t_s . \end{aligned}$$

Hence we easy obtain

$$r_s = \frac{\gamma^{(0)} - \gamma^{(1)}}{\gamma^{(0)} + \gamma^{(1)}} , \qquad t_s = 1 + r_s = \frac{2\gamma^{(0)}}{\gamma^{(0)} + \gamma^{(1)}} . \qquad (3.28)$$

Applying the same steps to the second algebraic system we obtain

$$r_p = \frac{\varepsilon^{(1)}\gamma^{(0)} - \varepsilon^{(0)}\gamma^{(1)}}{\varepsilon^{(1)}\gamma^{(0)} + \varepsilon^{(0)}\gamma^{(1)}} , \qquad t_p = \frac{2n^{(0)}n^{(1)}\gamma^{(0)}}{\varepsilon^{(1)}\gamma^{(0)} + \varepsilon^{(0)}\gamma^{(1)}} , \qquad (3.29)$$

where we used the relation $n^2 = \varepsilon$. A more conventional form of Fresnel coefficients uses the relation

$$\gamma_{s,p}^{(\kappa)} = n^{(\kappa)} \cos\varphi^{(\kappa)} .$$

in above formulae. Thus, we obtain

$$r_s = \frac{u_s^{(0-)}}{u_s^{(0+)}} = \frac{n^{(0)}\cos\varphi^{(0)} - n^{(1)}\cos\varphi^{(1)}}{n^{(0)}\cos\varphi^{(0)} + n^{(1)}\cos\varphi^{(1)}} , \qquad (3.30)$$

$$t_s = \frac{u_s^{(1+)}}{u_s^{(0+)}} = \frac{2n^{(0)}\cos\varphi^{(0)}}{n^{(0)}\cos\varphi^{(0)} + n^{(1)}\cos\varphi^{(1)}} \,, \tag{3.31}$$

$$r_p = \frac{u_p^{(0-)}}{u_p^{(0+)}} = \frac{n^{(1)}\cos\varphi^{(0)} - n^{(0)}\cos\varphi^{(1)}}{n^{(1)}\cos\varphi^{(0)} + n^{(0)}\cos\varphi^{(1)}} \,, \tag{3.32}$$

$$t_p = \frac{u_p^{(1+)}}{u_p^{(0+)}} = \frac{2n^{(0)}\cos\varphi^{(0)}}{n^{(1)}\cos\varphi^{(0)} + n^{(0)}\cos\varphi^{(1)}} \,. \tag{3.33}$$

Further, the alternative forms can be derived by elimination of the refraction angle $\varphi^{(1)}$ using Snell's law as

$$\left[n^{(1)}\cos\varphi^{(1)}\right]^2 = \left[n^{(1)}\right]^2 - \left[n^{(0)}\sin\varphi^{(0)}\right]^2 \,. \tag{3.34}$$

3.1.3.2 Reflectance and transmittance

From the practical point of view, we need to work with quantities directly representing energy distribution between reflected and trasmitted optical beam. To this purpose the **reflectance R and transmittance T** are introduced correspondingly to particular polarization state as

$$R = \left|\frac{u^{(0-)}}{u^{(0+)}}\right|^2 = |r|^2 \,, \tag{3.35}$$

$$T = \left|\frac{u^{(1+)}}{u^{(0+)}}\right|^2 \frac{\mathrm{Re}\left(n^{(1)}\cos\varphi^{(1)}\right)}{\mathrm{Re}\left(n^{(0)}\cos\varphi^{(0)}\right)} = |t|^2 \frac{\mathrm{Re}\left(n^{(1)}\cos\varphi^{(1)}\right)}{\mathrm{Re}\left(n^{(0)}\cos\varphi^{(0)}\right)} \,. \tag{3.36}$$

Example

At an interface between non-absorbing media $R + T = 1$ must hold. This fact is viewed in the Figs. 3.2, where the reflectance and transmittance at the planar interface air/SiO_2 are complementary at the graphs (a), (b) for lines of the same color representing one of two basic polarizations.

3.1.3.3 Brewster angle

The form of Fresnel coefficient (3.32) for p-polarized wave predicates that the reflectance R can be equal zero for non-absorbing materials (with real-valued refractove indices) – see the blue line in Figure 3.2(a). Such situation occurs at so called Brewster incidence angle when

$$n^{(1)}\cos\varphi^{(0)} = n^{(0)}\cos\varphi^{(1)} \,.$$

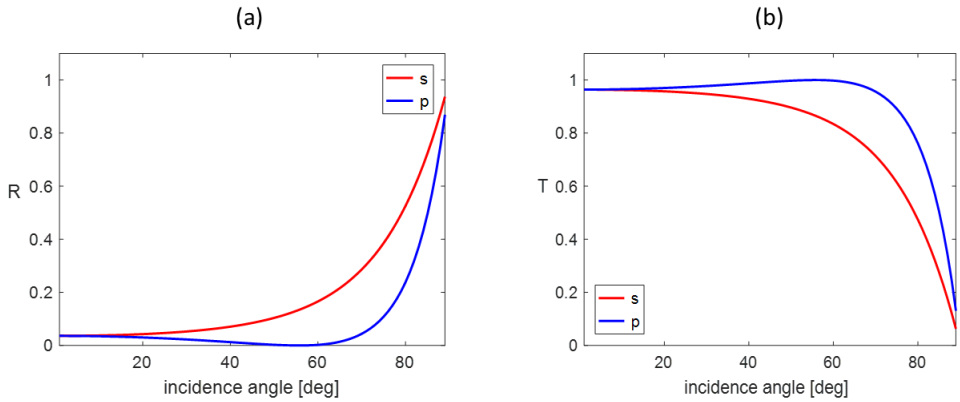

Fig. 3.2 Optical diffraction of the wave incoming from air to SiO_2 at the wavelength 632.8 nm ($n^{(0)} = 1,\ n^{(1)} = 1.469$). (a) Reflectance, (b) transmittance.

Hence we derive with the help of Snell's law for the **Brewster angle** $\varphi^{(0)} = \varphi_B$:

$$\operatorname{tg} \varphi_B = \frac{n^{(1)}}{n^{(0)}} \,. \tag{3.37}$$

A wave falling under the angle φ_B is fully refracted into substrate. This situation is conspicuously illustrated by ellipsometric angles in the Figure 3.3, where the minimum of $\tan \psi$ corresponds to the Brewster angle $\varphi_B = 55.76°$. Together, the phase shift changed in opposite one – see Figure 3.3(b).

3.1.3.4 Interface between perfect and absorbing media

Let a substrate is composed from absorbing material refractive index of which has non-zero imaginary part,

$$n^{(1)} = \nu^{(1)} - \mathrm{i}\kappa^{(1)} \,, \quad \kappa^{(1)} > 0.$$

As a consequence, Fresnel coefficients are complex valued what influences reflectometric and ellipsometric outputs as well. Among other, reflectance of p-polarized wave allways remains non-zero, nevertheless, at certain (pseudo-Brewster) incidence angle reaches its minimum. The Figure 3.4 demonstrates this situation at the interface air/iron by reflectometric and ellipsometric data.

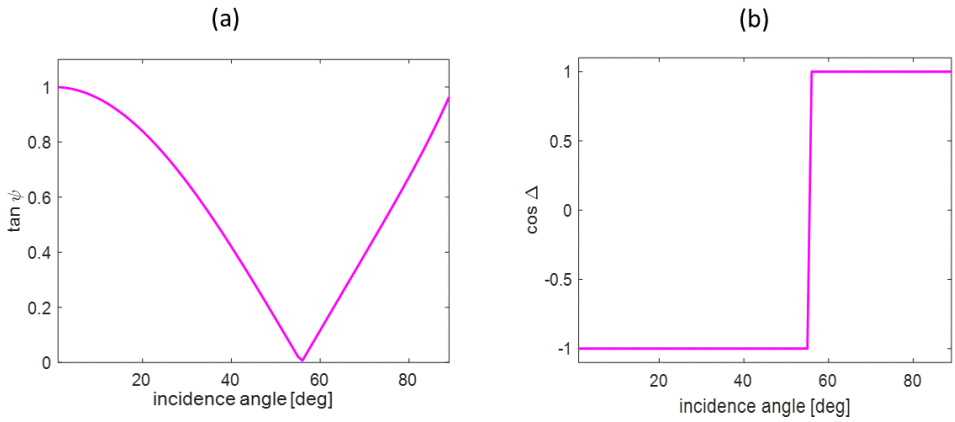

Fig. 3.3 Brewster angle demonstrated by ellipsometrical angles (see Fig. 3.2 for the input data).

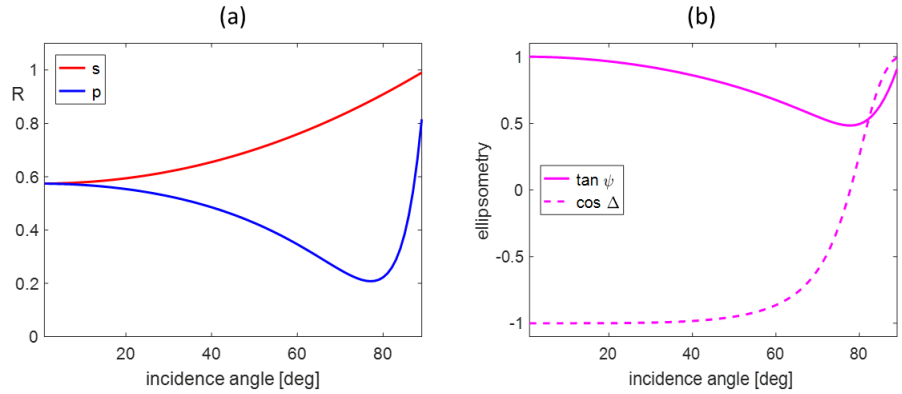

Fig. 3.4 Interface air/Fe ($n^{(0)} = 1$, $n^{(1)} = 2.87 - 3.46\mathrm{i}$): (a) reflectance, (b) ellipsometry.

3.1.3.5 Total reflection

A specific state is observed when the refractive index of superstrate is bigger than this one of substrate, i.e. $n^{(0)} > n^{(1)}$. At certain angle optical wave is refracted parallely with the interface because of $\varphi^{(1)} = \pi/2$. According Snell's

law we get **critical incidence angle** as

$$\varphi_c^{(0)} = \arcsin \frac{n^{(1)}}{n^{(0)}} \,. \tag{3.38}$$

It means that for $\varphi^{(0)} > \varphi_c^{(0)}$ in a lossless media the propagation constant is pure imaginary:

$$\gamma^{(1\pm)} = \pm\, n^{(1)} \cos\varphi^{(1)} = \pm\sqrt{\left(n^{(1)}\right)^2 - \left(n^{(0)} \sin\varphi^{(0)}\right)^2} \,. \tag{3.39}$$

A physically acceptable solution in wave traveling from the interface to the substrate in positive direction of the z axis with factor

$$\mathrm{e}^{-\mathrm{i}k_0\gamma^{(1)}z}$$

requires us to consider a negative sign in expression (3.39), which means exponentially decreasing character of this so called **evanescent wave**. The **penetration depth** δ_z denotes a distance at which the field intensity sinks to 1/e of input value. It depends not only on the material characteristics, but also on incidence angle and wavelength by the relation

$$\delta_z = \frac{1}{2k_0\sqrt{\left(n^{(0)} \sin\varphi^{(0)}\right)^2 - \left(n^{(1)}\right)^2}} \,. \tag{3.40}$$

Example

We demonstrate total reflection of optical beam ($\lambda = 632.8$ nm) by the passing from BK7 glass ($n^{(0)} = 1.5151$) into the air ($n^{(1)} = 1$).

The critical angle $\varphi_c^{(0)} = 41.3°$ is illustrated in the Figure 3.5(a) as a sudden reflectance growth that is similar for the both polarizations. The total reflection effect becomes evident also by ellipsometric output – see Figure 3.5(b). The response character in the incidence angle region $\varphi^{(0)} < \varphi_c^{(0)}$ is analogous as in the Figure 3.2(a) including the Brewster angle $\varphi_B = 33.4°$ in instantaneous case. Upon the critical angle we observe non-zero phase shift between principal polarizations.

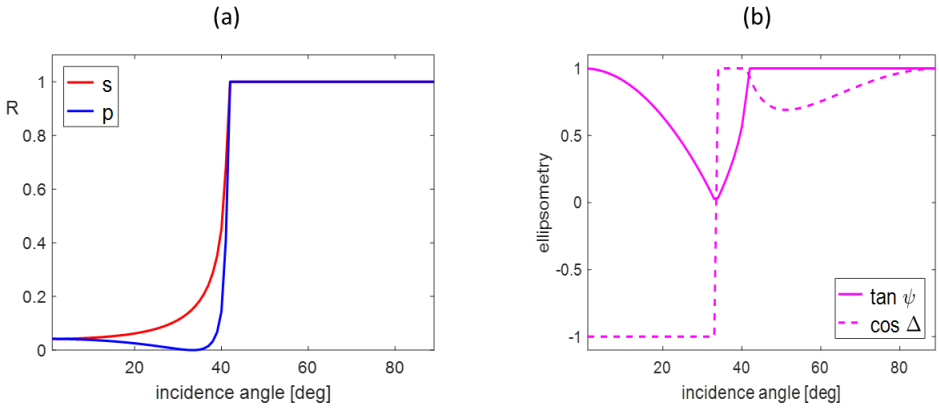

Fig. 3.5 Total reflection at interface glass/air ($n^{(0)} = 1.5151$, $n^{(1)} = 1$): (a) reflectance, (b) ellipsometry.

3.1.4 Interface between isotropic media and anisotropic substrate

3.1.4.1 Uniaxial crystal

In the isotropic superstrate the polarization matrix has an universal form (3.41),

$$\mathbf{D}^{(0)} = \begin{bmatrix} 1 & 1 & 0 & 0 \\ \gamma^{(0)} & -\gamma^{(0)} & 0 & 0 \\ 0 & 0 & \gamma^{(0)}/n^{(0)} & -\gamma^{(0)}/n^{(0)} \\ 0 & 0 & -n^{(0)} & -n^{(0)} \end{bmatrix} . \tag{3.41}$$

On the other hand, field characteristics in an anisotropic medium as propagation constants and polarization vectors must be derived with respect to given anisotropy type before the dynamical matrix construction. As an illustration consider uniaxial crystal introduced in the Subsection 2.2.2, where we derived polarization vectors (2.49) for the field $\boldsymbol{E}$ and (2.50) for the field $\boldsymbol{H}$. Thus, the polarization matrix of substrate corresponding to the general form (3.15)

is (by suppressed upper index)

$$\mathbf{D}^{(1)} = \begin{bmatrix} \gamma_1 & \varepsilon_1 & -\gamma_1 & \varepsilon_1 \\ \gamma_1^2 & \varepsilon_1\gamma_3 & \gamma_1^2 & -\varepsilon_1\gamma_3 \\ \gamma_1 & -\gamma_1^2 & -\gamma_1 & -\gamma_1^2 \\ -\varepsilon_1 & \varepsilon_1\gamma_3 & -\varepsilon_1 & -\varepsilon_1\gamma_3 \end{bmatrix}, \tag{3.42}$$

where we have by (2.48)

$$\gamma_1 = \sqrt{\varepsilon_1 - \beta^2}\,, \qquad \gamma_3 = \sqrt{\varepsilon_2 - \frac{\varepsilon_1+\varepsilon_2}{2\varepsilon_1}\beta^2}\,.$$

Evidently, an existence of hybrid modes is expected arising for the both linear polarizations of incident wave, so that two separate tasks must be solved to find amplitude coefficients of diffracted fields (3.16), (3.17):

$$\mathbf{D}^{(0)} \begin{bmatrix} u_s^{(0+)} \\ u_{ss}^{(0-)} \\ 0 \\ u_{sp}^{(0-)} \end{bmatrix} = \mathbf{D}^{(1)} \begin{bmatrix} u_{ss}^{(1+)} \\ 0 \\ u_{sp}^{(1+)} \\ 0 \end{bmatrix}, \qquad \mathbf{D}^{(0)} \begin{bmatrix} 0 \\ u_{ps}^{(0-)} \\ u_p^{(0+)} \\ u_{pp}^{(0-)} \end{bmatrix} = \mathbf{D}^{(1)} \begin{bmatrix} u_{ps}^{(1+)} \\ 0 \\ u_{pp}^{(1+)} \\ 0 \end{bmatrix}. \tag{3.43}$$

Although an estimate of unknown amplitude coefficients in general form is quite lengthy, the resolution of above algebraic systems becomes relatively easy with needed physical parameters.

3.1.4.2 Example

We turn back to the uniaxial rutile crystal discussed in the Subsection 2.2.2 including input data by the Excersise 2.2.6(2). Our aim is to find reflectance of reflected modes as a function of incidence angle. As in previous examples we suppose unit amplitude coefficient of input optical wave. By the above model we estimate amplitude coefficients for the both polarizations that enables to compute the reflectances

$$R_{ss} = \left|\frac{u_{ss}^{(0-)}}{u_s^{(0+)}}\right|^2, \qquad R_{pp} = \left|\frac{u_{pp}^{(0-)}}{u_p^{(0+)}}\right|^2, \qquad R_{ps} = \left|\frac{u_{ps}^{(0-)}}{u_p^{(0+)}}\right|^2.$$

Notice that resulting graphs in the Figure 3.6(a) are similar as in the Figure 3.4(a), where the iron substrate is of bigger absorption. The Figure 3.6(b) demonstrates the fact that the hybrid modes energy is in some orders smaller.

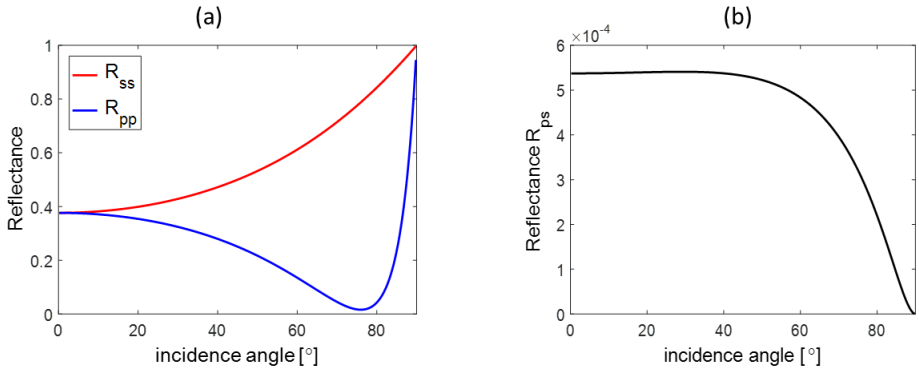

Fig. 3.6 Reflection at interface air/rutile. (a) Reflectance of principal modes, (b) reflectance R_{ps} of hybrid mode.

3.1.4.3 Eigen polarizations in anisotropic layers

If we are to solve the diffraction problem for a planar system consisting of both isotropic and anisotropic layers of finite thickness, it becomes obvious that the first type does not pose greater problems with reference to the previous explanation. The propagation constants and polarization vectors of the individual modes and thus also the matrix **D** can be easily determined in any isotropic layer by means of the procedure described in the previous text.

Similar analytic approach is also possible in the instance of an anisotropic media, however it is quite impractical in the case of complicated multilayers. From the methodological point of view it has however its significance. In the application presented in following chapters we mostly use an alternative method based on calculation of eigenvalues and eigenvectors of the matrix of the system obtained from Maxwell equations.

Classification of the forward and backward modes in outer (isotropic) regions is based on the principles corresponding to the used physical concept. Since the matrix algorithm immediates direct mode coupling, this step is not needed in the internal layers.

Consider a magnetically neutral medium with the permittivity described by the tensor $\boldsymbol{\varepsilon}$, for which the Maxwell's equations (2.7), (2.8) are of the form

$$\sqrt{\mu_0/\varepsilon_0}\left[\frac{\partial H_3}{\partial y}-\frac{\partial H_2}{\partial z}\right] = \mathrm{i}k_0(\varepsilon_{11}E_1+\varepsilon_{12}E_2+\varepsilon_{13}E_3)\ ,$$

$$\frac{\partial E_3}{\partial y}-\frac{\partial E_2}{\partial z} = -\mathrm{i}k_0\sqrt{\mu_0/\varepsilon_0}H_1\ ,$$

$$\sqrt{\mu_0/\varepsilon_0}\left[\frac{\partial H_1}{\partial z}-\frac{\partial H_3}{\partial x}\right] = \mathrm{i}k_0(\varepsilon_{21}E_1+\varepsilon_{22}E_2+\varepsilon_{23}E_3)\ ,$$

$$\frac{\partial E_1}{\partial z}-\frac{\partial E_3}{\partial x} = -\mathrm{i}k_0\sqrt{\mu_0/\varepsilon_0}H_2\ ,$$

$$\sqrt{\mu_0/\varepsilon_0}\left[\frac{\partial H_2}{\partial x}-\frac{\partial H_1}{\partial y}\right] = \mathrm{i}k_0(\varepsilon_{31}E_1+\varepsilon_{32}E_2+\varepsilon_{33}E_3)\ ,$$

$$\frac{\partial E_2}{\partial x}-\frac{\partial E_1}{\partial y} = -\mathrm{i}k_0\sqrt{\mu_0/\varepsilon_0}H_3\ .$$

The field components of waves propagating in the $x=0$ plane are written as

$$E_j = u\,e_j\mathrm{e}^{-\mathrm{i}k_0(\beta y+\gamma z)}\ ,\quad H_j = u\sqrt{\varepsilon_0/\mu_0}\,h_j\mathrm{e}^{-\mathrm{i}k_0(\beta y+\gamma z)}\ ,\quad j=x,\,y,\,z\ . \tag{3.44}$$

If we execute the derivatives by single space variables,

$$\frac{\partial}{\partial x}\equiv 0\cdot\ ,\quad \frac{\partial}{\partial y}\equiv -\mathrm{i}k_0\beta\cdot\ ,\quad \frac{\partial}{\partial z}\equiv -\mathrm{i}k_0\gamma\cdot\ , \tag{3.45}$$

then the above system of differential equations is transformed into algebraic one for unknown components of polarization vectors

$$\begin{aligned}
-\beta h_3+\gamma h_2 &= \varepsilon_{11}e_1+\varepsilon_{12}e_2+\varepsilon_{13}e_3\ , & -\beta e_3+\gamma e_2 &= -h_1\ ,\\
-\gamma h_1 &= \varepsilon_{21}e_1+\varepsilon_{22}e_2+\varepsilon_{23}e_3\ , & -\gamma e_1 &= -h_2\ ,\\
\beta h_1 &= \varepsilon_{31}e_1+\varepsilon_{32}e_2+\varepsilon_{33}e_3\ , & \beta e_1 &= -h_3\ .
\end{aligned} \tag{3.46}$$

Since only the tangential field components are needed to the application of boundary conditions, we eliminate the unknowns e_z, h_z; and, we rearrange the order of equations regarding the structure of dynamical matrix $\mathbf{D}$:

$$\begin{aligned}
\gamma e_1 &= h_2\ ,\\
\gamma h_2 &= \left(-\beta^2+\varepsilon_{11}-\frac{\varepsilon_{13}\varepsilon_{31}}{\varepsilon_{33}}\right)e_1+\left(\varepsilon_{12}-\frac{\varepsilon_{13}\varepsilon_{32}}{\varepsilon_{33}}\right)e_2+\frac{\beta\varepsilon_{13}}{\varepsilon_{33}}\,h_1\ ,\\
\gamma e_2 &= -\frac{\beta\varepsilon_{31}}{\varepsilon_{33}}\,e_1-\frac{\beta\varepsilon_{32}}{\varepsilon_{33}}\,e_2+\left(-1+\frac{\beta^2}{\varepsilon_{33}}\right)h_1\ ,\\
\gamma h_1 &= \left(-\varepsilon_{21}+\frac{\varepsilon_{23}\varepsilon_{31}}{\varepsilon_{33}}\right)e_1+\left(-\varepsilon_{22}+\frac{\varepsilon_{23}\varepsilon_{32}}{\varepsilon_{33}}\right)e_2-\frac{\beta\varepsilon_{23}}{\varepsilon_{33}}\,h_1\ .
\end{aligned}$$

This system can be written in the compact form

$$\gamma\boldsymbol{v}=\mathbf{G}\boldsymbol{v}\ , \tag{3.47}$$

where $\boldsymbol{v} = [e_x\, h_y\, e_y\, h_x]^\top$ and

$$\mathbf{G} = \begin{bmatrix} 0 & 1 & 0 & 0 \\ \varepsilon_{11} - \varepsilon_{13}\varepsilon_{31}/\varepsilon_{33} - \beta^2 & 0 & \varepsilon_{12} - \varepsilon_{13}\varepsilon_{32}/\varepsilon_{33} & \beta\varepsilon_{13}/\varepsilon_{33} \\ -\beta\varepsilon_{31}/\varepsilon_{33} & 0 & -\beta\varepsilon_{32}/\varepsilon_{33} & -1 + \beta^2/\varepsilon_{33} \\ -\varepsilon_{21} + \varepsilon_{23}\varepsilon_{31}/\varepsilon_{33} & 0 & -\varepsilon_{22} + \varepsilon_{23}\varepsilon_{32}/\varepsilon_{33} & -\beta\varepsilon_{23}/\varepsilon_{33} \end{bmatrix}. \tag{3.48}$$

As the solution of derived problem we obtain the eigenvalues γ_j, $j = 1, \ldots, 4$, and corresponding eigenvectors $\boldsymbol{v}_j$ of the matrix $\mathbf{G}$. The eigenvalues are immediately the propagation constants of eigenmodes; and, the eigenvectors represent the columns of dynamical matrix $\mathbf{D}$. In this way, we get adequate instruments to implement matrix formalism into the algorithm describing optical response from a multilayer in the next subsection.

3.2 Optical multilayers

3.2.1 Multilayer matrix construction

An optical structure is considered consisting of K homogeneous layers of the refractive indices n_κ divided by planar interfaces $z = z_\kappa$, $\kappa = 0, 1, \ldots, K$ – see Figure 3.7. Further we suppose that the semi-infinite regions $z < z_0$ and $z > z_K$ are isotropic whereas a κ-th layer of the thickness $t^{(\kappa)}$ between parallel planes $z = z_{\kappa-1}$, $z = z_\kappa$ of the relative permeability $\mu = 1$ can be characterized as anisotropic by the relative permittivity tensor $\boldsymbol{\varepsilon}$.

The wave coupling at single planar interface is described by the relation

$$\mathbf{D}^{(0)}\boldsymbol{u}^{(0)} = \mathbf{D}^{(1)}\boldsymbol{u}^{(1)}\,, \tag{3.49}$$

where $\mathbf{D}^{(0)}$, $\mathbf{D}^{(1)}$ are dynamical (or polarization) matrices of the superstrate and substrate, respectively; and, $\boldsymbol{u}^{(0)}$, $\boldsymbol{u}^{(1)}$ denote the vectors of amplitude coefficients. Consider a situation, when the medium (1) is of finite thickness $t^{(1)}$ and separated from the next medium (2) again by a planar interface. Thus, the wave coupling at the second interface can be written as

$$\mathbf{D}^{(1)}\mathbf{P}^{(1)}\boldsymbol{u}^{(1)} = \mathbf{D}^{(2)}\boldsymbol{u}^{(2)} \tag{3.50}$$

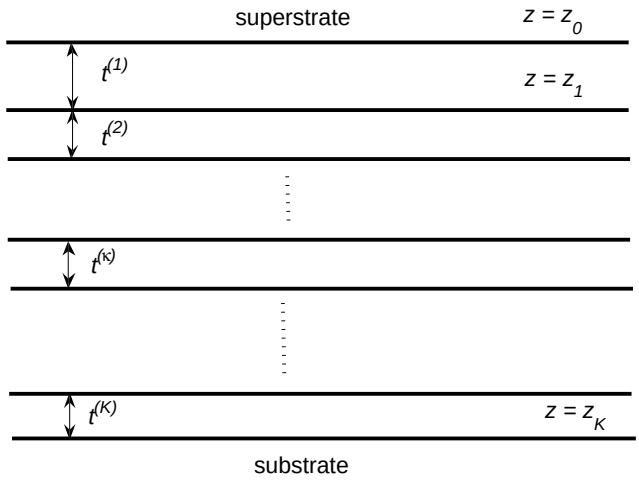

Fig. 3.7 Planar multilayer scheme.

with the **propagation matrix**

$$\mathbf{P}^{(1)} = \begin{bmatrix} \mathrm{e}^{-\mathrm{i}k_0\gamma_1^{(1)}t^{(1)}} & 0 & 0 & 0 \\ 0 & \mathrm{e}^{-\mathrm{i}k_0\gamma_2^{(1)}t^{(1)}} & 0 & 0 \\ 0 & 0 & \mathrm{e}^{-\mathrm{i}k_0\gamma_3^{(1)}t^{(1)}} & 0 \\ 0 & 0 & 0 & \mathrm{e}^{-\mathrm{i}k_0\gamma_4^{(1)}t^{(1)}} \end{bmatrix} \tag{3.51}$$

that express wave propagation through the layer (1). The relation between amplitude coefficients in the superstrate (0) and the medium (2) is obtained using (3.49) in the form

$$\mathbf{D}^{(1)}\mathbf{P}^{(1)}\left(\mathbf{D}^{(1)}\right)^{-1}\mathbf{D}^{(0)}\boldsymbol{u}^{(0)} = \mathbf{D}^{(2)}\boldsymbol{u}^{(2)}. \tag{3.52}$$

Hence

$$\boldsymbol{u}^{(0)} = \left(\mathbf{D}^{(0)}\right)^{-1}\mathbf{S}^{(1)}\mathbf{D}^{(2)}\boldsymbol{u}^{(2)}\,, \tag{3.53}$$

where the so called **characteristic matrix**

$$\mathbf{S}^{(1)} = \mathbf{D}^{(1)}\left(\mathbf{P}^{(1)}\right)^{-1}\left(\mathbf{D}^{(1)}\right)^{-1} \tag{3.54}$$

describes total effect of the finite layer ($\kappa = 1$). Since a contribution from another added layer has analogous representation, the resulting relation between

amplitude coefficents in superstrate ($\kappa = 0$) and substrate ($\kappa = K+1$) follows as

$$\boldsymbol{u}^{(0)} = \left(\mathbf{D}^{(0)}\right)^{-1} \mathbf{S}^{(2)} \cdots \mathbf{S}^{(K)} \mathbf{D}^{(K+1)} \boldsymbol{u}^{(K+1)} = \left(\mathbf{D}^{(0)}\right)^{-1} \mathbf{S} \mathbf{D}^{(K+1)} \boldsymbol{u}^{(K+1)} , \tag{3.55}$$

where

$$\mathbf{P}^{(\kappa)} = \mathrm{diag}\left(\mathrm{e}^{-\mathrm{i}k_0\gamma_q^{(\kappa)}h^{(\kappa)}},\, q = 1, \ldots, 4\right) ; \tag{3.56}$$

and,

$$\mathbf{S} = \prod_{\kappa=1}^{K} \mathbf{S}^{(\kappa)} , \qquad \mathbf{S}^{(\kappa)} = \mathbf{D}^{(\kappa)} \left(\mathbf{P}^{(\kappa)}\right)^{-1} \left(\mathbf{D}^{(\kappa)}\right)^{-1} \tag{3.57}$$

is the product of characteristic matrices of internal layers. Introducing the **characteristics** (or also **global**) **matrix of multilayer** as

$$\mathbf{M} = \left(\mathbf{D}^{(0)}\right)^{-1} \mathbf{S}\, \mathbf{D}^{(K+1)} , \tag{3.58}$$

the amplitude coefficients equation (3.55) takes the compact form

$$\boldsymbol{u}^{(0)} = \mathbf{M} \boldsymbol{u}^{(K+1)} . \tag{3.59}$$

Presented **Coupled Waves Method** (CWM) is also referred as Yeh's matrix formalism by the pilot article [12]. To the frequently citted works bringing detailled discussion of this approach belongs also the article [13].

3.2.2 Reflection and transmission

It is relevant to show a way to reflection and transmission characteristics. Consider at first the s-polarized incoming wave, for which the vectors of amplitude coefficients are of the form (3.16), (3.17). Thus, the problem (3.59) reads as

$$\begin{bmatrix} u_s^{(0+)} \\ u_{ss}^{(0-)} \\ 0 \\ u_{sp}^{(0-)} \end{bmatrix} = \begin{bmatrix} M_{11} & M_{12} & M_{13} & M_{14} \\ M_{21} & M_{22} & M_{23} & M_{24} \\ M_{31} & M_{32} & M_{33} & M_{34} \\ M_{41} & M_{42} & M_{43} & M_{44} \end{bmatrix} \begin{bmatrix} u_{ss}^{(K+1+)} \\ 0 \\ u_{sp}^{(K+1+)} \\ 0 \end{bmatrix} \tag{3.60}$$

that leads to the system

$$\begin{aligned} u_s^{(0+)} &= M_{11} u_{ss}^{(K+1+)} + M_{13} u_{sp}^{(K+1+)}, \\ u_{ss}^{(0-)} &= M_{21} u_{ss}^{(K+1+)} + M_{23} u_{sp}^{(K+1+)}, \\ 0 &= M_{31} u_{ss}^{(K+1+)} + M_{33} u_{sp}^{(K+1+)}, \\ u_{sp}^{(0-)} &= M_{41} u_{ss}^{(K+1+)} + M_{43} u_{sp}^{(K+1+)}. \end{aligned} \tag{3.61}$$

If we divide each equation by $u_s^{(0+)}$, then the requested coefficients are expressed by the global matrix $\mathbf{M}$ elements:

$$r_{ss} = \frac{u_{ss}^{(0-)}}{u_s^{(0+)}} = \frac{M_{21}M_{33} - M_{23}M_{31}}{M_{11}M_{33} - M_{13}M_{31}} \ , \tag{3.62}$$

$$r_{sp} = \frac{u_{sp}^{(0-)}}{u_s^{(0+)}} = \frac{M_{41}M_{33} - M_{43}M_{31}}{M_{11}M_{33} - M_{13}M_{31}} \ , \tag{3.63}$$

$$t_{ss} = \frac{u_{ss}^{(K+1+)}}{u_s^{(0+)}} = \frac{M_{33}}{M_{11}M_{33} - M_{13}M_{31}} \ , \tag{3.64}$$

$$t_{sp} = \frac{u_{sp}^{(K+1+)}}{u_s^{(0+)}} = -\frac{M_{31}}{M_{11}M_{33} - M_{13}M_{31}} \ . \tag{3.65}$$

A similar way leads to analogous results in case of p-polarized incident beam:

$$r_{pp} = \frac{u_{pp}^{(0-)}}{u_p^{(0+)}} = \frac{M_{11}M_{43} - M_{13}M_{41}}{M_{11}M_{33} - M_{13}M_{31}} \ , \tag{3.66}$$

$$r_{ps} = \frac{u_{ps}^{(0-)}}{u_p^{(0+)}} = \frac{M_{11}M_{23} - M_{13}M_{21}}{M_{11}M_{33} - M_{13}M_{31}} \ , \tag{3.67}$$

$$t_{pp} = \frac{u_{pp}^{(K+1+)}}{u_p^{(0+)}} = \frac{M_{11}}{M_{11}M_{33} - M_{13}M_{31}} \ , \tag{3.68}$$

$$t_{ps} = \frac{u_{ps}^{(K+1+)}}{u_p^{(0+)}} = -\frac{M_{13}}{M_{11}M_{33} - M_{13}M_{31}} \ . \tag{3.69}$$

No hybrid modes propagate in an isotropic structure, for which the global matrix is blockwise diagonal,

$$\mathbf{M} = \begin{bmatrix} M_{11} & M_{12} & 0 & 0 \\ M_{21} & M_{22} & 0 & 0 \\ 0 & 0 & M_{33} & M_{34} \\ 0 & 0 & M_{43} & M_{44} \end{bmatrix} \ , \tag{3.70}$$

therefore, the reflection and transmission coefficients take simplified form

$$r_s = \frac{M_{21}}{M_{11}} \ , \qquad t_s = \frac{1}{M_{11}} \ , \qquad r_p = \frac{M_{43}}{M_{33}} \ , \qquad t_p = \frac{1}{M_{33}} \ . \tag{3.71}$$

Moreover, setting $K = 0$ in (3.55) we obtain diffraction problem (3.14) at single interface,

$$\boldsymbol{u}^{(0)} = \left(\mathbf{D}^{(0)}\right)^{-1} \mathbf{D}^{(1)} \boldsymbol{u}^{(1)} \,, \tag{3.72}$$

with the unit characteristic matrix $\mathbf{S} = \mathbf{I}$. As a consequence, the formulae (3.71) lead directly to the Fresnel coefficients derived in the Subsection 3.1.3.1.

3.2.3 Implementation remarks

We are going to summarize fundamental steps of coupled waves algorithm to obtaining of reflection and transmission characteristics of planar multilayer:

(i) Assuming isotropical character of the sub- and superstrate material we estimate propagation constant in any layer. In the superstrate, from which the wave falls on the first interface under the angle φ, the propagation constants are defined as

$$\gamma_{s,p}^{(0)} = n^{(0)} \cos\varphi \,;$$

in the other isotropic layers include the substrate one holds

$$\gamma_{s,p}^{(\kappa)} = n^{(\kappa)} \cos\varphi^{(\kappa)} = \sqrt{\left(n^{(\kappa)}\right)^2 - \left(n^{(0)} \sin\varphi\right)^2} \,. \tag{3.73}$$

(ii) In an anisotropic layer with given permittivity tensor we compose the matrix $\mathbf{G}^{(\kappa)}$ by (3.48). Resolving the eigenvalue problem (3.47) we obtain the eigenvalues $\gamma_j^{(\kappa)}$ and (column) eigenvectors that form the dynamical matrix

$$\mathbf{D}^{(\kappa)} = \left[\boldsymbol{v}_1^{(\kappa)} \boldsymbol{v}_2^{(\kappa)} \boldsymbol{v}_3^{(\kappa)} \boldsymbol{v}_4^{(\kappa)}\right] \,. \tag{3.74}$$

(iv) Diagonal propagation matrix $\mathbf{P}^{(\kappa)}$ of the form (3.56) in arbitrary layer of the thickness $t^{(\kappa)}$ contains computed eigenvalues in the ordering by the matrix $\mathbf{D}$ structure.

(v) We derive the characteristic matrices $\mathbf{S}^{(\kappa)} = \mathbf{D}^{(\kappa)} \left(\mathbf{P}^{(\kappa)}\right)^{-1} (\mathbf{D}^{(\kappa)})^{-1}$ in the next step to obtain global characteristic matrix $\mathbf{S}$.

(vi) Finally, we resolve the algebraic system (3.55) for amplitude coefficients in the sub- and superstrate.

3.2.4 A single layer structure

An isotropic optical structure 'superstrate / thin layer / substrate' is treated as the simplest multilayer that we meet as one of fundamental constituents in the most planar optical systems, in particular in sensing devices, elements of optical circuits and waveguides. To have a better insight to its functionalizing we present more detailled derivation of global matrix including the reflection and transmission coefficients.

Denote $n^{(\kappa)} = \sqrt{\varepsilon^{(\kappa)}}$, $\kappa = 0, 1, 2$ material parameters of the superstrate, thin layer and substrate, respectively. The super- and substrate are semiinfinite regions, the thickness $t^{(1)}$ of internal layer is less than the wavelength λ of incoming optical beam. We seek for the global matrix $\mathbf{M}$ by (3.70) that we split into two 2×2 matrices $\mathbf{M}_s$ and $\mathbf{M}_p$ regarding the polarization of incident light. In agreement with (3.41) we get the polarization matrices

$$\mathbf{D}_s^{(\kappa)} = \begin{bmatrix} 1 & 1 \\ \gamma^{(\kappa)} & -\gamma^{(\kappa)} \end{bmatrix}, \quad (\mathbf{D_s}^{(\kappa)})^{-1} = \frac{1}{2\gamma^{(\kappa)}} \begin{bmatrix} \gamma^{(\kappa)} & 1 \\ \gamma^{(\kappa)} & -1 \end{bmatrix}, \tag{3.75}$$

$$\mathbf{D}_p^{(\kappa)} = \frac{1}{n^{(\kappa)}} \begin{bmatrix} \gamma^{(\kappa)} & -\gamma^{(\kappa)} \\ -\varepsilon^{(\kappa)} & -\varepsilon^{(\kappa)} \end{bmatrix}, \quad (\mathbf{D_p}^{(\kappa)})^{-1} = -\frac{n^{(\kappa)}}{2\gamma^{(\kappa)}} \begin{bmatrix} -\varepsilon^{(\kappa)} & \gamma^{(\kappa)} \\ \varepsilon^{(\kappa)} & \gamma^{(\kappa)} \end{bmatrix}. \tag{3.76}$$

Since $\gamma_s^{(\kappa)} = \gamma_p^{(\kappa)}$ in the isotropic case, the propagation matrix is the same for the both polarizations,

$$\mathbf{P}^{(1)} = \begin{bmatrix} \mathrm{e}^{-\mathrm{i}\tau} & 0 \\ 0 & \mathrm{e}^{\mathrm{i}\tau} \end{bmatrix}, \qquad \tau = \tau^{(1)} = k_0 \gamma^{(1)} t^{(1)}. \tag{3.77}$$

As the next step we construct characteristic matrices of internal layer:

$$\mathbf{S}_s^{(1)} = \mathbf{D}_s^{(1)} \left(\mathbf{P}^{(1)}\right)^{-1} (\mathbf{D}_s^{(1)})^{-1} = \frac{1}{2\gamma^{(1)}} \begin{bmatrix} \gamma^{(1)}(\mathrm{e}^{\mathrm{i}\tau} + \mathrm{e}^{-\mathrm{i}\tau}) & \mathrm{e}^{\mathrm{i}\tau} - \mathrm{e}^{-\mathrm{i}\tau} \\ \left(\gamma^{(1)}\right)^2 (\mathrm{e}^{\mathrm{i}\tau} - \mathrm{e}^{-\mathrm{i}\tau}) & \gamma^{(1)}(\mathrm{e}^{\mathrm{i}\tau} + \mathrm{e}^{-\mathrm{i}\tau}) \end{bmatrix},$$

or, in more concise form,

$$\mathbf{S}_s^{(1)} = \frac{1}{\gamma^{(1)}} \begin{bmatrix} \gamma^{(1)} \cos\tau & \mathrm{i}\sin\tau \\ \mathrm{i}\left(\gamma^{(1)}\right)^2 \sin\tau & \gamma^{(1)} \cos\tau \end{bmatrix}. \tag{3.78}$$

Similar steps give characteristic matrix for transversal magnetic field:

$$\mathbf{S}_p^{(1)} = \frac{1}{\gamma^{(1)}} \begin{bmatrix} \varepsilon^{(1)}\gamma^{(1)} \cos\tau & -\mathrm{i}\left(\gamma^{(1)}\right)^2 \sin\tau \\ -\mathrm{i}\left(\varepsilon^{(1)}\right)^2 \sin\tau & \varepsilon^{(1)}\gamma^{(1)} \cos\tau \end{bmatrix}. \tag{3.79}$$

The global matrices are given as the products of the form (3.58),

$$\mathbf{M}_s = \left(\mathbf{D}_s^{(0)}\right)^{-1} \mathbf{S}_s^{(1)} \mathbf{D}_s^{(2)} \,, \qquad \mathbf{M}_p = \left(\mathbf{D}_p^{(0)}\right)^{-1} \mathbf{S}_p^{(1)} \mathbf{D}_p^{(2)} \,. \tag{3.80}$$

Only the elements M_{11}, M_{21} of the $\mathbf{M}_s$ matrix, or, M_{33}, M_{43} of the $\mathbf{M}_p$ one are needed to establish the reflection and transmission coefficients by the relations (3.71). Omitting tedious matrix multiplication, resulting matrix elements appears in the case of s-polarization

$$M_{11} = \frac{1}{2\gamma^{(0)}\gamma^{(1)}} \left[\left(\gamma^{(0)}\gamma^{(1)} + \gamma^{(1)}\gamma^{(2)}\right) \cos\tau + \mathrm{i} \left(\gamma^{(0)}\gamma^{(2)} + \left(\gamma^{(1)}\right)^2\right) \sin\tau \right] \,, \tag{3.81}$$

$$M_{21} = \frac{1}{2\gamma^{(0)}\gamma^{(1)}} \left[\left(\gamma^{(0)}\gamma^{(1)} - \gamma^{(1)}\gamma^{(2)}\right) \cos\tau + \mathrm{i} \left(\gamma^{(0)}\gamma^{(2)} - \left(\gamma^{(1)}\right)^2\right) \sin\tau \right] \,. \tag{3.82}$$

For the p-polarized incident wave we introduce following notation:

$$\begin{aligned} p_1 &= \varepsilon^{(1)}\varepsilon^{(2)}\gamma^{(0)}\gamma^{(1)} - \varepsilon^{(0)}\varepsilon^{(1)}\gamma^{(1)}\gamma^{(2)} \,, \\ p_2 &= (\varepsilon^{(1)})^2\gamma^{(0)}\gamma^{(2)} - \varepsilon^{(0)}\varepsilon^{(2)}(\gamma^{(1)})^2 \,, \\ p_3 &= \varepsilon^{(1)}\varepsilon^{(2)}\gamma^{(0)}\gamma^{(1)} + \varepsilon^{(0)}\varepsilon^{(1)}\gamma^{(1)}\gamma^{(2)} \,, \\ p_4 &= (\varepsilon^{(1)})^2\gamma^{(0)}\gamma^{(2)} + \varepsilon^{(0)}\varepsilon^{(2)}(\gamma^{(1)})^2 \,. \end{aligned}$$

Thus, we have

$$M_{33} = \frac{1}{2\gamma^{(0)}\gamma^{(1)}} \frac{n^{(0)}}{n^{(2)}} \left[p_3 \cos\tau + \mathrm{i} p_4 \sin\tau \right] \,, \tag{3.83}$$

$$M_{43} = \frac{1}{2\gamma^{(0)}\gamma^{(1)}} \frac{n^{(0)}}{n^{(2)}} \left[p_1 \cos\tau + \mathrm{i} p_2 \sin\tau \right] \,. \tag{3.84}$$

Finally, the reflection and transmission coefficients result in the form

$$r_s = \frac{\left(\gamma^{(0)}\gamma^{(1)} - \gamma^{(1)}\gamma^{(2)}\right) \cos\tau + \mathrm{i} \left(\gamma^{(0)}\gamma^{(2)} - (\gamma^{(1)})^2\right) \sin\tau}{\left(\gamma^{(0)}\gamma^{(1)} + \gamma^{(1)}\gamma^{(2)}\right) \cos\tau + \mathrm{i} \left(\gamma^{(0)}\gamma^{(2)} + (\gamma^{(1)})^2\right) \sin\tau} \,, \tag{3.85}$$

$$r_p = \frac{p_1 \cos\tau + \mathrm{i} p_2 \sin\tau}{p_3 \cos\tau + \mathrm{i} p_4 \sin\tau} \,, \tag{3.86}$$

$$t_s = (1 + r_s) \cos\tau - \mathrm{i} \frac{\gamma^{(0)}}{\gamma^{(1)}} (1 - r_s) \sin\tau \,, \tag{3.87}$$

$$t_p = \sqrt{\frac{\varepsilon^{(0)}}{\varepsilon^{(2)}}} \left[(1 + r_p) \cos\tau - \mathrm{i} \frac{\varepsilon^{(1)}}{\varepsilon^{(0)}} \frac{\gamma^{(0)}}{\gamma^{(1)}} (1 - r_p) \sin\tau \right] \,. \tag{3.88}$$

3.3 Selected applications

This section is devoted to typical applications, when an interaction of light beam with optical nanostructures is modeled using coupled waves method. We present here relatively simple situations, more complicated models we meet in the next chapters.

3.3.1 An interface with metallic film

We start with isotropic optical structure composed from the glass substrate covered by ultrathin (5 nm) gold film, as the superstrate the air is assumed. Reflection response for the both basic linear polarizations has been accomplished directly with the help of analytical formulae derived in previous subsection.

Resulting simulations were obtained at the yellow light wavelength (589.3 nm) for the corresponding refractive indices $n^{(0)} = 1$ (air), $n^{(1)} = 0.28 - 3.07\mathrm{i}$ (Au) and $n^{(2)} = 1.517$ (BK7 glass).

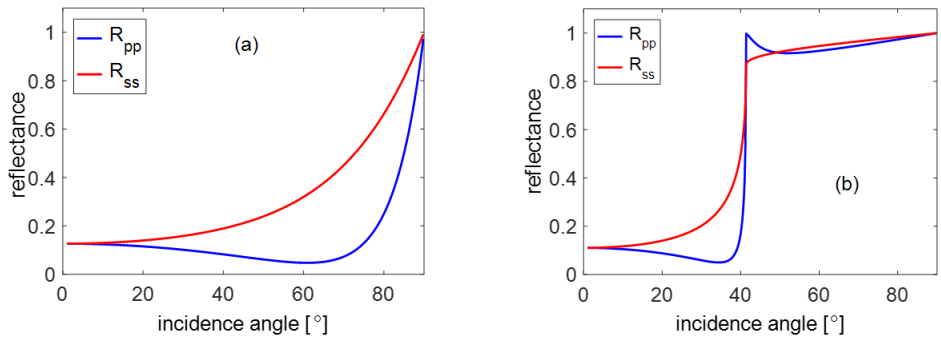

Fig. 3.8 The system air/Au/glass: (a) external reflection (b) internal reflection.

Two different situation are considered with regard to the direction of light propagation. In the first case the external reflection is modeled when the incident wave impinges upon the Au film from the air superstrate. Due to absorption in the gold film we observe **pseudo-Brewster angle** at reflection minimum of p-polarized wave – see Figure 3.8(a).

Similar effect occurs in the Figure 3.8(b), where the wave propagates from the glass substrate, but only for the incidence angles less than critical angle 40° – cf. also the Figure 3.5. For the greater incidence angles the total reflection predominates at the interface SiO_2/Au.

3.3.2 Prism coupling

In the subsection 3.1.3.5 we discussed the total reflection of an optical wave. Among other, this situation occur when a light beam rises from optical prism into ambient medium with lower refractive index. Thus, arising evanescent wave can be coupled through a thin layer (gap) into another component of optical structure. Prism coupling belongs to frequently used applications of this phenomena, which is a traditional experimental method of light coupling and decoupling in planar layered structures. The prism coupling has proven useful in generation of surface plasmons (SPR – **Surface Plasmon Resonance**), in studying of surfaces and nanostructures by means of the **Total Internal Reflection Ellipsometry** (TIRE) method, and, in sensorics. In all these cases we require the electromagnetic wave to impinge on prism base under bigger than critical angle for generation of an evanescent wave in the coupling gap area.

The coupling between the prism and the sample can be basically changed in two ways (maintaining the working wavelength). On the one hand mechanically, when the geometric dimensions of the coupling gap are altered, and on the other by a change of refractive index in the coupling gap. In the latter case, various kinds of so called immersion liquids are used.

In order to illustrate coupling properties of a gap, we present the example of reflection response at the wavelength 632.8 nm from the lossless TIR system, in which the bismut-germanate prism ($n^{(0)} = 2.54$) is separated from the garnet glass substrate ($n^{(2)} = 2.20$) by the thin air gap ($n^{(1)} = 1$). The reflectance as a function of incidence angle is demonstrated in the Figure 3.9 for the s-polarized light beam; gap thickness is referred in the figure legend.

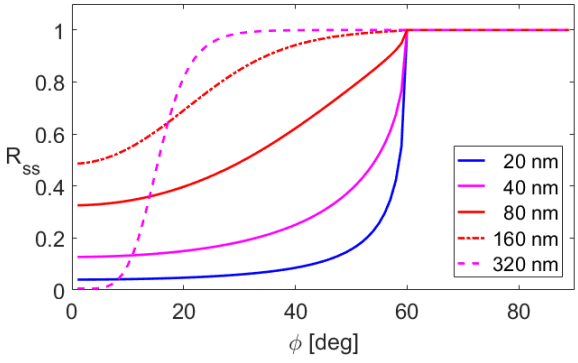

Fig. 3.9 Air gap coupling ability as a function of its thickness.

If the air gap is very thin (here, tens of nm's), then the evanescent wave

penetrates the substrate, therefore, we register total reflection on a fictitious prism/substrate interface (59.88°). A growing gap thickness causes coupling attenuation so, that we observe only total reflection at the prism/air interface at the critical angle 23.15° at hihgest value 320 nm.

3.3.3 Magnetooptics

Single internal nanolayer postured in the previous examples that means $K = 1$ in the multilayer model. A growing number of layers such as absorbing media demand solely the use of matrix algorithm that we demonstrate by magneto-optically active iron nanolayer of the 150 nm width embedded in between the glass substrate and gold film of the system discussed in the Subsection 3.3.1 – see the scheme in Figure 3.10. Here, we have two absorbing internal layers ($K = 2$), moreover, we will model an influence of the iron component anisotropy by magnetooptical response.

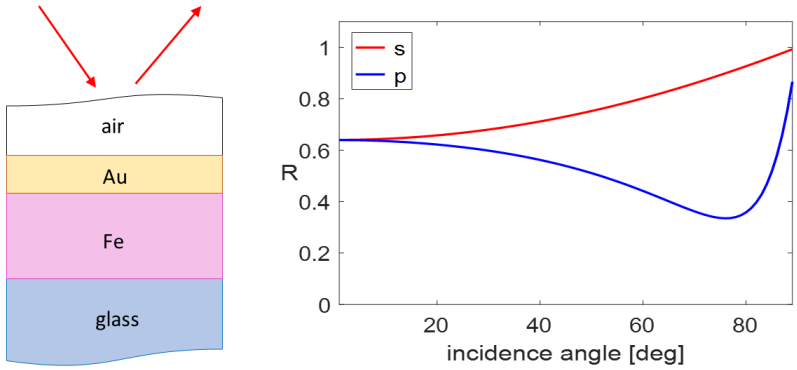

Fig. 3.10 The multilayer scheme with reflection response.

The material parameters of the glass substrate and Au film are preserved at the wavelength 589.3 nm, where the iron refractive index $n_{Fe} = 1.6207 - 1.8415\mathrm{i}$ and the Voigt magneto-optical parameter $q = 0.0022 + 0.0173\mathrm{i}$ [14] are used. The resulting reflectance at above picture is very similar to this one in the Figure 3.8, however, with the higher response caused by reflection at the Au/Fe interface.

If the inserted ferromagnetic layer is exposed to an external magnetic field, the artificial anisotropy of permittivity causes a change of light beam polarization state as we analysed in the Subsection 2.2.3. Assuming the magnetization

vector acting paralelly to the incidence plane we obtain longitudinal MO Kerr effect that is modeled in the Figure 3.11 by the rotation and ellipticity for the both polarizations of incoming wave.

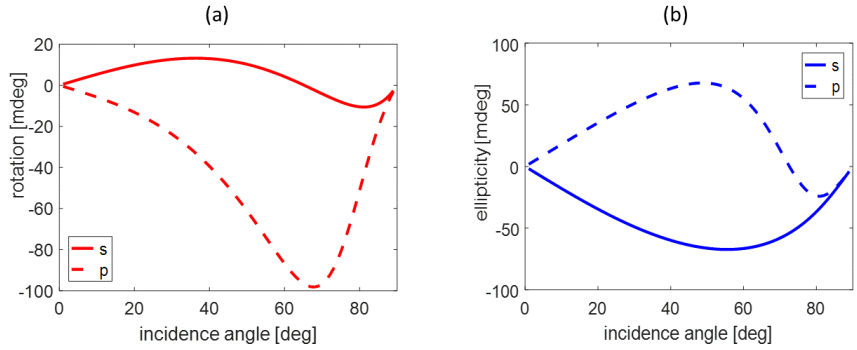

Fig. 3.11 Magnetooptical angles.

3.3.4 Spectral ellipsometry

Untill now we demonstrated the angular dependence of several optical characteristics at fixed wavelength. However, material properties are functions of the wavelength that plays important role in sensorics, surface diagnostics and so on. Following example shows spectral dependence of ellipsometrical angles obtained as reflection response from the oxidized silicon bulk.

Pulse thermal oxidation of the silicon surface leads to creation of a SiO_2 film, whose thickness depends among other on temperature and pulse duration. Ellipsometric curves in the Figure 3.12 were obtained in the spectral region from 250 to 680 nm for the 5 nm thickness of oxidized layer. Dispersion function of the SiO_2 was computed by well-known **Sellmeier formula**

$$\varepsilon(\lambda) = 1 + \sum_m \frac{A_m \lambda^2}{\lambda^2 - B_m} \,, \tag{3.89}$$

where A_m, B_m are given parameters. In particular, the coefficients $A = 1.336$, $B = 92.61$ were used by $m = 1$. Optical function of the silicon substrate has been interpolated from the data referred in [15].

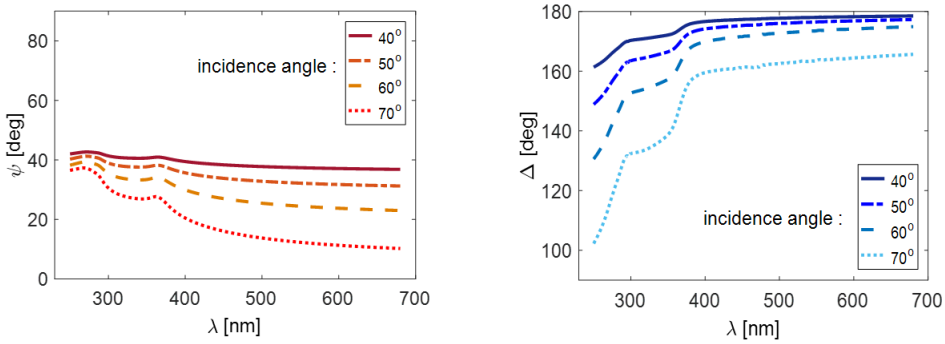

Fig. 3.12 Ellipsometric angles at selected angles of incidence.

3.3.5 Inverse problems

3.3.5.1 Theoretical framework

The applications presented so far focused on determination of ellipsometric or reflectometric characteristics of optical structures represented generally by a function $\mathcal{F}$. The geometric and material parameters of the system and the attributes of the incident optical beam served as parameters, namely its wavelength λ and the angle of incidence $\varphi^{(0)}$. Models approached this way represent the so called **direct problems**.

In practice we often meet a situation when we know experimentally obtained data and our task is to obtain information on the optical system properties as for example thicknesses of layers or their material composition (optical functions) from these data. As algorithms for direct problems are usually relatively complicated, we are not able to implement the inversion of the function $\mathcal{F}$ and to define some of its arguments as the required output immediately. This is why the inverse problem is usually conceived in such manners, that for the target set of desired parameters a suitably chosen so called **merit function** (or **cost function**) $\mathcal{J}$ takes the minimum value. This must depend on both, the numeric values obtained from the direct solution of the problem and the experimental data for a given selection of the remaining independent variables. The term **parameter fitting** is often use in this context. Several questions naturally arise, to which attention has to be paid in formulation of inverse problems. The most important ones are as follows:

- selection of the cost function with possible inclusion of weighting coefficients (e.g. if the individual measurements are loaded with different

errors etc.),

- selection of the numeric algorithm for the cost function minimization (these are non-linear problems with some exceptions),
- possible addition of certain limits for fitted parameters.

3.3.5.2 Example

As an example of a simple inverse problem we are going to present main steps of fitting procedure for determination of the thickness of a thin planar film based on ellipsometric data. We are thus going to consider planar structure discussed in previous subsection, i.e. consisting of three parallel media – air superstrate over the oxidized silicon substrate, for which we are able to formulate and solve a direct ellipsometric problem, where $K = 1$:

$$\begin{bmatrix} \psi \\ \Delta \end{bmatrix} = \mathcal{F}\left(t^{(1)},\, \varphi,\, \lambda,\, \varepsilon^{(0)},\, \varepsilon^{(1)},\, \varepsilon^{(2)}\right) , \tag{3.90}$$

where SiO_2 film thickness $t^{(1)}$, which is a fitted value, is the first among the parameters of the function $\mathcal{F}$. Let us also assume that we have the values of the angles ψ and Δ available, measured on the scale of wavelengths $\lambda_1, , \lambda_2, \ldots, \lambda_J$ for a particular angle of incidence φ. Material parameters are also considered given. The cost function for the inputs formulated this way can be considered for example in the following form:

$$\mathcal{J}(\psi_{\text{num}}, \Delta_{\text{num}}, \psi_{\text{exp}}, \Delta_{\text{exp}}) = \sum_{i=1}^{J} \left\{ [\operatorname{tg}\psi_{\text{num}}(\lambda_i) - \operatorname{tg}\psi_{\text{exp}}(\lambda_i)]^2 + [\cos\Delta_{\text{num}}(\lambda_i) - \cos\Delta_{\text{exp}}(\lambda_i)]^2 \right\} , \tag{3.91}$$

where $\psi_{\text{num}}, \Delta_{\text{num}}$ are calculated, and $\psi_{\text{exp}}, \Delta_{\text{exp}}$ experimental (input) values.

At the beginning of fitting process we need to input the "starting" value $t_0^{(1)}$, determined for example by a qualified estimation. The procedure then runs as follows: a direct problem is solved for the given thickness, i.e. the functional (3.90) is calculated, and the obtained output values are applied in calculation of the value of the cost function (3.91). Now – in dependence on the algorithm structure – we perform correction of the parameter $t_0^{(1)}$, to a new value $t_1^{(1)}$, and the whole procedure is repeated. In the individual steps we examine whether the cost function value is decreasing and the correction is thereto adjusted, until the required accuracy is achieved.

The film thickness $t^{(1)}$ that minimizes the functional $\mathcal{J}$ is the sought parameter of the optical system.

The measurement of the ellipsometric angles was performed within the spectral interval 250 - 700 nm with the step 5 nm at incidence angle 65° with the accuracy of 10^{-4} degrees. The numeric processing was implemented by an own programme code in Matlab applying the FMINSEARCH procedure. A comparison of the ellipsometric curves from the experiments and from the theoretical model applying the fit is shown in Fig. 3.13.

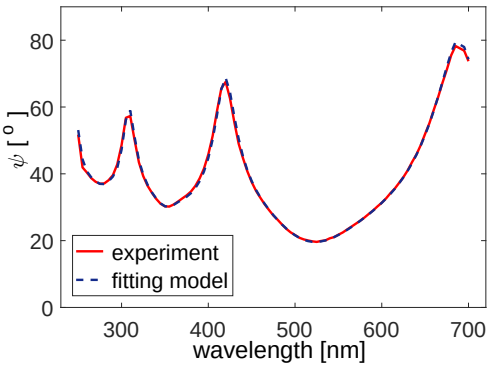

Fig. 3.13 Oxidation layer thickness fitting (determined thickness 447 nm).

3.3.6 Excersise

3.3.6.1

Derive Fresnel coefficients (3.29) as the Eq. (3.27) solution.

3.3.6.2

Verify the formula (3.87).

3.3.6.3

Uniaxial crystal of calcite is one from typical materials that exhibit optical birefringence – see Fig. 3.14. Our aim is to estimate the refraction angles corresponding to the ordinary and extraordinary refractive indices n_0, n_e, respectively.
Two situations are considered:

(I) crystal optical axis is parallel to the coordinate axis x_2,

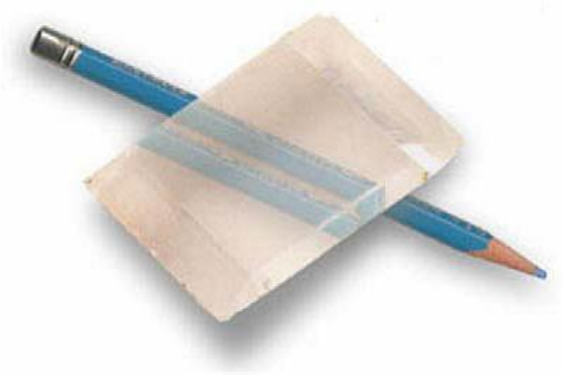

Fig. 3.14 Birefringence at calcite crystal.

(II) optical axis rotated about the x_3 axis by the angle $\phi = 45°$.

Input data:
wavelength $\lambda = 589.3$ nm,
incidence angle from the air) $\varphi^{(0)} = 60°$,
ordinary refractive index of calcite $n_o = 1.6854$,
extraordinary refractive index of calcite $n_e = 1.4864$.

3.3.6.4

Estimate graphical dependence between penetration depth δ of evanescent wave and the incidence angle φ at the interface SF10 glass/water. Use optical functions at the wavelength $\lambda = 633$ nm e.g. by the reference [16].

3.3.6.5

Consider the situation as in previous problem with added BK7 glass substrate. Demonstrate the coupling forces as a function of water gap thickness t_g performing graphical comparison of the reflectance for the gap dimensions $t_g = 70$ nm and $t_g = 700$ nm.

Chapter 4

Planar Optical Waveguides

4.1 Introduction

Optical waveguides are the basic elements for confinement and transmission of light over various distances, ranging from tens or hundreds of μm in integrated photonics to hundreds or thousands of km in long-distance fiber-optic transmission. Optical waveguides also form key structures in semiconductor lasers, and act as passive and active devices such as waveguide couplers and modulators. They are used also as components in integrated optical circuits, as the transmission medium in long distances for light wave communications, or for biomedical imaging. Here we discuss the planar dielectric waveguide (Fig. 4.1) specifically from the configuration, waveguide mode, field distribution, and dispersion relation aspects.

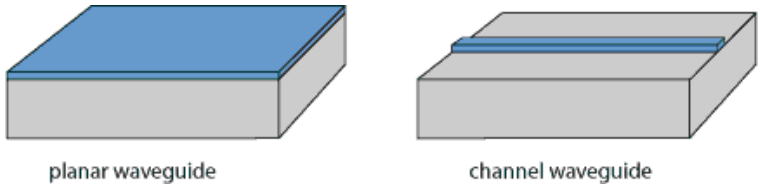

Fig. 4.1 Planar and strip waveguides.

We can classify the waveguide according to

- the constuction structure: planar, strip, or fiber waveguides,
- refractive index distribution: step or gradient index,
- the material: glass, polymer, semiconductor,

- the mode structure: single-mode, multi-mode.

The basic structure of a dielectric waveguide consists of a longitudinally extended high-index optical medium, called the **core**, which is transversely surrounded by low-index media, called the **cladding**. A guided optical wave propagates in the waveguide along its longitudinal direction. The core of a planar waveguide is also called the film, while the upper and lower cladding layers are called the cover and the substrate.

A waveguide in which the index profile has abrupt changes between the core and the cladding is called a **step-index waveguide**, while one in which the index profile varies gradually is called a **graded-index waveguide**. We will focus on the step-index waveguide for our discussion. The refractive index of the core $n^{(2)}$ must be greater than the refractive indices of surrounding media, in particular it must hold

$$n^{(1)} < n^{(3)} < n^{(2)} \tag{4.1}$$

so that total reflection at the both interfaces occurs – see the Figure 4.2. There are two critical angles associated with the internal reflections at the upper and lower interfaces,

$$\varphi_{c1} = \arcsin \frac{n^{(1)}}{n^{(2)}}\,, \qquad \varphi_{c2} = \arcsin \frac{n^{(3)}}{n^{(2)}}\,, \tag{4.2}$$

$\varphi_{c1} < \varphi_{c2}$ because $n^{(1)} < n^{(2)}$.

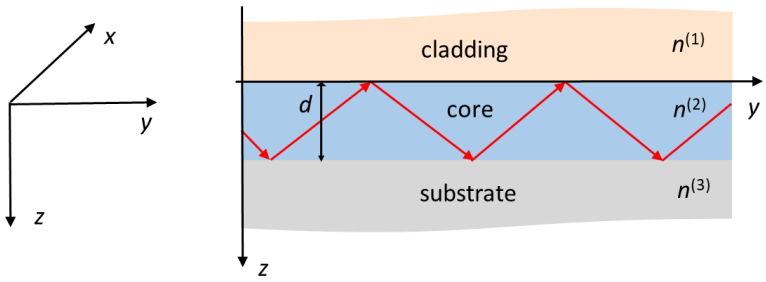

Fig. 4.2 Planar waveguide scheme.

4.2 Dispersion relations

4.2.1 Transverse resonance

As the wave is reflected back and forth between the two interfaces, it interferes with itself. A guided mode can exist only when a transverse resonance condition is satisfied, i.e. the repeatedly reflected wave has constructive interference with itself. In other words, the **self-consistency condition** must hold: the phase shift between the two waves must be 0 or a multiple of 2π.

Suppose internal reflection at a given "zig-zag" angle $\varphi^{(2)} > \varphi_{c2}$ at the both interfaces, where $|r^{(12)}| = |r^{(23)}| = 1$ for the Fresnel coefficients independently on polarization state. Thus

$$r^{(12)} = \exp\{2\mathrm{i}\theta^{(12)}\} \,, \qquad r^{(23)} = \exp\{2\mathrm{i}\theta^{(23)}\} \,, \tag{4.3}$$

where $\theta^{(12)}(\varphi^{(2)})$ and $\theta^{(23)}(\varphi^{(2)})$ are the phase angles. Since the wave reproduces itself, it holds

$$-2\theta^{(12)} - 2\theta^{(23)} + 2k_0\gamma^{(2)}d = 2\pi m \,, \qquad m = 0,\, 1,\, 2,\, \ldots \,. \tag{4.4}$$

Hence we obtained one of possible features of the **waveguide characteristic equation**,

$$k_0\gamma^{(2)}d = \theta^{(12)} + \theta^{(23)} + \pi m \,. \tag{4.5}$$

Unlike the critical angles the phase shifts, $2\theta^{(12)}$ and $2\theta^{(23)}$, caused by the internal reflection at the angle $\varphi^{(2)}$ depend on the polarization. Therefore, the TE and TM waves have different solutions for the transverse resonance condition (4.5) resulting in different mode characteristics for a given mode number m.

4.2.2 Dispersion relations

Resonance states in a waveguide system correspond to the poles (singularities] of generalized Fresnel coefficients derived in the Subsection 3.2.2. This fact is expressed by the condition

$$M_{11}M_{33} - M_{13}M_{31} = 0 \,, \tag{4.6}$$

or, in the case of isotropic materials,

$$M_{11} = 0 \qquad \text{for TE wave} \,, \tag{4.7}$$

$$M_{33} = 0 \qquad \text{for TM wave} \,. \tag{4.8}$$

In the first case thw relation (3.81) gives

$$\left(\gamma^{(1)}\gamma^{(2)} + \gamma^{(2)}\gamma^{(3)}\right)\cos\tau + \mathrm{i}\left(\gamma^{(1)}\gamma^{(3)} + (\gamma^{(2)})^2\right)\sin\tau = 0$$

that can be rewritten in the form

$$\operatorname{tg}\tau = \mathrm{i}\frac{\gamma^{(1)}\gamma^{(2)} + \gamma^{(2)}\gamma^{(3)}}{\gamma^{(1)}\gamma^{(3)} + (\gamma^{(2)})^2}\ , \qquad \tau = k_0\gamma^{(2)}d\ . \tag{4.9}$$

The transverse propagation constants $\gamma^{(1)}$, $\gamma^{(3)}$ in surrounding media are imaginary due the total reflection, therefore, one is useful to introduce real constants $g^{(1)}$, $g^{(3)}$ as

$$\gamma^{(1)} = -\mathrm{i}g^{(1)}\ , \qquad g^{(1)} = \sqrt{(n^{(2)}\sin\varphi^{(2)})^2 - (n^{(1)})^2}\ , \tag{4.10}$$

$$\gamma^{(3)} = -\mathrm{i}g^{(3)}\ , \qquad g^{(3)} = \sqrt{(n^{(2)}\sin\varphi^{(2)})^2 - (n^{(3)})^2}\ . \tag{4.11}$$

Now, the relation (4.9) gains the real form

$$\operatorname{tg}\tau = \frac{\dfrac{g^{(1)}}{\gamma^{(2)}} + \dfrac{g^{(3)}}{\gamma^{(2)}}}{1 - \dfrac{g^{(1)}}{\gamma^{(2)}}\dfrac{g^{(3)}}{\gamma^{(2)}}}\ . \tag{4.12}$$

To obtain the patameter τ we use following formula:

$$\operatorname{arctg}\frac{a+b}{1-ab} = \operatorname{arctg} a + \operatorname{arctg} b\ .$$

Thus,

$$\tau = \operatorname{arctg}\frac{g^{(1)}}{\gamma^{(2)}} + \operatorname{arctg}\frac{g^{(3)}}{\gamma^{(2)}} + m\pi\ , \tag{4.13}$$

where m is a non-negative integer.

In case of TM wave (p-polarized light beam, i.e. $M_{33} = 0$) we set equal to zero the expression (3.83). Hence

$$p_3\cos\tau + \mathrm{i}p_4\sin\tau = 0\ , \tag{4.14}$$

where

$$p_3 = \varepsilon^{(2)}\varepsilon^{(3)}\gamma^{(1)}\gamma^{(2)} + \varepsilon^{(1)}\varepsilon^{(2)}\gamma^{(2)}\gamma^{(3)}\ ,$$
$$p_4 = (\varepsilon^{(2)})^2\gamma^{(1)}\gamma^{(3)} + \varepsilon^{(1)}\varepsilon^{(3)}(\gamma^{(2)})^2$$

(see the Subsection 3.2.4). Similarly as in the TE case, we obtain

$$\operatorname{tg}\tau = \mathrm{i}\frac{\varepsilon^{(2)}\varepsilon^{(3)}\gamma^{(1)}\gamma^{(2)} + \varepsilon^{(1)}\varepsilon^{(2)}\gamma^{(2)}\gamma^{(3)}}{(\varepsilon^{(2)})^2\gamma^{(1)}\gamma^{(3)} + \varepsilon^{(1)}\varepsilon^{(3)}(\gamma^{(2)})^2}\ , \tag{4.15}$$

and, final real-valued form

$$\operatorname{tg}\tau = \frac{\dfrac{\varepsilon^{(2)}g^{(1)}}{\varepsilon^{(1)}\gamma^{(2)}} + \dfrac{\varepsilon^{(2)}g^{(3)}}{\varepsilon^{(3)}\gamma^{(2)}}}{1 - \dfrac{\varepsilon^{(2)}g^{(1)}}{\varepsilon^{(1)}\gamma^{(2)}}\dfrac{\varepsilon^{(2)}g^{(3)}}{\varepsilon^{(3)}\gamma^{(2)}}} \ . \tag{4.16}$$

Again, a conversion to inverse tangent is possible,

$$\tau = \operatorname{arctg}\frac{\varepsilon^{(2)}g^{(1)}}{\varepsilon^{(1)}\gamma^{(2)}} + \operatorname{arctg}\frac{\varepsilon^{(2)}g^{(3)}}{\varepsilon^{(3)}\gamma^{(2)}} + m\pi \ . \tag{4.17}$$

4.2.3 Equivalence of resonance relations

Let we show that above dispersion relations are in accordance with transverse resonance condition (4.5)

$$k_0\gamma^{(2)}d = \theta^{(12)} + \theta^{(23)} + \pi m \ .$$

Without loss of generality we can consider resonance condition of the TE polarized wave

$$\left(\gamma^{(1)}\gamma^{(2)} + \gamma^{(2)}\gamma^{(3)}\right)\cos\tau + \mathrm{i}\left(\gamma^{(1)}\gamma^{(3)} + (\gamma^{(2)})^2\right)\sin\tau = 0 \ ,$$

where we replace goniometrical functions by complex exponentials as

$$\cos\tau = \frac{1}{2}\left(\mathrm{e}^{\mathrm{i}\tau} + \mathrm{e}^{-\mathrm{i}\tau}\right) \ , \qquad \sin\tau = \frac{1}{2\mathrm{i}}\left(\mathrm{e}^{\mathrm{i}\tau} - \mathrm{e}^{-\mathrm{i}\tau}\right) \ .$$

Simple rearrangements lead to following formula:

$$1 + \frac{\gamma^{(1)} - \gamma^{(2)}}{\gamma^{(1)} + \gamma^{(2)}}\,\frac{\gamma^{(2)} - \gamma^{(3)}}{\gamma^{(2)} + \gamma^{(3)}}\mathrm{e}^{-2\mathrm{i}\tau} = 0 \ , \tag{4.18}$$

where the fractions represent Fresnel reflection coefficients $r_s^{(12)}$, $r_s^{(23)}$ at the waveguide interfaces – see (3.28). However, we must set $r_s^{(21)} = -r_s^{(12)}$ instead $r_s^{(12)}$ at the interface between waveguide and cladding, so that the resonance condition results as

$$1 - r_s^{(12)}r_s^{(23)}\mathrm{e}^{-2\mathrm{i}\tau} = 0 \ . \tag{4.19}$$

Taking Eq. (4.3) in account for totally reflected wave, we obtain the resonance condition (4.5) putting $1 = \mathrm{e}^{-2\mathrm{i}m\pi}$.

4.2.4 Electromagnetic field model

Dispersion relation can be derived directly by solution of Maxwell's equations in the layers of waveguide system. This approach is valuable to its universality that is of use in another optical structures modeling. Consider TE polarized wave in waveguide system by the Figure 4.2, where the isotropic non-absorbing materials are supposed. With regard to boundary conditions we target the tangential components E_x, H_y of electromagnetic intesities composed from forward and backward wave in the expression (2.22). In particular, only the backward wave propagates in the superstrate, and, similarly, only forward wave lives in the substrate. Thus, the electric field component can be expressed as

$$E_x = \mathrm{e}^{-\mathrm{i}k_0\beta y}\begin{cases} A^{(1)}\mathrm{e}^{\mathrm{i}k_0\gamma^{(1)}z}\,, & z<0\,,\\ A^{(2-)}\mathrm{e}^{\mathrm{i}k_0\gamma^{(2)}z}+A^{(2+)}\mathrm{e}^{-\mathrm{i}k_0\gamma^{(2)}z}\,, & 0<z<d,\\ A^{(3)}\mathrm{e}^{-\mathrm{i}k_0\gamma^{(3)}z}\,, & z<d\,. \end{cases} \tag{4.20}$$

It is easy to derive from Maxwell's equations that it holds in the TE case

$$H_y = -\frac{\mathrm{i}}{k_0}\sqrt{\frac{\varepsilon_0}{\mu_0}}\frac{\partial E_x}{\partial z}\ . \tag{4.21}$$

Hence

$$H_y = \sqrt{\frac{\varepsilon_0}{\mu_0}}\mathrm{e}^{-\mathrm{i}k_0\beta y}\begin{cases} \gamma^{(1)}A^{(1)}\mathrm{e}^{\mathrm{i}k_0\gamma^{(1)}z}\,, & z<0\,,\\ \gamma^{(2)}A^{(2-)}\mathrm{e}^{\mathrm{i}k_0\gamma^{(2)}z}-\gamma^{(2)}A^{(2+)}\mathrm{e}^{-\mathrm{i}k_0\gamma^{(2)}z}\,, & 0<z<d,\\ -\gamma^{(3)}A^{(3)}\mathrm{e}^{-\mathrm{i}k_0\gamma^{(3)}z}\,, & z<d\,. \end{cases} \tag{4.22}$$

The constants $A^{(1)}$, $A^{(2-)}$ $A^{(2+)}$, $A^{(3)}$ can be obtained as a solution of algebraic problem following from boundary conditions application at the interfaces:

$$\begin{aligned} &E_x^{(1)}(0) = E_x^{(2)}(0) \quad \dots \quad A^{(1)} = A^{(2-)} + A^{(2+)}\ ,\\ &H_y^{(1)}(0) = H_y^{(2)}(0) \quad \dots \quad \gamma^{(1)}A^{(1)} = \gamma^{(2)}A^{(2-)} - \gamma^{(2)}A^{(2+)}\ ,\\ &E_x^{(2)}(d) = E_x^{(3)}(d) \quad \dots \quad A^{(2-)}\mathrm{e}^{\mathrm{i}k_0\gamma^{(2)}d} + A^{(2+)}\mathrm{e}^{-\mathrm{i}k_0\gamma^{(2)}d} = A^{(3)}\mathrm{e}^{-\mathrm{i}k_0\gamma^{(3)}d}\ ,\\ &H_y^{(2)}(d) = H_y^{(3)}(d) \quad \dots \quad \gamma^{(2)}\left(A^{(2-)}\mathrm{e}^{\mathrm{i}k_0\gamma^{(2)}d} - A^{(2+)}\mathrm{e}^{-\mathrm{i}k_0\gamma^{(2)}d}\right) = -\gamma^{(3)}A^{(3)}\mathrm{e}^{-\mathrm{i}k_0\gamma^{(3)}d}\ . \end{aligned}$$

The term $A^{(3)}\exp\{-\mathrm{i}k_0\gamma^{(3)}d\}$ can be eliminated in the last two equations. Thus, to get a non-trivial solution of the reduced equation system, the follow-

ing determinant must be zero (again, $k_0\gamma^{(2)}d = \tau$):

$$\begin{vmatrix} 1 & -1 & -1 \\ \gamma^{(1)} & -\gamma^{(2)} & \gamma^{(2)} \\ 0 & \mathrm{e}^{\mathrm{i}\tau} & \mathrm{e}^{-\mathrm{i}\tau} \\ 0 & (\gamma^{(2)}+\gamma^{(3)})\mathrm{e}^{\mathrm{i}\tau} & -(\gamma^{(2)}-\gamma^{(3)})\mathrm{e}^{-\mathrm{i}\tau} \end{vmatrix} = 0 \ ,$$

where the columns ordering relates to the constants $A^{(1)}$, $A^{(2-)}$, $A^{(2+)}$. The evaluated expression

$$(\gamma^{(1)}+\gamma^{(2)})(\gamma^{(2)}+\gamma^{(3)}) + (\gamma^{(1)}-\gamma^{(2)})(\gamma^{(2)}-\gamma^{(3)})\mathrm{e}^{-2\mathrm{i}\tau} = 0 \qquad (4.23)$$

is in accordance with the formula (4.18) in previous subsection. Analogous way leads to the dispersion relation in the case of TM polarized field.

4.3 Waveguide modes

4.3.1 Classification

A waveguide mode is a transverse field pattern whose amplitude and polarization profiles remain constant along the longitudinal coordinate. Before a discussion about structure of waveguide field we proceed to more physically objective formulation of dispersion equations (4.13) and (4.17). To this purpose we introduce frequently used waveguide parameter as the **effective refractive index**

$$N = n^{(1)} \sin\varphi^{(2)} \ . \qquad (4.24)$$

Thus, the modified propagation constants $g^{(1)}$, $g^{(3)}$ in surrounding media take the forms

$$g^{(1)} = \sqrt{N^2 - (n^{(1)})^2} \ , \qquad g^{(3)} = \sqrt{N^2 - (n^{(3)})^2} \ . \qquad (4.25)$$

The unified form of **dispersion relation** of a dielectric waveguide can be written as

$$k_0 d\sqrt{(n^{(2)})^2 - N^2} = \mathrm{arctg}\left[\left(\frac{n^{(2)}}{n^{(1)}}\right)^{2c}\sqrt{\frac{N^2-(n^{(1)})^2}{(n^{(2)})^2-N^2}}\right] +$$

$$+ \quad \mathrm{arctg}\left[\left(\frac{n^{(2)}}{n^{(3)}}\right)^{2c}\sqrt{\frac{N^2-(n^{(3)})^2}{(n^{(2)})^2-N^2}}\right] + m\pi \ , \qquad c = \begin{cases} 0 & (\text{TE wave}), \\ 1 & (\text{TM wave}) \end{cases} \ . \qquad (4.26)$$

where the condition $n^{(1)} < n^{(3)} < N < n^{(2)}$ holds for the guided modes. These are denoted regarding the polarization state as TE_0, TM_0, TE_1, TM_1 etc. Besides the **guided modes** we can classify the two kinds of the **radiation modes** (see Figure 4.3):

- substrate mode, when $n^{(1)} < N < n^{(3)} < n^{(2)}$,
- superstrate mode, when $N < n^{(1)} < n^{(3)} < n^{(2)}$.

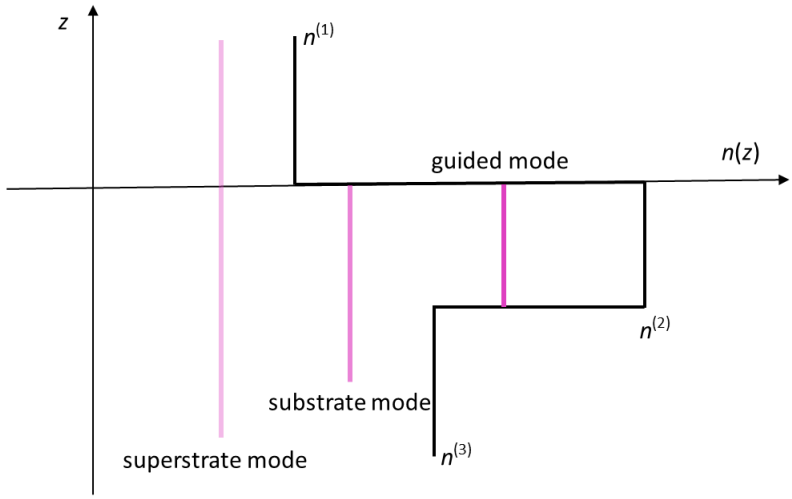

Fig. 4.3 Areas of waveguide modes.

Resolving dispersion equation with regard to the m-th mode effective refractive index N_m needs an appropriate numerical method. A solution exists only for finite number of mode indices m, because left-hand side term is less than $\sqrt{(n^{(2)})^2 - (n^{(3)})^2}$, and, the function 'arctg' values move from 0 to $\pi/2$. The m-th mode vanishes, when $N_m = n^{(3)}$, i.e. by the **critical waveguide thickness**

$$d_{m,crit} = \frac{1}{k_0\sqrt{(n^{(2)})^2 - (n^{(3)})^2}} \left\{ \text{arctg} \left[\left(\frac{n^{(2)}}{n^{(3)}} \right)^{2c} \frac{\sqrt{(n^{(3)})^2 - (n^{(1)})^2}}{\sqrt{(n^{(2)})^2 - (n^{(3)})^2}} \right] + m\pi \right\} . \tag{4.27}$$

Since $n^{(2)} > n^{(3)}$ the TM modes have slightly greater critical thickness than TE modes.

Dispersion diagram is an usual tool to demonstrate graphically dispersion characteristics of guided modes. Typically it represents dependence

between effective refractive index N and **waveguide thickness** d at a fixed wavelength.

Example

The Figure 4.4 is performed for bismuth-doped iron garnet waveguide (Bi:GIG) prepared on a gallium–gadolinium garnet (GGG) substrate. Refractive indices of these materials at the wavelength 633 nm ($n^{(2)} = 2.4619$ for Bi:GIG, $n^{(3)} = 1.9648$ for the GGG substrate [17]) enable to clearly analyze waveguiding properties.

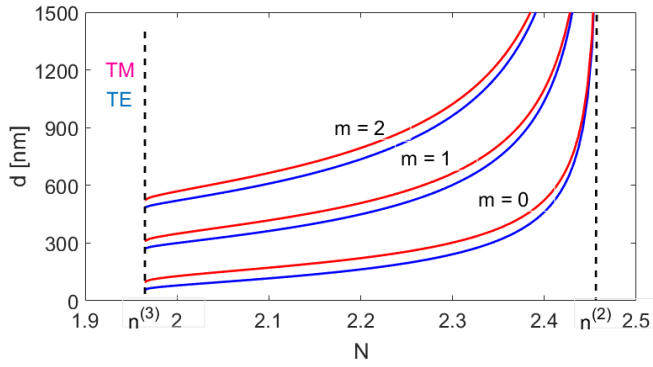

Fig. 4.4 Dispersion diagram of the Bi:GIG waveguide.

All dispersion curves are situated in the interval $\langle n^{(3)}, n^{(2)} \rangle$, the critical thicknesses increase with the mode number m from the critical values $d = 58$ nm and $d = 97$ nm for the TE_0 and TM_0 modes, respectively. By any choose of the waveguide layer thickness the number of guided modes can be estimated at corresponding horizontal line.

4.3.2 Symmetric waveguide

There are two noticeable waveguide types – the **waveguide with weak guidance** and **symmetric waveguide** that we will discuss separately. In a symmetric waveguide refractive indices of the substrate and superstrate are iden-

tical, $n^{(3)} = n^{(1)}$. The symbolic dispersion relation takes the simplified form

$$\operatorname{tg}\tau = 2 \begin{cases} \dfrac{g^{(1)}\gamma^{(2)}}{\left(\gamma^{(2)}\right)^2 - \left(g^{(1)}\right)^2}, & \text{(TE)}, \\ \dfrac{\left(n^{(1)}n^{(1)}\right)^2 g^{(1)}\gamma^{(2)}}{\left(n^{(1)}\gamma^{(2)}\right)^2 - \left(n^{(2)}g^{(1)}\right)^2}, & \text{(TM)}\ . \end{cases} \tag{4.28}$$

Thus, the common dispersion equation (4.26) follows as

$$k_0 d\sqrt{(n^{(2)})^2 - N^2} = 2\ \text{arctg}\left[\left(\frac{n^{(2)}}{n^{(1)}}\right)^{2c}\sqrt{\frac{N^2 - (n^{(1)})^2}{(n^{(2)})^2 - N^2}}\right] + m\pi\ . \tag{4.29}$$

This result means that critical thickness of the zero-order modes is zero; in other words, in the symmetric waveguide a mode can be allways excited.

Example

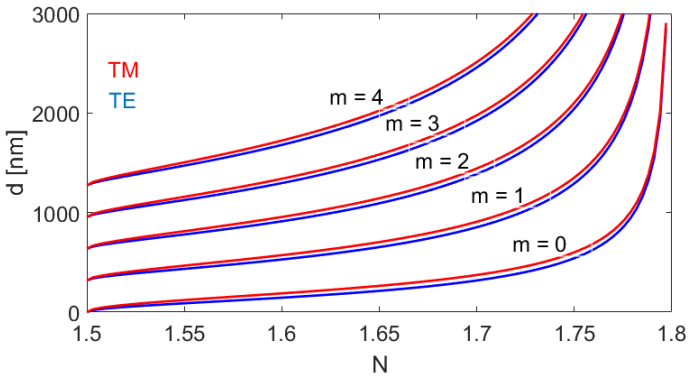

Fig. 4.5 Dispersion diagram of the symmetric waveguide modes.

We demonstrate a symmetrical case by the waveguide, in which the aluminium-dopped zinc oxide (AZO, $n^{(2)} = 1.8$) is sandwiched between glass plates ($n^{(1)} = 1.5$). The Figure 4.5 shows obtained dipersion diagram for the first five modes.

In the subsection 4.2.4 the algebraic system for the TE field components in any layer of waveguide system has been derived; a very similar one can be also obtained in the case of TM polarization. In the both cases it has an one-parametric solution for the constants $A^{(1)}$, $A^{(2+)}$, $A^{(2-)}$, $A^{(3)}$. Setting someone as the parameter and normalize resulting expressions we obtain

Tab. 4.1 Mode parameters to the Figure 4.6, the other data by the Figure 4.5.

mode order m	waveguide thickness d [nm]	effective refractive index N
0	140	1.563
2	600	1.545

graphical dependence of the field components on the normal coordinate z – see Figure 4.6 including the data in Table 4.1.

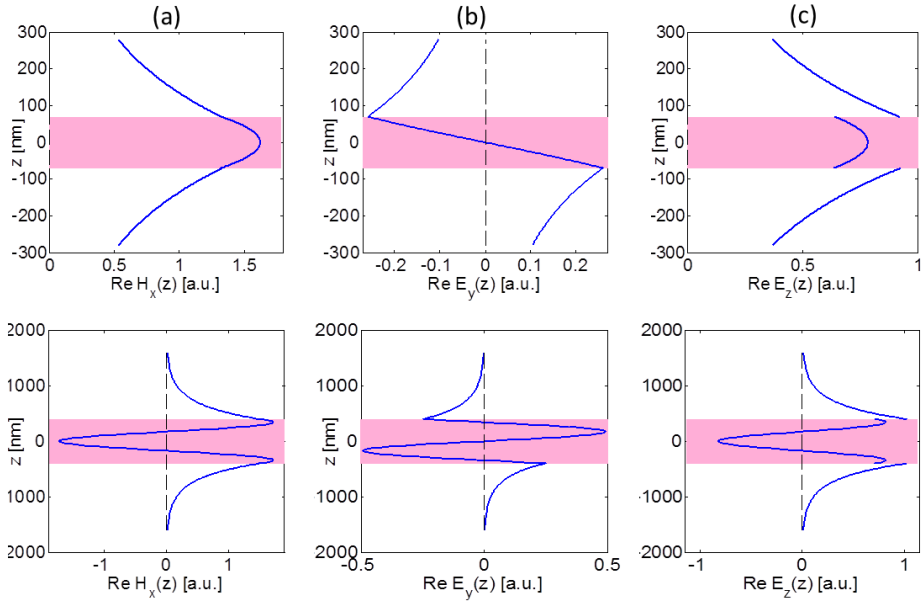

Fig. 4.6 The field components in a symmetrical waveguide: the TM_0 mode in upper row, the TM_2 mode in lower row.

Since the dependence on variable y is the same in each layer, we set $y = 0$ without loss of generality. Notice that the tangential components H_x and E_y are continuous at interfaces (the columns (a), (b) in the Figure) unlike the normal component E_z. In all the cases the field exponentially decreases outwards the waveguiding layer because of evanescent wave character, whereas the guided wave has harmonic character. This property is better apparent by the TM_2 mode.

4.3.3 Weakly guided modes

These modes are excited in a waveguide, the superstrate refractive index $n^{(1)}$ of which is expressive less than the other two indices being of small difference.

Several important consequences of this waveguide construction follow from modified dispersion relations. The dispersion lines of TE and TM modes in dispersion diagram are very close – see Figure 4.7. Further, supposing $n^{(2)} \approx n^{(3)} >> n^{(1)}$ we have also $\gamma^{(2)} \approx g^{(3)} >> \gamma^{(1)}$. Thus, the both relations (4.13) and (4.17) become the same simplified form

$$\operatorname{tg} \tau = \frac{g^{(3)}}{\gamma^{(2)}} \ , \tag{4.30}$$

therefore, the dispersion equation contains only two material parameters:

$$k_0 d \sqrt{(n^{(2)})^2 - N^2} = 2 \ \operatorname{arctg} \frac{\sqrt{N^2 - (n^{(3)})^2}}{\sqrt{(n^{(2)})^2 - N^2}} + m\pi \ . \tag{4.31}$$

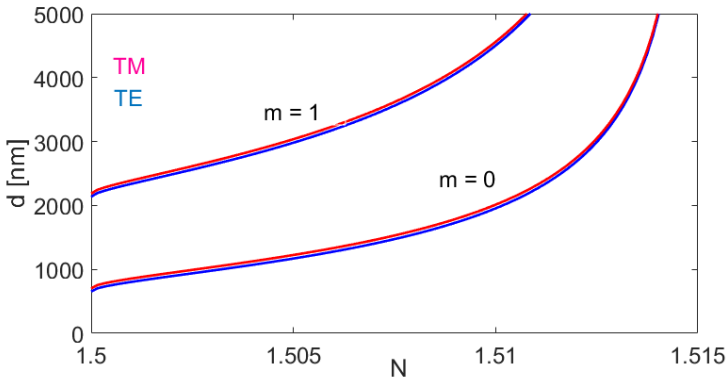

Fig. 4.7 Dispersion diagram of the first two mode in asymmetric waveguide: air superstrate ($n^{(1)} = 1$), BK7 glass waveguiding layer ($n^{(2)} = 1.5151$), glass ($n^{(3)} = 1.5$).

In the case of weak guidance the obvious relation $(\gamma^{(2)})^2 + (g^{(3)})^2 = (n^{(2)})^2 - (n^{(3)})^2$ motivates to introduce the frequently used dimensionless parameter

$$V = k_0 d \sqrt{(n^{(2)})^2 - (n^{(3)})^2} \tag{4.32}$$

called **normalized frequency**. It contains all physical quantities influencing giuded modes. Especially, a guidance condition of the m-th order mode follows easy from (4.31) as

$$V > \frac{1}{2}(2m+1)\pi \ .$$

Energy of weakly guided wave is concentrated near the optically thinner superstrate so that this waveguide type is referred as asymmetric one. This fact is cleary viewed, when the field components in waveguiding structure are analyzed. Graphical output performed similarly as in previous subsection is presented in the Figure 4.8 for the TM_0 mode and the data by the Figure 4.7.

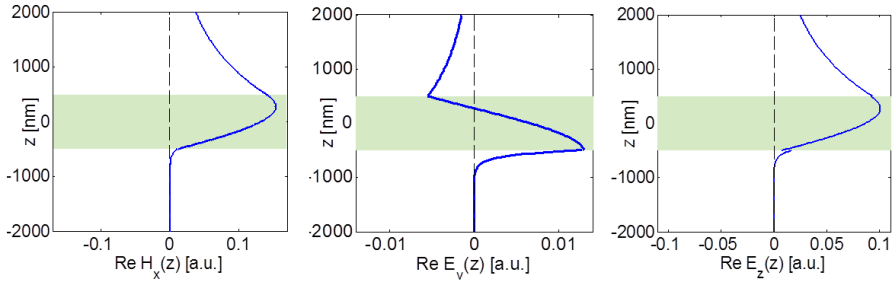

Fig. 4.8 The field components of the TM_0 mode in an asymmetric waveguide ($d = 100$ nm, $N = 1.503$).

4.3.4 Waveguiding structures with coupling prism

Weakly guided modes can be easy coupled and decoupled that enables construction of sensing devices, optical circuits elements and another applications. A widely used method is based on the implementation of coupling prism with refractive index higher than this one of waveguiding medium. A thin low index coupling gap between prism and waveguide layer allows prospective 'tunning' of such system by a change of the thickness and/or material properties. Consider again the Bi:GIG waveguiding structure as in the Subsection 4.3.1 that is supplied by the rutile coupling prism ($n^{(0)} = 2.54$ at the wavelegth 633 nm) – see the scheme 4.9(a). Simulation of the reflectometric response at Figure 4.9(b) shows the resonance dips of the first three guided modes for the both polarizations. The highest mode number $m = 2$ follows from the chosen waveguide thickness $d = 650$ nm (cf. Figure 4.4).

In order to reach the one-mode waveguide regime the thickness d must be less than critical thickness of the second-order mode. Here, this condition is satisfied for the waveguide thickness $d = 120$ nm (Figure 4.10(a)). The coupling forces decrease by the growing gap thickness. The Figure 4.10(b) illustrates this fact for the two times bigger gap thickness in the 650 nm waveguiding structure by the Figure 4.9(b).

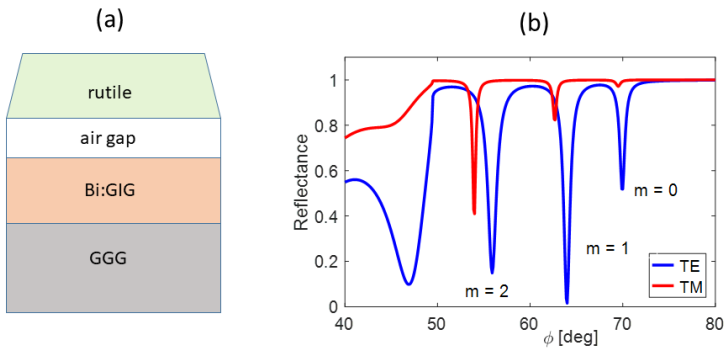

Fig. 4.9 Reflectometric output from a waveguide. (a) High-index waveguide scheme, (b) resonance dips (gap thickness $t_g = 50$ nm).

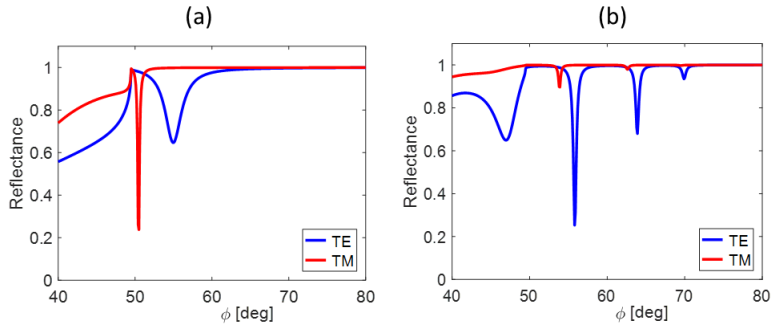

Fig. 4.10 (a) One-mode waveguide configuration: $d = 120$ nm, $t_g = 50$ nm, (b) coupling condition weakening: $d = 100$ nm, $t_g = 650$ nm.

4.3.5 Excersise

4.3.5.1

Compute critical thicknesses of the air/AZO/SiO_2 waveguide for the both TE and TM modes on the orders 0, 1, 2. Use the refractive indices 1/1.8/1.5.

4.3.5.2

Why the critical thickness of a symmetric waveguide is the same for the both principal polarizations?

4.3.5.3

How we do choose the thickness of a weakly guiding waveguide with the parameters by the Fig. 4.7 (at the wavelength 633 nm) to the second order mode guidance?

Chapter 5

Plasmon Waves

5.1 Plasmon polaritons in planar structures

5.1.1 Plasmon wave generation

The term **surface plasmons** refers to multiple excitations of electrons coupled to the interface between a dielectric and a conductor. The real part of the permittivity of the used metal, $\mathrm{Re}\,(\varepsilon_m)$, then has to be negative and its size greater than the size of the permittivity of the adjacent dielectric ε_d,

$$|\mathrm{Re}\,(\varepsilon_m)| > \varepsilon_d \ ;$$

the imaginary part has to be small enough at the same time. At optical wavelengths, this condition is fulfilled by several (noble) metals of which gold and silver the most commonly used. Owing to high loss in the metal, the surface plasmon waves propagate with high attenuation in the visible and near-infrared spectral regions.

Total reflection in transition from an optically denser medium to an optically rarer medium is used in the first case. The phenomena occurrence is caused either on metal surface "by aspiration" of an evanescent wave from a thin dielectric layer, a so called gap (**Otto configuration** – Fig. 5.1a) or directly in thin metal film by excitation of electrons (**Kretschmann-Raether** configuration – Fig. 5.1b). In the case of a grating diffraction occurs on an interface having periodicity comparable with the wavelength of the impinging beam. As a result of interference, reflected and transmitted modes are produced on one hand and evanescent modes propagating along the interface, which may also excite surface plasmons, are produced on the other hand (Fig. 5.1c). We must stress that it is necessary in all these cases that the incident wave is linearly polarized in the plane of incidence, i.e., it exhibits transversal magnetic (TM) polarization. This fact is explained in the next subsection.

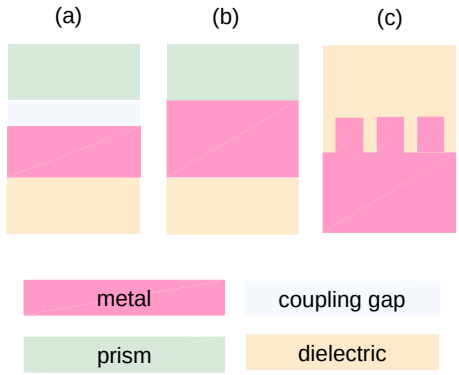

Fig. 5.1 Configuration for excitation of plasmon waves: (a) Otto, (b) Kretschmann-Raether, (c) metal grating.

5.1.2 Surface plasmon dispersion relations

Plasmon waves that freely move along a surface represent propagating electromagnetic waves, and, form a class of quasi-particles called **plasmon polaritons**. At first, we consider a sandwich optical structure 'superstrate/thin metallic film/substrate' with the permittivities $\varepsilon^{(1)}$, $\varepsilon^{(2)}$, $\varepsilon^{(3)}$, respectively, for which we aim to derive components of electromagnetic field vectors $\boldsymbol{E} = (0,\, E_y,\, E_z)$, $\boldsymbol{H} = (H_x,\, 0,\, 0)$ for a TM incident wave. This situation can be viewed as a waveguide system discussed in previous chapter in the Subsection 4.2.4. Similarly as in the mentioned case we start with the transversal component H_x that we write in accordance with (4.20) as

$$H_x = \mathrm{e}^{-\mathrm{i}k_0\beta y} \begin{cases} C^{(1)}\mathrm{e}^{\mathrm{i}k_0\gamma^{(1)}z}\,, & z < 0\,, \\ C^{(2-)}\mathrm{e}^{\mathrm{i}k_0\gamma^{(2)}z} + C^{(2+)}\mathrm{e}^{-\mathrm{i}k_0\gamma^{(2)}z}\,, & 0 < z < d, \\ C^{(3)}\mathrm{e}^{-\mathrm{i}k_0\gamma^{(3)}z}\,, & z < d\,. \end{cases} \tag{5.1}$$

Tangential component of the field $\boldsymbol{E}$ follows from Maxwell's equations in the form

$$E_y = -\frac{\mathrm{i}}{k_0\varepsilon}\sqrt{\frac{\mu_0}{\varepsilon_0}}\frac{\partial H_x}{\partial z}\,, \tag{5.2}$$

i.e.,

$$E_y = \sqrt{\frac{\mu_0}{\varepsilon_0}}\mathrm{e}^{-\mathrm{i}k_0\beta y}\begin{cases}\gamma^{(1)}/\varepsilon^{(1)}A^{(1)}\mathrm{e}^{\mathrm{i}k_0\gamma^{(1)}z}\,, & z<0\,,\\ \gamma^{(2)}/\varepsilon^{(2)}\left(A^{(2-)}\mathrm{e}^{\mathrm{i}k_0\gamma^{(2)}z}-A^{(2+)}\mathrm{e}^{-\mathrm{i}k_0\gamma^{(2)}z}\right)\,, & 0<z<d,\\ -\gamma^{(3)}/\varepsilon^{(3)}A^{(3)}\mathrm{e}^{-\mathrm{i}k_0\gamma^{(3)}z}\,, & z<d\,.\end{cases} \tag{5.3}$$

To exploit a similarity with the TE field discussed in the Subsections 4.2.2-4 we denote

$$\hat{\gamma}^{(\kappa)} = \frac{\gamma^{(\kappa)}}{\varepsilon^{(\kappa)}}\,, \qquad \kappa = 1,\,2,\,3\,. \tag{5.4}$$

Thus, we obtain congenerous algebraic system performed by application of boundary conditions for the constants $C^{(\kappa)}$, the singularity of which implies the **resonance condition**

$$1+\frac{\hat{\gamma}^{(1)}-\hat{\gamma}^{(2)}}{\hat{\gamma}^{(1)}+\hat{\gamma}^{(2)}}\,\frac{\hat{\gamma}^{(2)}-\hat{\gamma}^{(3)}}{\hat{\gamma}^{(2)}+\hat{\gamma}^{(3)}}\mathrm{e}^{-2\mathrm{i}\tau}=0\,. \tag{5.5}$$

Applying the sign change at the first interface (see the Subsection 4.2.3 for explanation), the previous formula can be easy rearranged using Fresnel coefficients for TM wave:

$$1-r_p^{(12)}r_p^{(23)}\mathrm{e}^{-2\mathrm{i}\tau}=0\,, \qquad \tau=\mathrm{i}k_0\gamma^{(2)}d\,. \tag{5.6}$$

Notably, to guide plasmon polaritons, a single metal/dielectric interface suffices. The dispersion relation of those polaritons can be derived from Eqs. (4.18) and (5.6), if we put $d\to\infty$. In this way, we get

$$\gamma^{(1)}+\gamma^{(2)} = 0\,, \tag{5.7}$$

$$\hat{\gamma}^{(1)}+\hat{\gamma}^{(2)} = 0 \tag{5.8}$$

for the TE and TM polarizations, respectively. In superstrate, the propagation constant $\gamma^{(1)}=\sqrt{\varepsilon^{(1)}}\cos\varphi$ represents a harmonic wave at the incidence angle φ. In metallic substrate, the evanescent wave propagates with constant $\gamma^{(2)}=-\mathrm{i}\sqrt{\beta^2-\varepsilon^{(2)}}$, where $\beta=\sqrt{\varepsilon^{(1)}}\sin\varphi$.

The dispersion equation for the TE polarization has no solution. This means that a single dielectric/metal interface does not support any wave of TE type. At the same time, the equation for the TM polaritons has one solution, which is given by

$$\frac{\gamma^{(1)}}{\varepsilon^{(1)}}+\frac{\gamma^{(2)}}{\varepsilon^{(2)}}=0\,, \tag{5.9}$$

Hence,

$$\beta=\sqrt{\frac{\varepsilon^{(1)}\varepsilon^{(2)}}{\varepsilon^{(1)}+\varepsilon^{(2)}}}\,. \tag{5.10}$$

Usually, this result is referred in the form that emphasizes the **plasmon resonance angle** φ_{SP}. Assuming an incoming wave from lossless medium (e.g. prism) with the tangential wavevector component $k_y = k_0\beta = k_0 n_i \sin\varphi$ we have

$$n_i \sin\varphi_{SP} = \frac{n_d n_m}{\sqrt{n_d^2 + n_m^2}} , \tag{5.11}$$

where n_d and n_m are refractive indices of dielectric and metal.

5.1.3 Examples

5.1.3.1 Kretschmann configuration

The basic model situation is illustrated in Figure 5.2 by the course of the transversal component of magnetic intensity at the wavelength $\lambda = 632.8$ nm. The wave propagates from the left to right; a harmonic wave is incoming from the prism, exponential character of the evanescent wave in total reflection is clearly visible.

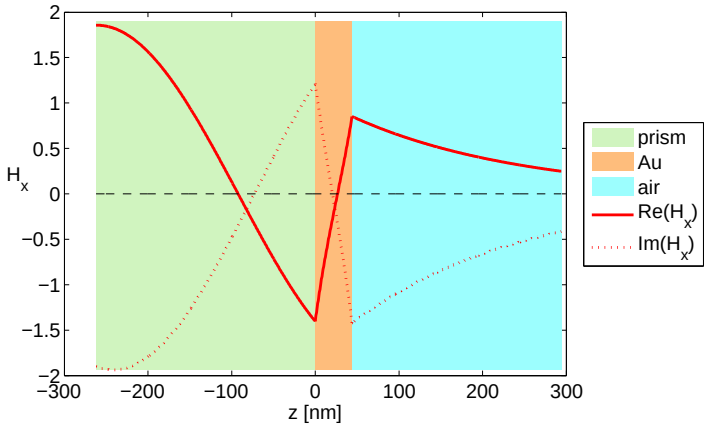

Fig. 5.2 Transversal component of intensity $\boldsymbol{H}_x$ as a function of the coordinate perpendicular to the interfaces (44 nm thick Au layer).

5.1.3.2 Otto configuration

Plasmon waves cannot be directly registered outside an optical system, however their existence can be proven, e.g., as a local decrease of energy of a reflected beam. From the viewpoint of experimental applications, the Otto

configuration is often more attractive. In the case of metal layer damage the prism does not have to be replaced like in Kretschmann configuration. The reflection response in Fig. 5.3 is the result, the theoretical model is accompanied by experimental data obtained in the laboratory of the Institute of Physics of VŠB-TUO Ostrava few years ago.

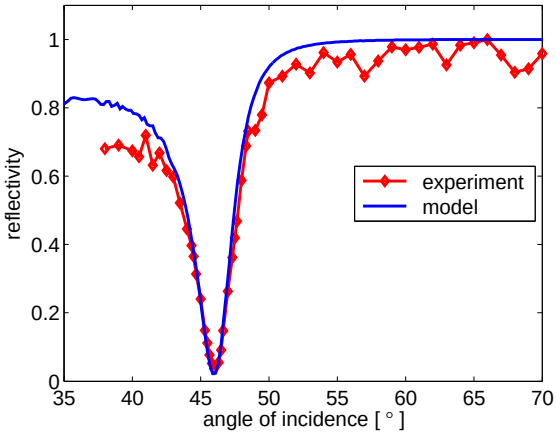

Fig. 5.3 Otto configuration: model comparison with the experiment.

In accordance with experimental setup the system 'prism/gap (400 nm)/gold (44 nm)/glass' for wavelength 632.8 nm was modeled with corresponding refractive indices $n^{(0)} = 1.5151$ (prism of borosilicate glass BK7), $n^{(1)} = 1$ (air coupling gap), $n^{(2)} = 0.1428 - 3.5429\mathrm{i}$ (Au film) and $n^{(3)} = 1.76$ (glass base of heavy flint glass SF10).

5.2 Surface pasmon polariton applications

5.2.1 Plasmonic sensing principle

Surface plasmon resonance (SPR) has become a widely accepted optical technique for studying biological and chemical interactions. Among other, detecting small changes in analyte concentration in complex solutions remains challenging, e.g. because of the need of distinguishing the interaction of interest from other effects. In particular, non-specific binding and/or background refractive index changes are problematic in the multi-component analytes, e.g. in medicine, food safety and environmental applications.

Typically, the SPR sensor is characterized by its **sensitivity**, **penetration depth**, and perhaps even by **full width of half-minimum** (FWHM) of the reflectance dip. In the angular interrogation mode the traditional sensing device has angular sensitivity of 50-100 deg/RIU, where RIU denotes refractive index units.

Tab. 5.1 Example of modeled sensitivity analysis of SPR.

aerosol refraction index $n^{(s)}$	1.00	1.02	1.05
resonance angle φ_{SP} [°]	43.654	44.865	46.745

The following model problem for planar system in Kretschmann-Raether configuration for optical TIR structure can serve as an illustrative example of SPR sensitivity. Optical nanostructure consists of a prism (BK7 glass), 50 nm thick Au film and substrate, which is air or as the case may be aerosol. The Table 5.1 obtained for wavelength 690 nm shows how a very small change of aerosol refraction index (in practice for example a change of adjacent media contamination) affects the SPR system response expressed by reflectance R_p. A mere one hundredth difference in refraction index values induces a shift of the resonance minimum by degrees, as also seen in Fig. 5.4.

Sensitivity (S) is the standard parameter of evaluation of SPR sensor sensitivity. In case of angular interrogation this one is defined as the ratio of resonance angle change to the change of the refractive index of the examined medium – analyte $n_a = n^{(s)}$:

$$S = \frac{\Delta\varphi_{\mathrm{SP}}}{\Delta n_a} \qquad [\mathrm{deg/RIU}] \ . \tag{5.12}$$

In presented example the simple calculation gives

$$S = \frac{3.091}{0.05} \approx 61 \quad \mathrm{deg/RIU} \ .$$

If the reflectance shift ΔR at fixed incidence angle is detected instead SPR dip angular shift, the sensitivity moves about 30 RIU^{-1} [18]. Figure 5.5 demonstrates a scheme of reflectance interrogation mode at fixed reference angle of incidence 53.2 deg for the structure 'SF10 glass prism/44 nm Au film/water' at the wavelength 633 nm. For this sensing configuration the sensitivity S is introduced as

$$S = \frac{\Delta R_p}{\Delta n_a} \qquad [1/\mathrm{RIU}] \ . \tag{5.13}$$

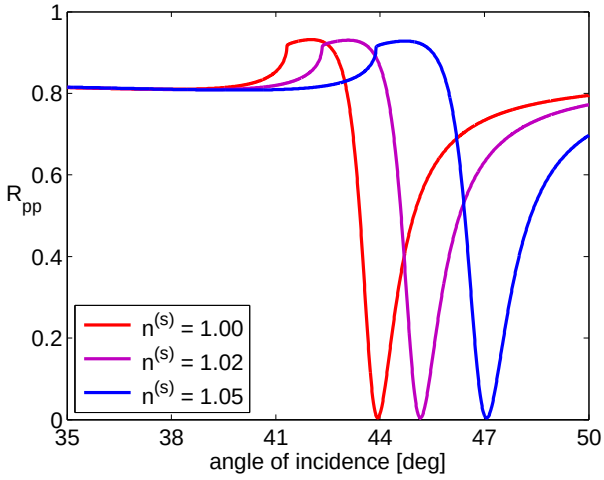

Fig. 5.4 Kretschmann configuration – dependence on substrate refraction index $n^{(s)}$.

The violet curves corrrespond to the analyte refractive indices n_a from 1.331 to 1.335 by the 0.001 step. Since the $\Delta R_p = 0.05$ increment depends linearly on Δn_a, the established sensitivity $S = 50$ RIU^{-1} is the same at any sub-interval.

Depending on applied measuring method the **resolution limit** less than 10^{-4} RIU can be achieved [19]. Denote $\varphi_{\mathrm{SP},min}$, $\Delta R_{p,min}$ the minimal measurable values in the previous model situations. Thus, the refractive index resolution limits follow as

$$\min(\Delta n_a) = \frac{\varphi_{\mathrm{SP},min}}{S}, \qquad \min(\Delta n_a) = \frac{\Delta R_{p,min}}{S}\ , \tag{5.14}$$

respectively. Supposing $\varphi_{\mathrm{SP},min} = 0.01$ deg, $\Delta R_{p,min} = 0.01$, we can expect the resolution limits 1.6×10^{-4} and 2×10^{-4} RIU.

5.2.2 MIM and IMI plasmonic structures

Penetration depth gives quite reliable indication of the usable distance, at which the SPR device is sensitive to changes in the analyte (≈ 200 nm at optical frequencies). In order to improve sensing parameters, several different ways were suggested to enhance detection limit of SPR sensors, penetration depth of those or specific application conditions. implementation of insulator-metal-insulator (IMI) or metal-insulator-metal (MIM) substructures that produce long-range surface plasmons (LR SPP) with lower absorption losses [20, 21];

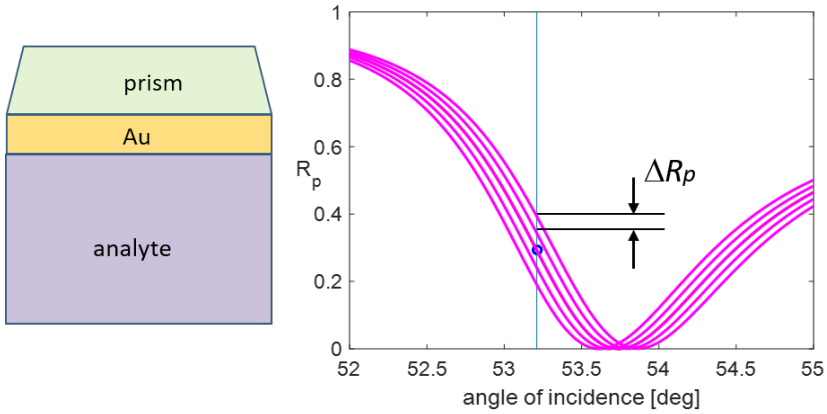

Fig. 5.5 Kretschmann configuration – a scheme of reflectance interrogation mode.

In **multiple-interface systems** the surface plasmon polaritons (SPPs) associated with individual interfaces can interact with each other. Considering the SPPs excited on two metal-dielectric interfaces one finds that plasmonic modes can be supported by either a thin metal film embedded in dielectric (insulator-metal-isnsulator structure, IMI) or by a thin dielectric layer surrounded by metal (metal-insulator-metal structure, MIM). Such optical substructure can be viewed as a waveguide system with specific properties (see e.g. [22]), therefore, again we can use the resonance condition (4.18) modified for TM wave as (5.6).

We will discuss the the MIM configuration considering a symmetric variant with the same metallic materials as the sub- and superstrate ($\varepsilon^{(3)} = \varepsilon^{(1)}$), for simplicity. In this case the relation (5.6) reads

$$1 - \left(\frac{\hat{\gamma}^{(1)} - \hat{\gamma}^{(2)}}{\hat{\gamma}^{(1)} + \hat{\gamma}^{(2)}} \right)^2 \mathrm{e}^{-2\mathrm{i}\tau} = 0 \,, \qquad \hat{\gamma}^{(\kappa)} = \frac{\gamma^{(\kappa)}}{\varepsilon^{(\kappa)}} \,. \tag{5.15}$$

If we write this equation as the product

$$\left(\mathrm{e}^{\mathrm{i}\tau} - \frac{\hat{\gamma}^{(1)} - \hat{\gamma}^{(2)}}{\hat{\gamma}^{(1)} + \hat{\gamma}^{(2)}} \right) \left(\mathrm{e}^{\mathrm{i}\tau} + \frac{\hat{\gamma}^{(1)} - \hat{\gamma}^{(2)}}{\hat{\gamma}^{(1)} + \hat{\gamma}^{(2)}} \right) = 0 \,, \tag{5.16}$$

then the two different solution lead to two types of SPPs. Generally, dispersion relation of this symmetric MIM structure gives four resonance states that represent two plasmonic and two photonic modes [22], particular setup of which depends on material as well as geometrical parameters of SPR structure. The roots of obtained equation can be found using appropriate numerical method, usually under certain additional assumptions [20].

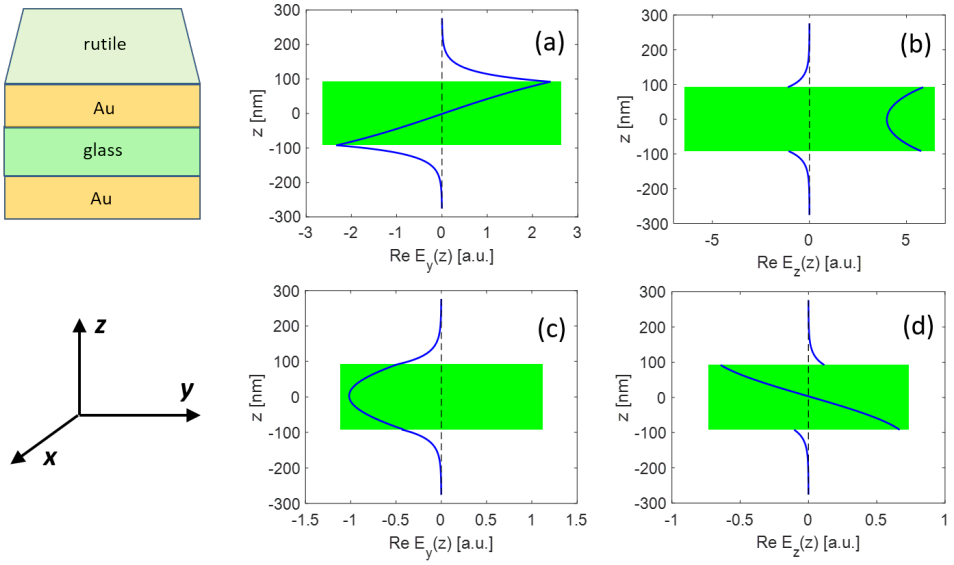

Fig. 5.6 Electric field components in the MIM structure Au – SiO_2 184 nm – Au coupled with rutile prism. (**a,b**) LR SPP with odd longitudinal field symmetry at resonance incidence angle 19.8 deg. (**c,d**) SR SPP with even symmetry of longitudinal field $E_y(z)$, incidence angle 44.4 deg.

Considering the rutile prism and SiO_2 gap between gold layers as an example, the photonic (i.e. guided) modes cannot exist in this system. On the other hand, one SPP mode survives for all values d of gap thickness. This mode exhibits odd symmetry of longitudinal electric field component E_y, and, consequently even symmetry of transversal component E_z (normal to the interface, incidence plane is perpendicular to the x axis) – see Figure 5.6a,b. For sufficiently thick dielectric interlayer also the other SPP type is supported having opposite characteristics of corresponding electric field components (Figure 5.6c,d). In agreement with described properties, these SPPs are termed asymmetric or symmetric ones. In the both cases, the longitudinal components are continuous regarding the boundary conditions.

Note, that frequently used nomenclature works with the **long-range** (LR) SPP in the case of asymmetric longitudinal component, and **short-range** (SR) SPP in opposite situation. This notation is typical for IMI plasmonic structures, where propagation length of the symmetric SPP is expressively less than of the asymmetric one. For the clarity, we also keep the LR/SR symbolics in this text.

The size of single MIM parts importantly influences the parameters of

plasmonic resonance states that brings an advantage in several applications. The thicknesses of lossy metallic layers must be sufficiently small in real situations. Therefore, the 44 nm gold film at the wavelength 633 nm in applied

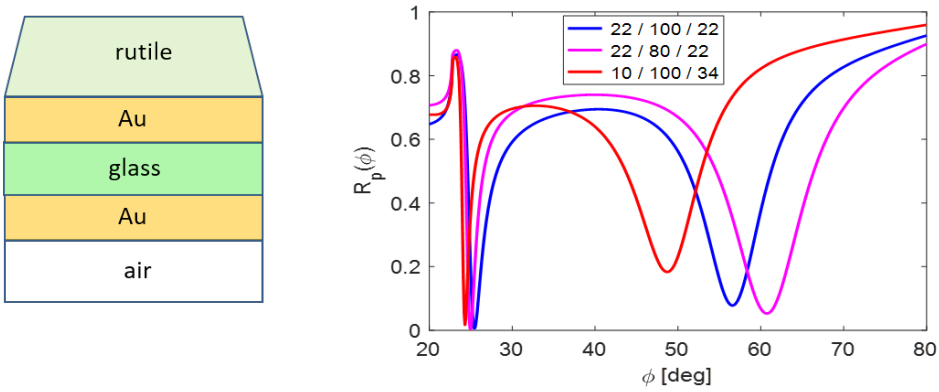

Fig. 5.7 Plasmonic resonance states in the MIM structure with thin Au films: the LR SPR minima on the left ($\phi \approx 25^o$); the SR SPR dips on the right. The nanometer values of layer thicknesses in the legend are ordered from the closest to the prism to the air substrate.

Kretschmann configuration is used in presented simulations. The Figure 5.7 illustrates excitation of the both kinds of SPPs for two states with symmetric geometry but of different dielectric slab, and the asymmetric case, when the first gold layer thickness predominates. LR SPPs excited close to 25 deg exhibit small dependence on MIM geometry, whereas the SR SPPs are hardly modified.

5.2.3 Excersise

5.2.3.1

Why the surface plasmon polariton can be excited at single dielectric/metal interface only for TM polarized light wave?

5.2.3.2

Estimate the SP resonance angle at the planar silver/water interface for the TM polarized wave. Use following data for refractive indices (at the wavelength 633 nm):
$n_p = 1.72$ (SF10 prism), $n_m = 0.16 - 3.81\mathrm{i}$ (silver), $n_d = 1.33$ (water).

Excersises in Chapters 2-5: Answers and Solutions

2.2.6.1

$$\mathbf{R} = \begin{bmatrix} 1 & 0 & 0 \\ 0 & 0 & 1 \\ 0 & -1 & 0 \end{bmatrix}$$

2.2.6.2

Ordinary beam is linearly polarized in the plane $y = x$, extra-ordinary one exhibits elliptical polarization – see Figure below.

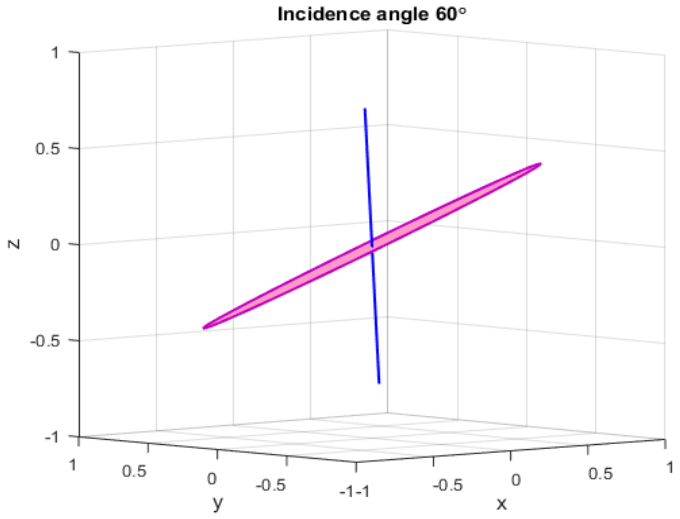

3.3.6.3

(I) $\varphi_o^{(1)} = \varphi_e^{(1)} = 31.48°$, no birefringence occurs

(II) $\varphi_o^{(1)} = 31.48°$, $\varphi_e^{(1)} = 38.12°$

3.3.6.4

Upon the critical angle $\varphi_c = 50.6°$ the penetration depth rapidly decreases – see figure on the next page.

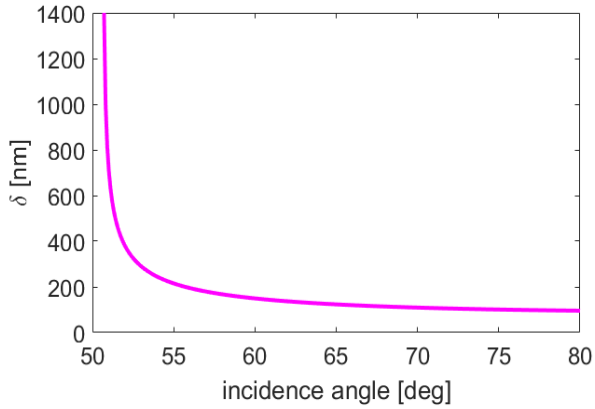

To the Excersise 3.3.6.4.

4.3.5.1

mode order m	0	1	2
TE	85	403	721
TM	131	450	768

4.3.5.2
See Eq. (4.27) for $n^{(1)} = n^{(3)}$.

4.3.5.3
$d > 3.7\mu$m

5.2.3.1
see the Subsection 5.1.2

5.2.3.2
$\varphi_{SP} = 50.44°$

Bibliography

[1] B. Maxum, *Field Mathematics for Electromgnetics, Photonics and Material Science*, SPIE Press, Bellingham, WA, U.S.A., 2004.

[2] S. Hess, *Tensors for Physics*, Springer, 2015.

[3] J. A. Kong, *Electromagnetic Wave Theory*, EMW Publ., Cambridge, MA, USA, 2000.

[4] Š. Višňovský, *Optics in Magnetic Multilayers and Nanostructures*. CRC Press, Boca Raton, U.S.A., 2006.

[5] P. H. Lissberger, M. R. Parker, Theory of the Voigt effect in gyroelectric media. *Int. J. Magnet.* I (1971), 209-218.

[6] R. M. Osgood III, S. D. Bader, B. M. Clemens, R. L. White, H. Matsuyama, Second-order magneto-optic effects in anisotropic thin films. *J. Magn. Magn. Mat.* 182 (1998), 297-323.

[7] J. Vlček, O. Bárta, J. Pištora, Quadratic magneto-optical effect in Fe, Ni and Co. In: *12th Czech-Slovak-Polish Optical Conference on Wave and Quantum Aspects of Contemporary Optics* (J. Peřina, M. Hrabovský and J. Křepelka Eds.), *Proc. of SPIE*, Vol. 4356 (2001), 254-261.

[8] J. Pištora, J. Vlček, M. Lesňák, *Optical Approaches for Nanotechnologies*, CERM, Brno, 2018.

[9] R. M. A. Azzam, N. M. Bashara, *Ellipsometry and Polarized Light*, North-Holland Publ. Comp., Amsterdam - New York - Oxford, 1977.

[10] E. Collett, *Field Guide to Polarization*, SPIE Press, Bellingham, WA, U.S.A., 2005.

[11] M. Schubert, B. Rheinländer, J. A. Woollam, B. Johs, C. M. Herzinger, Extension of rotating-analyzer ellipsometry to generalized ellipsometry: determination of the dielectric function tensor from uniaxial TiO_2. *J. Opt. Soc. Am.* A, Vol. 13 (1996), 901-908.

[12] P. Yeh, Optics of anisotropic layered media: a new 4x4 matrix algebra. *Surf. Sci.* 96 (1980), 41-53.

[13] Š. Višňovský, Magneto-optical ellipsometry. *Czech. J. Phys.*, B 36 (1986), 625-650.

[14] Š. Višňovský, R. Krishnan, M. Nývlt, V. Prosser, Optical behaviour of Fe in magnetic multilayers. *J. Magn. Soc. Jpn.* 20 (1996), 41.

[15] M. Bass, *Handbook of Optics II*, McGraw-Hill, New York, 1995.

[16] https://refractiveindex.info/...

[17] J. Pištora, J. Vlček, P. Otipka, M. Cada, Plasmonic nanostructures with waveguiding effect. *PNFA* 31 (2018), 22-26.

[18] S. Isaacs, E. Harté, I. D. Alves, I. Abdulahim, Improved detection of plasmon waveguide resonance using diverging beam, liquid crystal retarder, and application to lipid orientation determination. *Sensors* 48 (2019), 1402.

[19] B. A. Prabowo, A. Purwidyantri, K.-Ch. Liu, Surface Plasmon Resonance Optical Sensor: A Review on Light Source Technology. *Biosensors* 8 (2018), 80.

[20] S. I. Bozhevolnyi, T. Sondergaard, General properties of slow-plasmon resonant nanostructures: nano-antennas and resonantors. *Opt. Expr.* 15, No. 17 (2007), 10869.

[21] V. Chabot, Y. Miron, M. Grandbois, P. G. Charette, Long range surface plasmon resonance for increased sensitivity in living cell biosensing through greate probing depth. *Sens. & Act. B Chem.* 174 (2012), 94-101.

[22] J. Park et al., Resonant tunneling of surface plasmon polariton in the plasmonic nano-cavity. *Opt. Expr.* 16, No. 21 (2008), 16903.